Electronic supplementary information for

Metal-Free FRET† Macrocycles of Perylenediimide and Aza-BODIPY for Multifunctional Sensing

Kavita Rani and Sanchita Sengupta*

Department of Chemical Sciences, Indian Institute of Science Education and Research (IISER) Mohali, Punjab-140306, India.

Table of Contents

1. Materials and methods

All chemicals and solvents were purchased from commercial suppliers and used without further purification.

NMR Spectroscopy: ^{1}H, ^{13}C, ^{11}B and ^{19}F spectra were recorded on BrukerBiospinAvance III FT-NMR 400 MHz spectrometer at room temperature. Tetramethyl silane (TMS) was used as internal standard.

Mass Spectroscopy: High-resolution mass spectra were recorded with Waters QTOF mass spectrometer. Software used for acquiring mass spectra was Flex Control, Bruker (USA) and software used for analyzing mass spectra was Flex Analysis 3.1.

UV/Vis absorption and fluorescence spectroscopy: UV/Vis and near-NIR spectral measurements were carried out with Carey 5000 UV/Vis spectrophotometer using a quartz cuvette with 1 cm path length. Steady state emission and excitation studies were carried out with Hitachi F7000 fluorescence spectrophotometer equipped with R928F photomultiplier expandable up to 900 nm.

Temperature dependent fluorescence spectroscopy: Temperature-dependent fluorescence of samples were measured using temperature-controlled cuvette holder for Hitachi F7000 spectrophotometer (Luma 40) from Quantum Northwest. Luma 40 temprature controller was used for measurements in the temperature range of 0 $^{\circ}$C to 100 $^{\circ}$C.

Time resolved fluorescence spectra: Time resolved fluorescence spectra were measured using time correlated single photon counting (TCSPC) model from Fluorocube, Horiba Jobin Yvon, NJ equipped with picosecond laser diodes as excitation source. A 590 nm and 635 nm laser diode were used as a light source for the excitation of samples and the instrument response function (IRF) was collected using Ludox (colloidal silica) solution. The width (FWHM) of IRF was ~250 ps. The optical pulse durations from < 70 ps were used. Highly integrated picosecond PMT modules as well as micro channel plate PMTs were used for the time resolution.

Cyclic voltammetry: The electrochemical measurements were recorded using CHI-610 electrochemical workstation from CH Instruments (USA), with a conventional three electrode single-compartment cell consisting of a glassy carbon as the working electrode, Ag/AgCl containing 1M KCl solution as the reference electrode, and Pt wire as the counter electrode. Cyclic voltammetry measurements were performed at a scan-rate of 100 mV/s. Tetrabutylammonium hexafluorophosphate (TBAHFP) (Alfa Aesar) (0.1M) dissolved in pre-dried DCM was used as a supporting electrolyte. The solutions were purged with nitrogen prior

to measurement. The electrochemical potential was internally calibrated against the standard ferrocene/ferrocenium (Fc/Fc^+) redox couple prior to each measurement.

Spectroelectrochemistry: Spectroelectrochemical measurements were performed using a cell assembly (SEC-C) supplied by BAS Inc (Japan) and the assembly comprised of a Pt counter electrode, a Pt gauze working electrode, and an Ag/AgCl reference electrode in a 1.0 mm path length quartz cell. The absorption spectra were measured using an ocean optics set up connected in absorbance mode and using the FLAME spectrometer. Voltages were swept in the range of -2 V to +2 V, dry DCM was used as solvent and TBAHFP was used as the supporting electrolyte. The solutions were purged with nitrogen for 10 min prior to spectroelectrochemical measurements.

Dynamic light scattering (DLS) Measurements: DLS experiments have been performed on a Malvern Zetasizer Nano ZS90 instrument.

2. Synthesis procedures

Synthesis of donor subchromophore

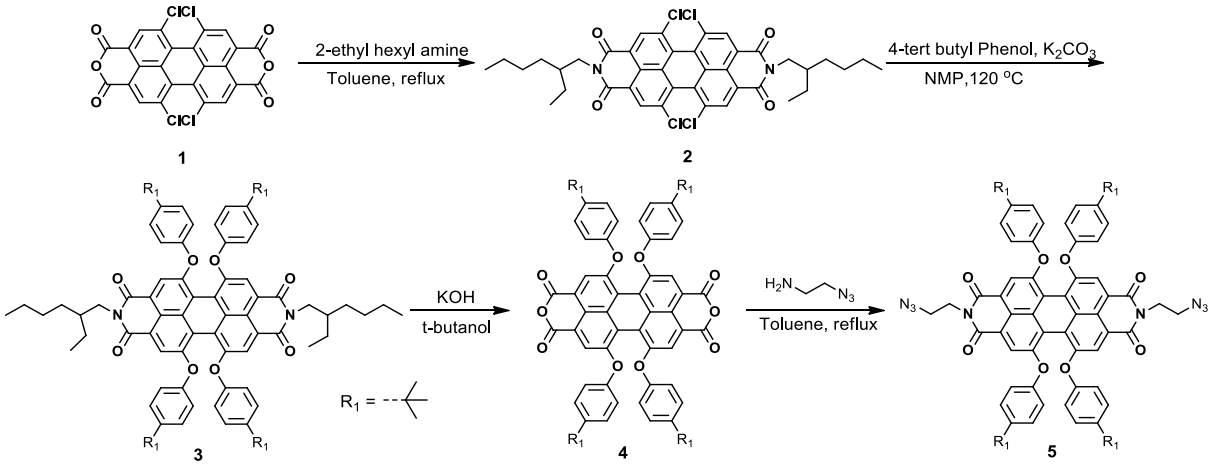

Scheme S1. Synthesis of donor precursor PDI **5**.

Synthesis of compound 1

Compound **1** was synthesized according to literature procedure.[1]

Synthesis of compound 2

The crude compound **1** (5 g, 9.43 mmol) was dissolved in dry toluene (100 mL), 2-ethylhexylamine (3.10 mL, 18.86 mmol) was added and refluxed for 24 h. Then solvent was removed under reduced pressure and compound was purified by column chromatography with dichloromethane (DCM) /hexane (1/3) as eluent to obtain compound **2** as red solid.[1]

Yield: 5.12 g (72 %).

^{1}H NMR (400 MHz, $CDCl_3$) δ (ppm): 8.68 (s, 4 H), 4.21 – 4.10 (m, 4 H), 1.98 – 1.91 (m, 2 H), 1.43 – 1.32 (m, 16 H), 0.97 – 0.88 (m, 12 H).

^{13}C NMR (100 MHz, $CDCl_3$) δ (ppm): 162.74, 135.49, 133.15, 131.56, 128.70, 123.44, 123.34, 44.71, 38.10, 30.80, 28.75, 24.10, 23.21, 14.27, 10.71.

Synthesis of compound 3

Compound **2** (5 g, 6.64 mmol), 4-tert-butylphenol (12.00 g, 79.73 mmol) and K_2CO_3 (11.02 g, 79.73 mmol) were dissolved in dry N-methyl-2-pyrrolidone (NMP) (60 mL) under nitrogen atmosphere. The reaction mixture was stirred for 24 h at 120 ^{o}C. After being cooled to room temperature (RT), 2 M HCl was added and a precipitate was formed, filtered and washed with water/methanol mixture. Subsequently, crude product was purified by column chromatography with DCM/hexane (1/2) as eluent to obtain **3** as purple solid.[1]

Yield: 5.3 g (66 %).

^{1}H NMR (400 MHz, CD_2Cl_2) δ (ppm): 8.14 (s, 4 H), 7.28 (d, J = 8 Hz, 8 H), 6.85 (d, J = 8 Hz, 8 H), 4.07 – 3.95 (m, 4 H), 1.86 – 1.80 (m, 2 H), 1.31 – 1.26 (m, 52 H), 0.89 – 0.84 (m, 12 H).

^{13}C NMR (100 MHz, CD_2Cl_2) δ (ppm): 164.08, 156.35, 153.67, 147.87, 133.44, 127.17, 123.16, 120.98, 120.36, 120.07, 119.77, 44.63, 38.52, 34.82, 31.76, 31.28, 29.29, 24.57, 23.58, 14.42, 10.95.

Synthesis of compound 4

Compound **3** (4 g, 3.31 mmol) was added to the solution of potassium hydroxide (2.80 g, 50 mmol) dissolved in *t*-butanol (60 mL) and refluxed for 24 h. Subsequently, the reaction mixture was cooled to RT and HCl (2M) was added and reaction mixture was heated at 100 °C for 3-4 h. The precipitate was formed and filtered, washed with water and dried in oven and further purified by silica column chromatography using DCM /hexane (1/1) as eluent to obtain compound **4** as purple solid.

Yield: 2.7 g (83 %).

^{1}H NMR (400 MHz, CD_2Cl_2) δ (ppm): 8.17 (s, 4 H), 7.30 (d, J = 8 Hz, 8 H), 6.86 (d, J = 8 Hz, 8 H), 1.30 (s, 36 H).

^{13}C NMR (100 MHz, CD_2Cl_2) δ (ppm): 160.35, 156.84, 153.14, 148.53, 133.98, 127.41, 122.02, 121.95, 119.81, 119.19, 34.88, 31.72.

Synthesis of compound 5

Compound **4** (1 g, 1.02 mmol) was dissolved in dry toluene (40 mL) and 2-azidoethanamine (437 mg, 5.08 mmol) was added. The reaction mixture was refluxed for 24 h followed by evaporation of solvent under reduced pressure. The crude product was purified by silica column chromatography using DCM/hexane (2/1) as eluent and purple solid compound was obtained.

Yield: 1.10 g (97 %).

^{1}H NMR (400 MHz, $CDCl_3$) δ (ppm): 8.24 (s, 4 H), 7.25 – 7.23 (m, 8 H), 6.83 (d, J = 8 Hz, 8 H), 4.37 (t, J = 8 Hz, 4 H), 3.62 (t, J = 4 Hz, 4 H), 1.29 (s, 32 H).

^{13}C NMR (100 MHz, $CDCl_3$) δ (ppm): 163.58, 156.17, 152.89, 147.54, 133.06, 126.85, 122.16, 120.86, 120.22, 119.63, 119.46, 48.98, 39.10, 34.52, 31.59.

HRMS (ESI): *m/z* calcd for $C_{68}H_{65}N_8O_8^+$ [M+ H]$^+$: 1121.4920, Found: 1121.4924.

Synthesis of acceptor subchromophore

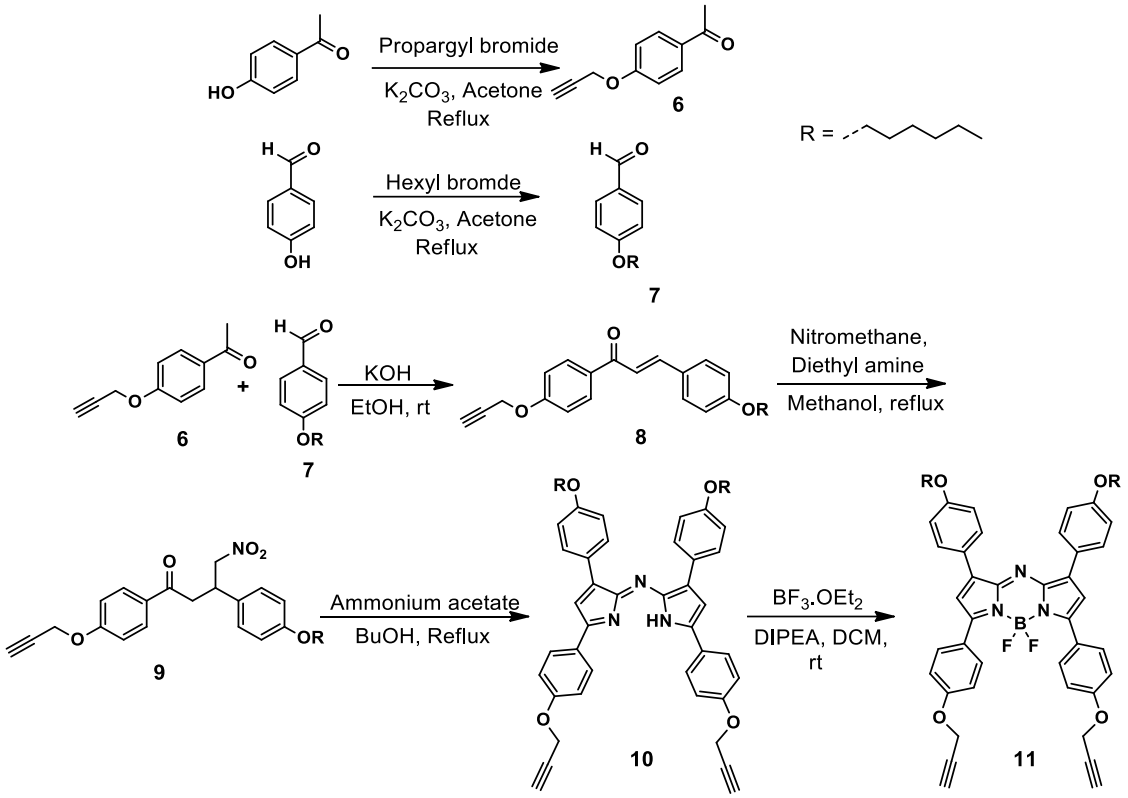

Scheme S2. Synthesis of acceptor precursor ABDP **11**.

Synthesis of compound 6

4-hydroxyacetophenone (5 g, 36.72 mmol), potassium carbonate (7.6 g, 55.08 mmol) and propargyl bromide (6.55 g, 55.08 mmol) were dissolved in anhydrous acetone (50 mL) under nitrogen atmosphere and mixture was refluxed for 5 h. After being cooled to RT, the reaction mixture was filtered followed by removing the solvent of the filtrate, the crude product was

obtained which was purified by recrystallization from methanol and white solid compound **6** was obtained.

Yield: 4.8 g (75 %).

^{1}H NMR (400 MHz, $CDCl_3$) δ (ppm): 7.97 – 7.93 (m, 2 H), 7.04 – 7.00 (m, 2 H), 4.76 (d, *J* = 4 Hz, 2 H), 2.56 (s, 3 H), 2.55 (t, *J* = 4 Hz, 1 H).

^{13}C NMR (100 MHz, $CDCl_3$) δ (ppm): 196.82, 161.33, 131.07, 130.59, 114.63, 77.82, 76.25, 55.90, 26.49.

Synthesis of compound 7

4-hydroxybenzaldehyde (6 g, 49.13 mmol), potassium carbonate (10.18 g, 73.70 mmol) and 1-bromohexane (10.30 mL, 73.70 mmol) were dissolved in anhydrous acetone (60 mL) under nitrogen atmosphere and mixture was refluxed for 8 h under nitrogen atmosphere. Subsequently, the solvent was removed under reduced pressure and ethyl acetate (EA) was added to the crude mixture and washed with water and dried over sodium sulphate. Further solvent was evaporated under reduced pressure and crude product was purified by silica column chromatography with hexane/EA (5/1) as eluent, compound **7** was obtained as colourless oil.

Yield: 8.1 g (80 %).

^{1}H NMR (400 MHz, $CDCl_3$) δ (ppm): 9.86 (s, 1 H), 7.81 (d, *J* = 8 Hz, 2 H), 6.98 (d, *J* = 8 Hz, 2 H), 4.02 (t, *J* = 8 Hz, 2 H), 1.83-1.76 (m, 2 H), 1.49-1.42 (m, 2 H), 1.36-1.31 (m, 4 H), 0.90 (t, *J* = 8 Hz, 3 H).

Synthesis of compound 8

Compound **6** (4.76 g, 27.32 mmol) was dissolved in ethanol (70 mL) followed by dropwise addition of aqueous potassium hydroxide (6.13 g, 109.28 mmol). Subsequently, compound **7** (5.63 g, 27.32 mmol) was dissolved in ethanol (20 mL) and was slowly added dropwise to the reaction mixture and stirred overnight at RT. A precipitate was formed that was filtered and washed with ethanol. Compound **8** was further purified by recrystallization from methanol, and obtained as light yellow colour crystals.

Yield: 9.4 g (95 %).

^{1}H NMR (400 MHz, $CDCl_3$) δ (ppm): 8.04 (d, *J* = 8 Hz, 2H), 7.78 (d, *J* = 16 Hz, 1 H), 7.59 (d, *J* = 8 Hz, 2H), 7.42 (d, *J* = 16 Hz, 1 H), 7.06 (d, *J* = 8 Hz, 2H), 6.92 (d, J = 8 Hz, 2H), 4.78 (d, *J* = 2 Hz, 2 H), 4.00 (t, *J* = 8 Hz, 2 H), 2.56 (t, *J* = 4 Hz, 1 H), 1.83 – 1.76 (m, 2 H), 1.51 – 1.43 (m, 2 H), 1.37 – 1.33 (m, 4 H), 0.91 (t, *J* = 8 Hz, 3 H).

^{13}C NMR (100 MHz, $CDCl_3$) δ (ppm): 188.91, 161.34, 161.14, 144.28, 132.29, 130.73, 130.26, 127.62, 119.41, 115.02, 114.77, 77.98, 76.28, 76.22, 68.32, 55.99, 31.68, 29.25, 25.81, 22.72,14.16.

HRMS (ESI): *m/z* calcd for $C_{24}H_{27}O_3^+$ $[M+H]^+$: 363.1955 , Found: 363.1960.

Synthesis of compound 9

Diethylamine (13.00 mL, 125.53 mmol) and nitromethane (6.73 mL, 125.53 mmol) were added to the solution of compound **8** (9.11 g, 25.11 mmol) in ethanol (100 mL) and the mixture was refluxed for 24 h. After being cooled to RT, solvent was evaporated under reduced pressure and EA was added to crude mixture and washed with water. Further solvent was evaporated under reduced pressure and crude was purified by silica column chromatography with hexane/EA (2/1) as eluent, compound **9** was obtained as a yellowish oil.

Yield: 8.5 g (56 %).

^{1}H NMR (400 MHz, $CDCl_3$) δ (ppm): 7.91 (d, J = 8 Hz, 2 H), 7.17 (d, J = 8 Hz, 2 H), 7.00 d, J = 8 Hz, 2 H), 6.84 (d, J = 8 Hz, 2 H), 4.81 – 4.75 (m, 3 H), 4.65 – 4.60 (m, 1 H), 4.18 – 4.11 (m, 1 H), 3.91 (t, J = 8 Hz, 2 H), 3.42 – 3.30 (m, 2 H), 2.55 (t, J = 4 Hz, 1 H), 1.78 – 1.71 (m, 2 H), 1.47 – 1.40 (m, 2 H), 1.34 – 1.30 (m, 4 H), 0.90 (t, J = 8 Hz, 3 H).

^{13}C NMR (100 MHz, $CDCl_3$) δ (ppm): 199.58, 161.66, 158.74, 130.91, 130.39, 130.30, 128.55, 115.02, 114.83, 80.01, 77.72, 76.42, 76.39, 68.07, 55.96, 41.44, 38.82, 31.68, 29.31, 25.82, 22.72, 14.17.

HRMS (ESI): *m/z* calcd for $(M+H)^+$ 424.2118:, Found: 424.2117.

Synthesis of compound 10 and 11

Compound **9** (3.5 g, 8.26 mmol) and ammonium acetate (31.85 g, 413.22 mmol) were dissolved in 50 mL of anhydrous butanol. The reaction mixture was refluxed for 24 h. After being cooled to RT, the precipitate was filtered and washed with water and methanol to give blue solid product **10**. This compound was used for the next step without further purification.

Yield: 1.55 g (25 %).

Compound **10** (1.5 g, 1.98 mmol) was dissolved in dry DCM (150 mL) under nitrogen atmosphere, diisopropylethylamine (DIPEA) (4.14 mL, 23.76 mmol) was added and reaction mixture was stirred for 10 minutes followed by the addition of boron trifluoride-diethyl etherate (4.40 mL, 35.62 mmol) and stirred at RT for 24 h under nitrogen atmosphere. Subsequently, the reaction mixture was washed with a saturated aqueous NH_4Cl solution, saturated sodium chloride and water. The organic layer was dried over sodium sulphate and the solvent was

evaporated under reduced pressure. The crude product was purified by column chromatography with DCM/hexane (1/2) as eluent to obtain purple solid compound **11**.[1,2]

Yield: 1.51 g (95 %).

^{1}H NMR (400 MHz, $CDCl_3$) δ (ppm): 8.05 (t, J = 8 Hz, 8 H), 7.07 (d, J = 8 Hz, 4 H), 6.98 (d, J = 8 Hz, 4 H), 6.92 (s, 2 H), 4.76 (d, J = 4 Hz, 2 H), 4.04 (t, J = 8 Hz, 4 H), 2.57 (t, J = 4 Hz, 2 H), 1.87 – 1.80 (m, 4 H), 1.52 – 1.47 (m, 4 H), 1.41 – 1.35 (m, 8 H), 0.93 (t, J = 8 Hz, 6 H).

^{13}C NMR (100 MHz, $CDCl_3$) δ (ppm): 160.53, 159.70, 131.53, 130.91, 125.34, 115.06, 114.80, 78.22, 76.13, 68.32, 55.98, 31.76, 29.36, 25.89, 22.78, 14.21.

^{11}B NMR (128 MHz, $CDCl_3$) δ (ppm): 1.04 (t, ^{1}J (B-F) = 32 Hz, 1 B).

^{19}F NMR (376 MHz, $CDCl_3$) δ (ppm): -131.28 (q, ^{1}J (F-B) = 30 Hz, 2 F).

HRMS (ESI): *m/z* calcd for $C_{50}H_{51}BF_2N_3O_4$ $[M+H]^+$: 806.3935, Found: 806.3931.

Synthesis of triad T, macrocycle M1 and pentad P

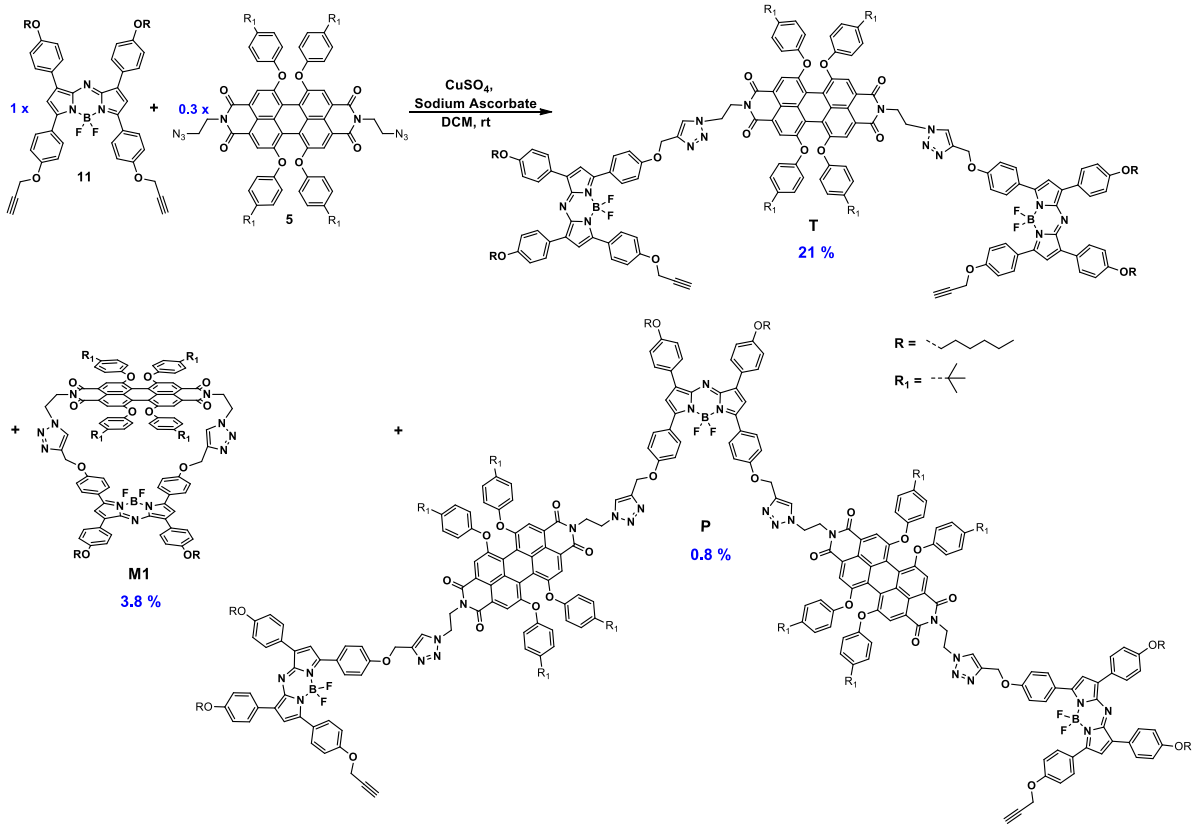

Scheme S3. Synthesis of triad **T**, macrocycle **M1** and pentad **P**.

Aza-BODIPY compound **11** (1.00 equiv.) (550 mg, 0.68 mmol) and PDI **5** (0.3 equiv.) (230.00 mg, 0.20 mmol) were dissolved in DCM: H_2O: Ethanol (12:1:1) (60 mL) solvent mixture and purged with nitrogen for 25-30 minutes. Then sodium ascorbate (872 mg, 0.044 mmol) was added and after 10 min purging with nitrogen, copper sulphate (5.48 mg, 0.022 mmol) was

added under nitrogen atmosphere and the reaction was stirred at RT. After the complete consumption of limiting reactant PDI **5** as monitored by TLC, the reaction was stopped and the mixture was washed with water and dried with sodium sulphate. The crude product was purified using column chromatography first with DCM as eluent to recover the reactant aza-BODIPY **11 (**275 mg) as first eluted compound from column and further eluting with DCM/EA (95/5) compound **T** (second spot in TLC) was obtained as purple compound in 21 % yield (115 mg).[1,2]

Macrocycle **M1** was isolated from the above reaction mixture (third spot in TLC) by washing the mixture with EA as it was soluble in EA followed by further purification 3-4 times using silica column chromatography with DCM/EA (90/10) as eluents and obtained as a purple solid (15 mg, 3.8 %).

Compound P was isolated from the above reaction mixture as fourth spot in TLC and purified by column chromatography using DCM/EA (80/20) as eluents as a purple solid (9 mg, 0.8 %).

Triad T

^{1}H NMR (400 MHz, $CDCl_3$) δ (ppm): 8.15 (s, 4 H), 8.04 – 7.95 (m, 16 H), 7.66 (s, 2 H), 7.20 (d, J = 8 Hz, 8 H), 7.04 – 6.93 (m, 16 H), 6.89 (s, 2 H), 6.84 (s, 2 H), 6.78 (d, J = 8 Hz, 8 H), 5.21 (s, 4 H), 4.72 (d, J = 4 Hz, 4 H), 4.68 (d, J = 8 Hz, 4 H), 4.58 (s, 4 H), 4.0.3 (t, J = 4 Hz, 8 H), 2.54 (t, J = 4 Hz, 2 H), 1.86 – 1.76 (m, 8 H), 1.53 – 1.46 (m, 8 H), 1.39 – 1.35 (m, 16 H), 1.28 (s, 36 H), 0.93 (t, J = 8 Hz, 12 H).

^{13}C NMR (100 MHz, $CDCl_3$) δ (ppm): 163.28, 160.44, 160.41, 160.38, 159.62, 157.46, 155.98, 152.95, 147.39, 145.26, 145.14, 143.96, 142.95, 142.82, 132.95, 131.53, 130.84, 126.76, 125.29, 125.24, 124.88, 123.46, 121.86, 121.04, 120.27, 119.58, 119.34, 117.11, 114.99, 114.69, 78.21, 76.20, 76.16, 68.30, 62.21, 55.94, 55.19, 47.86, 40.01, 34.48, 31.75, 31.58, 29.36, 25.87, 22.76, 14.20.

^{11}B NMR (128 MHz, $CDCl_3$) δ (ppm): 0.95 (t, ^{1}J (B-F) = 32 Hz, 2 B).

^{19}F NMR (376 MHz, $CDCl_3$) δ (ppm): -130.86 – -131.14 (m, 4 F).

HRMS (ESI): *m/z* calcd for $(M+Na)^+$ $(C_{168}H_{164}B_2F_4N_{14}NaO_{16})^+$: 2754.2464 Found: 2754.5583.

m/z calcd for $(M+2Na)^{2+}$ $(C_{168}H_{164}B_2F_4N_{14}O_{16}Na_2)^{2+}$: 1389.1195, Found: 1389.1185.

HRMS (MALDI): *m/z* calcd for $(M+Na)^+$ $(C_{168}H_{164}B_2F_4N_{14}NaO_{16})^+$: 2754.2464 Found: 2754.3640.

Macrocycle M1

^{1}H NMR (400 MHz, $CDCl_3$) δ (ppm): 8.18 (s, 4 H), 8.04 (d, *J* = 12 Hz, 8 H), 7.40 (s, 2 H), 7.22 (d, *J* = 8 Hz, 8 H), 6.98 (d, *J* = 12 Hz, 4 H), 6.93 (s, 2 H), 6.89 - 6.80 (m, 12 H), 5.05 (s, 4 H), 4.84 (s, 4 H), 4.58 (s, 4 H), 4.04 (t, *J* = 8 Hz, 4 H), 1.85 - 1.80 (m, 4 H), 1.52 - 1.48 (m, 4 H), 1.39 - 1.36 (m, 8 H), 1.28 - 1.25 (32 H), 0.93 (t, *J* = 8 Hz, 6 H).

^{13}C NMR (100 MHz, $CDCl_3$) δ (ppm): 163.22, 160.51, 157.54, 156.08, 152.91, 147.57, 145.33, 143.49, 142.85, 133.14, 131.60, 131.55, 130.87, 126.86, 125.31, 124.98, 123.43, 121.66, 121.17, 119.58, 119.30, 114.76, 68.31, 62.02, 52.82, 48.34, 39.86, 34.50, 31.75, 31.57, 29.83, 29.36, 25.88, 22.76, 14.20.

^{11}B NMR (128 MHz, $CDCl_3$) δ (ppm): 1.09 (t, ^{1}J (B-F) = 32 Hz, 1 B).

^{19}F NMR (376 MHz, $CDCl_3$) δ (ppm): -131.72 (q, ^{1}J (F-B) = 33.84 Hz, 2 F).

HRMS (ESI): *m/z* calcd for $(M+H)^+$ $(C_{118}H_{115}BF_2N_{11}O_{12})^+$: 1926.8782, Found: 1926.7845.

m/z calcd for $(M+Na)^+$ $(C_{118}H_{114}BF_2N_{11}NaO_{12})^+$: 1948.8602, Found: 1948.7806.

HRMS (MALDI): *m/z* calcd for $(M+H)^+$ $(C_{118}H_{115}BF_2N_{11}O_{12})^+$: 1926.8782, Found: 1926.9504.

m/z calcd for $(M+Na)^+$ $(C_{118}H_{114}BF_2N_{11}NaO_{12})^+$: 1948.8602, Found: 1948.9384.

Pentad P

^{1}H NMR (400 MHz, $CDCl_3$) δ (ppm): 8.13 (d, *J* = 2 Hz, 8 H), 8.03 – 7.94 (m, 24 H), 7.66 (d, *J* = 4 Hz, 4 H), 7.20 – 7.18 (m, 16 H), 7.03 – 6.92 (m, 24 H), 6.87 (s, 2 H), 6.83 (s, 4 H), 6.78 – 6.76 (m, 16 H), 5.20 (s, 8 H), 4.72 – 4.66 (m, 12 H), 4.56 (s, 8 H), 4.02 (t, *J* = 6.68 Hz, 12 H), 2.53 (t, *J* = 2 Hz, 2 H), 1.86 – 1.79 (m, 12 H), 1.51 – 1.46 (m, 12 H), 1.38 – 1.35 (m, 24 H), 1.27 (s, 72 H), 0.93 (t, *J* = 6.76 Hz, 18 H).

^{13}C NMR (100 MHz, $CDCl_3$) δ (ppm): 163.26, 160.42, 160.37, 160.33, 159.61, 157.77, 155.95, 152.93, 147.37, 145.24, 145.12, 143.98, 143.94, 142.90, 142.73, 132.93, 131.50, 130.83, 126.74, 125.27, 125.24, 124.85, 123.43, 121.83, 121.02, 120.26, 119.56, 119.32, 117.06, 114.97, 114.67, 78.20, 76.72, 76.22, 68.30, 62.20, 55.94, 47.83, 40.01, 34.47, 31.75, 31.58, 29.36, 25.88, 22.76, 14.21.

^{11}B NMR (128 MHz, $CDCl_3$) δ (ppm): 0.93 (t, ^{1}J (B-F) = 32 Hz, 3 B).

^{19}F NMR (376 MHz, $CDCl_3$) δ (ppm): -130.93 – -131.10 (m, 6 F).

HRMS (ESI): *m/z* calcd for $[(C_{286}H_{278}B_3F_6N_{25}O_{28} - C_{168}H_{164}B_2F_4N_{14}O_{16}) + Na^+]$:1948.8602, Found 1948.7483.

HRMS (MALDI): *m/z* calcd for $[(C_{286}H_{278}B_3F_6N_{25}O_{28} - C_{168}H_{164}B_2F_4N_{14}O_{16}) + Na^+]$:1948.8602, Found 1948.9413.

For pentad **P** only mass for fragments ions were observed in both ESI and MALDI techniques.

Synthesis of macrocycle M2

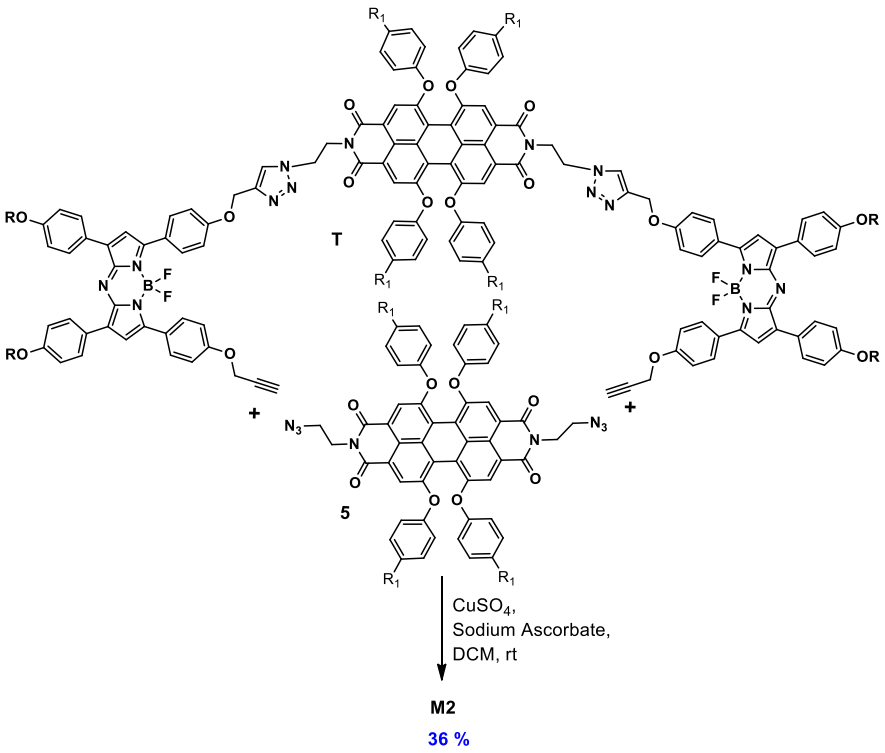

Scheme S4. Synthesis of macrocycle **M2**.

Triad compound **T** (120 mg, 0.044 mmol) was dissolved in (DCM: H_2O: Ethanol 12:1:1) (240 mL) solvent and purged with nitrogen for 25-30 minutes, while compound PDI **5** (49.23 mg, 0.044 mmol) was dissolved in DCM (100 mL), filled in syringe, and connected to syringe pump, sodium ascorbate (8.72 mg, 0.044 mmol) and copper sulphate (5.48 mg, 0.022 mmol) was added under nitrogen atmosphere to the reaction mixture. The addition of **5** was started dropwise (0.1 mL/min) to this mixture for about 15 h under nitrogen atmosphere. After the complete consumption of reactants as monitored by TLC, the mixture was washed with water and dried using sodium sulphate and solvent was removed under reduced pressure. The crude was purified using column chromatography with DCM/EA (75/25) as eluents and compound **M2** was obtained as a purple solid compound.[1,2]

Yield: 61 mg (36 %).

^{1}H NMR (400 MHz, $CDCl_3$) δ (ppm): 8.09 (s, 8 H), 7.97 – 7.92 (m, 8 H), 7.68 – 7.64 (m, 4 H), 7.17 (d, J = 8 Hz, 16 H), 6.94 (d, J = 8 Hz, 16 H), 6.82 – 6.73 (m, 20 H), 5.16 (s, 8 H), 4.67 (s, 8 H), 4.56 (s, 8 H), 4.02 (t, J = 8 Hz , 8 H), 1.86 – 1.79 (m, 8 H), 1.54 – 1.46 (m, 8 H), 1.39 – 1.36 (m, 16 H), 1.24 (s, 72 H), 0.93 (t, J = 7 Hz, 12 H).

^{13}C NMR (100 MHz, $CDCl_3$) δ (ppm): 163.20, 160.39, 160.32, 155.93, 152.90, 152.82, 147.36, 145.14, 143.93, 132.89, 131.51, 130.80, 126.73, 125.24, 124.85, 123.48, 121.71, 120.94,

120.13, 119.46, 119.30, 114.94, 114.67, 68.30, 62.15, 54.91, 47.85, 39.99, 34.45, 31.76, 31.56, 29.36, 25.88, 22.76, 14.21.

^{11}B NMR (128 MHz, $CDCl_3$) δ (ppm): 0.92 (t, ^1J (B-F) = 32 Hz, 2 B).

^{19}F NMR (376 MHz, $CDCl_3$) δ (ppm): -131.04 – -131.32 (m, 4 F).

HRMS (ESI): *m/z* calcd for $(M + 2Na)^{2+}$ $(C_{236}H_{228}B_2F_4N_{22}O_{24}Na_2)^{2+}$: 1949.8636, Found: 1949.7632.

HRMS (MALDI): *m/z* calcd for $(M + Na)^{+}$ $(C_{236}H_{228}B_2F_4N_{22}O_{24}Na)^{+}$: 3874.7311, Found: 3874.7583.

m/z calcd for $(M + 2Na)^{2+}$ $(C_{236}H_{228}B_2F_4N_{22}O_{24}Na_2)^{2+}$: 1949.8636, Found: 1949.7722.

3. NMR spectra

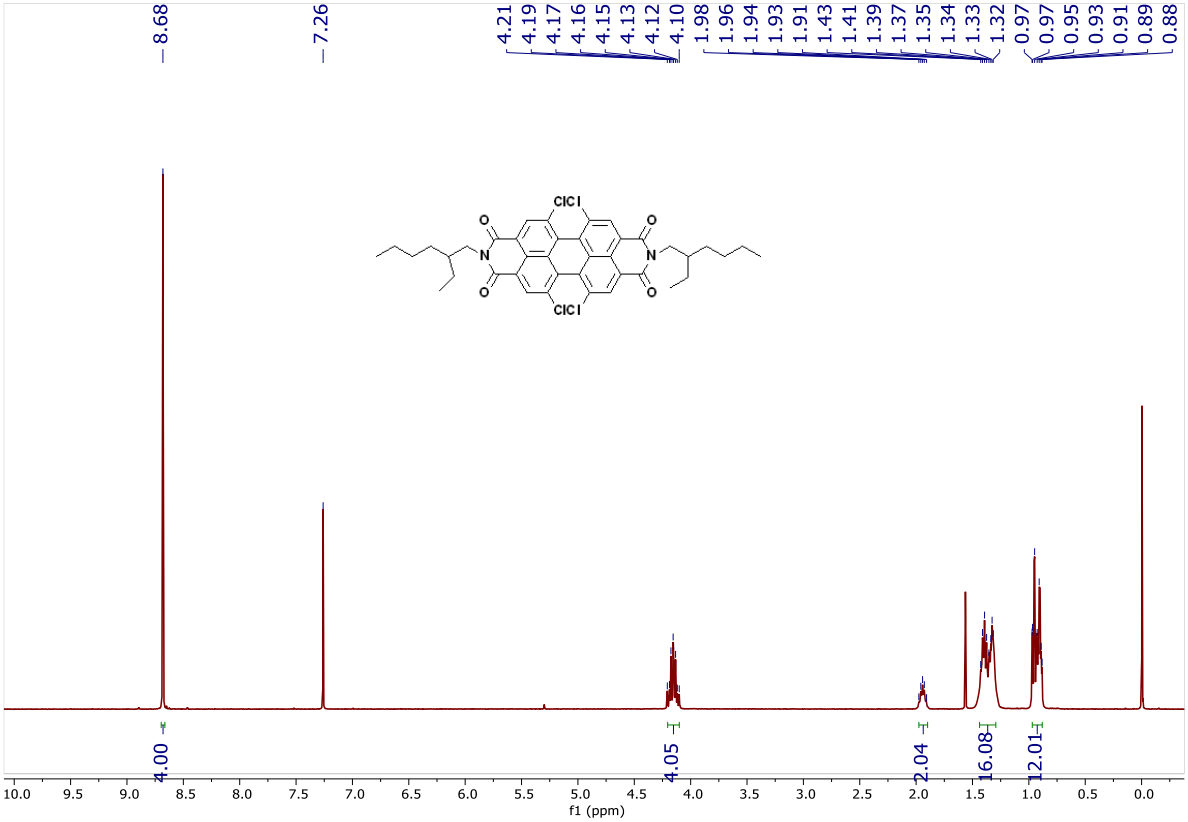

^{1}H NMR of compound **2** in $CDCl_3$.

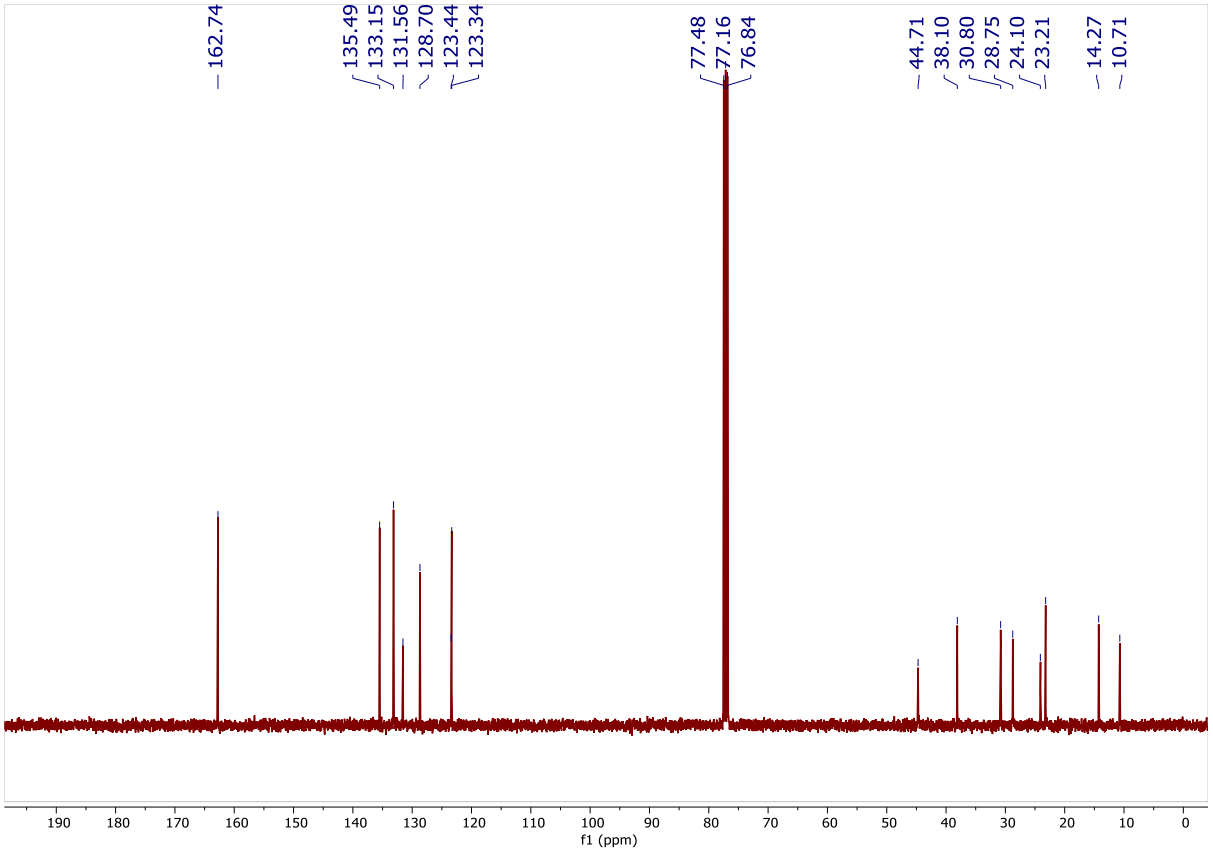

^{13}C NMR of compound **2** in $CDCl_3$.

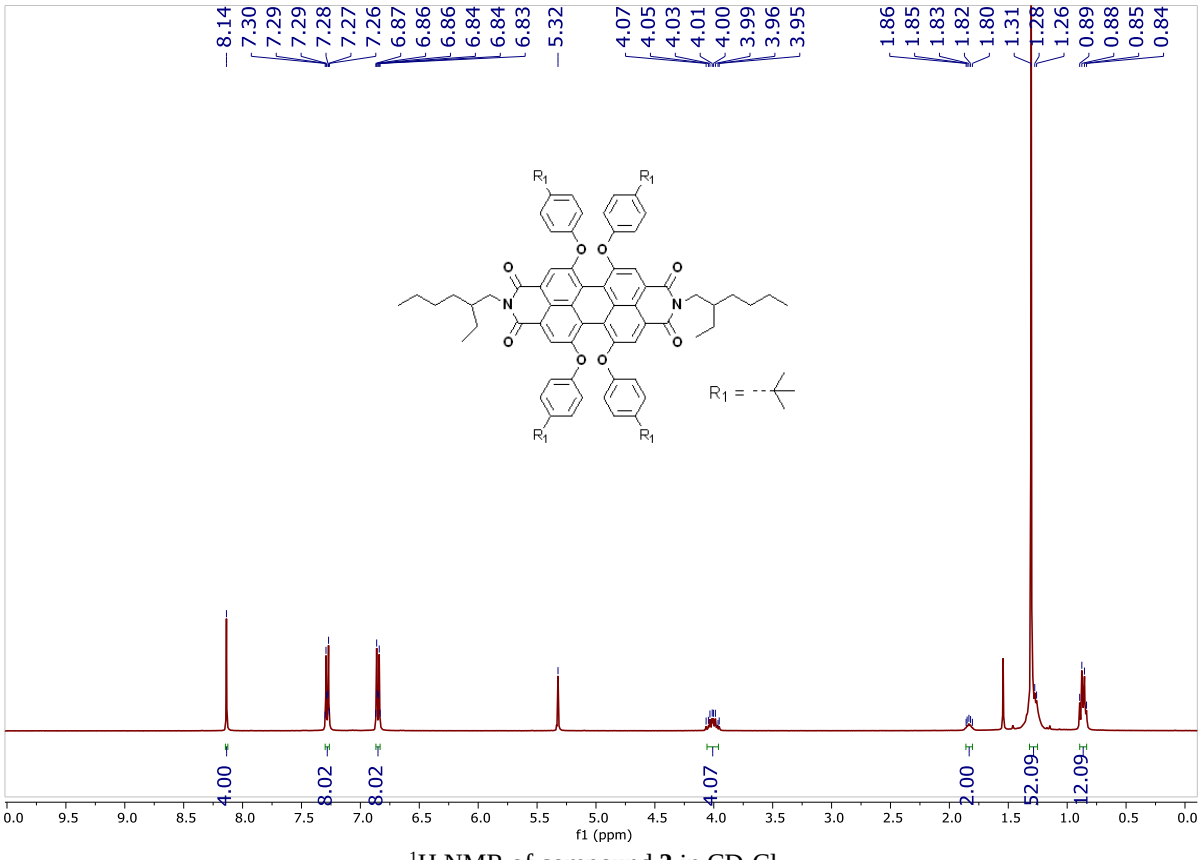

^{1}H NMR of compound **3** in CD_2Cl_2.

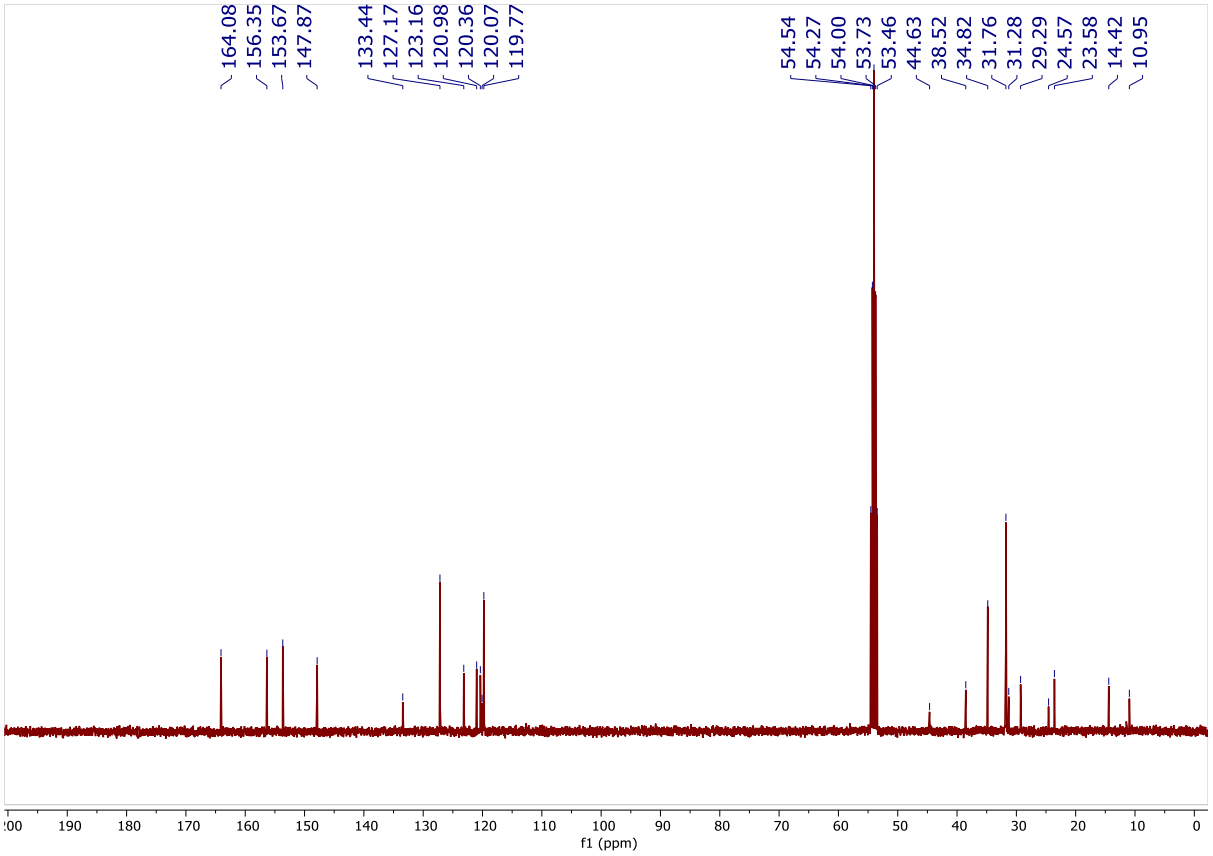

^{13}C NMR of compound **3** in CD_2Cl_2.

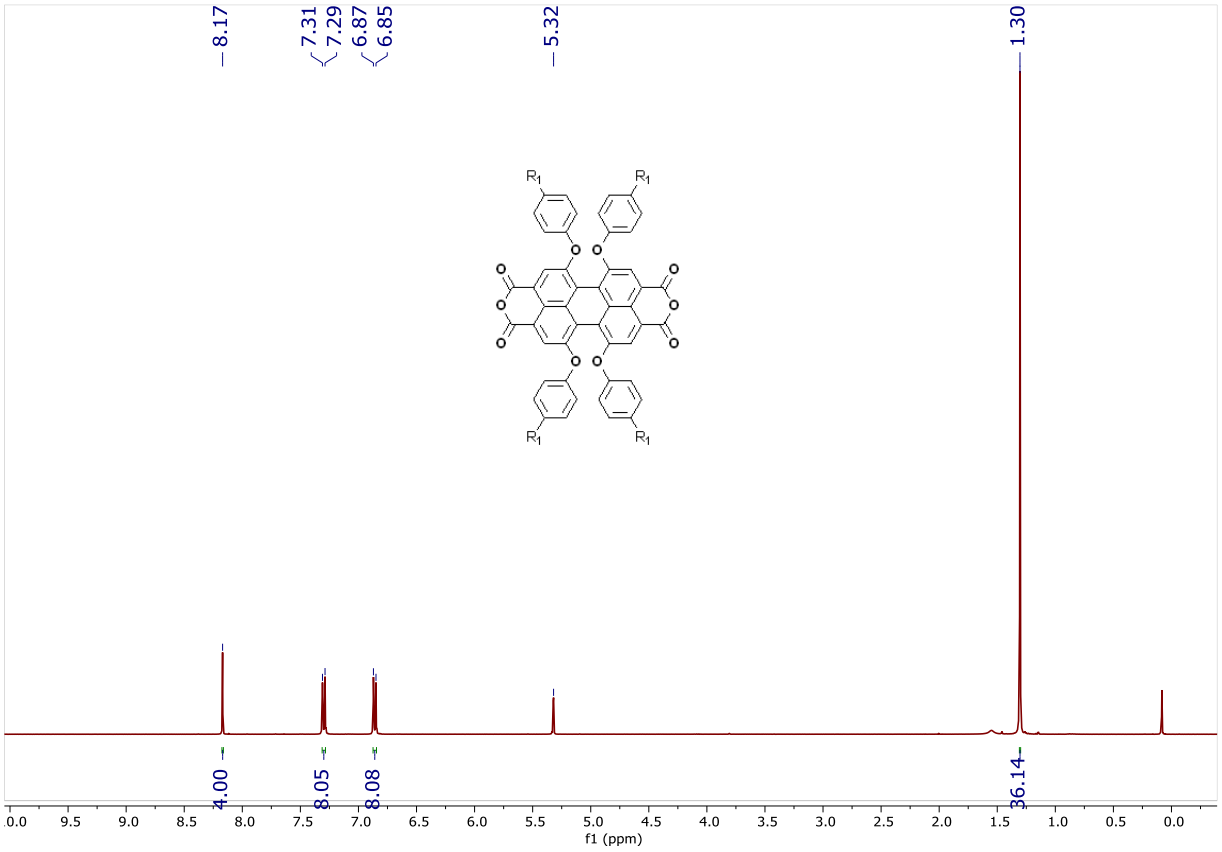

^{1}H NMR of compound **4** in CD_2Cl_2.

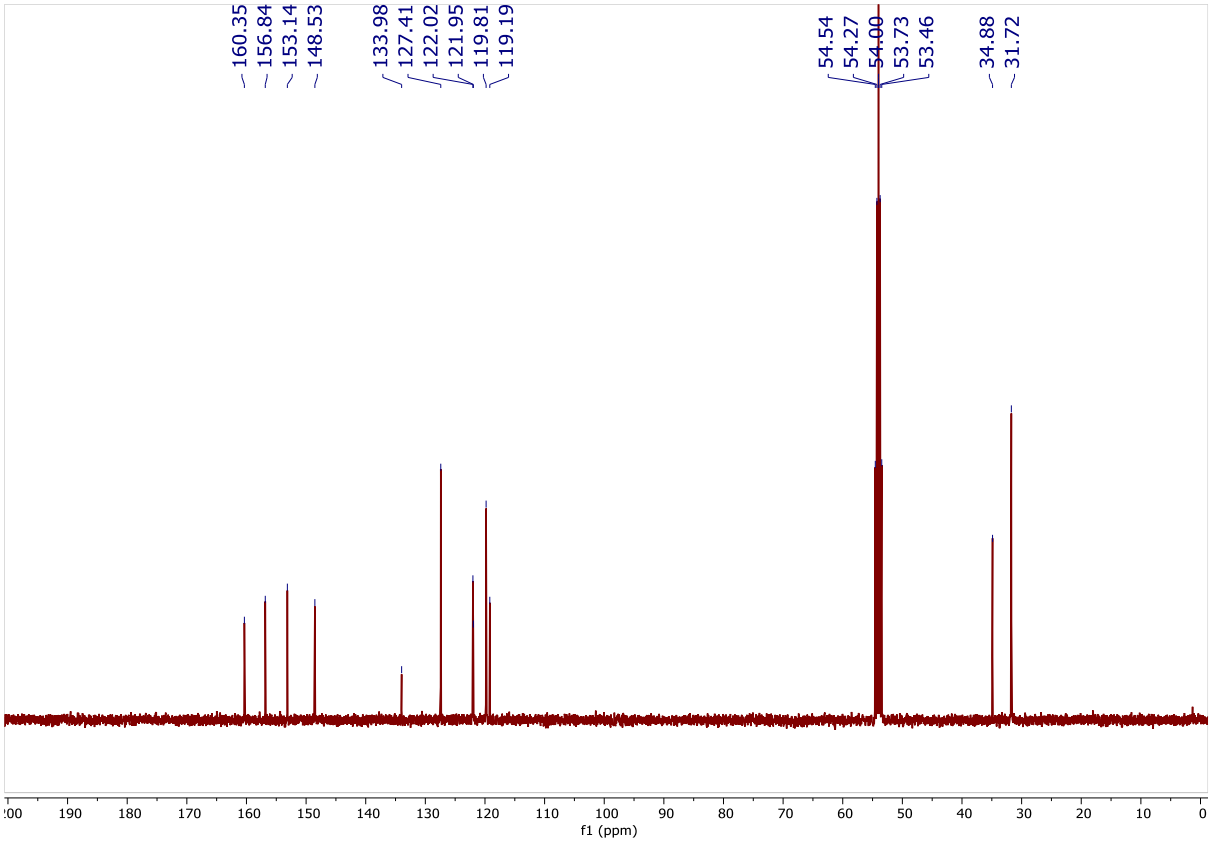

^{13}C NMR of compound **4** in CD_2Cl_2.

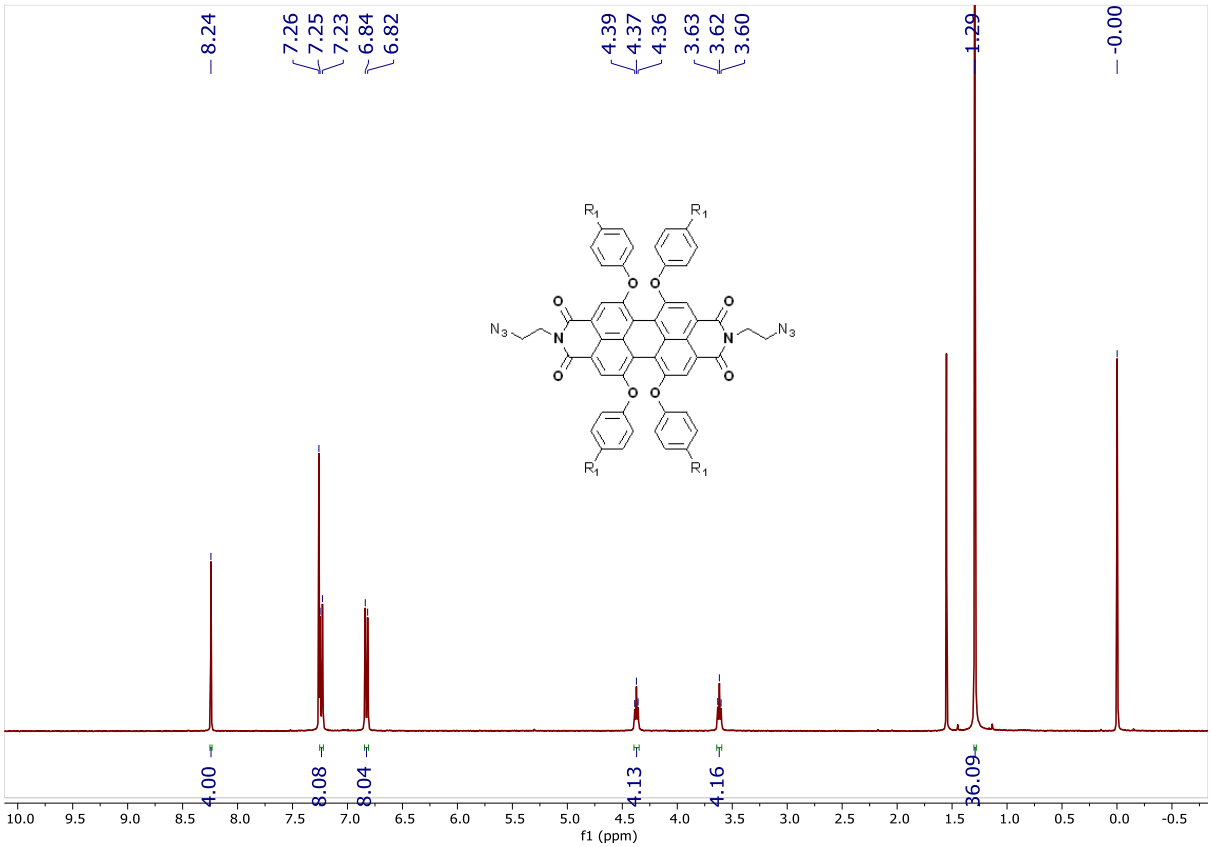

^{1}H NMR of compound **5** in $CDCl_3$.

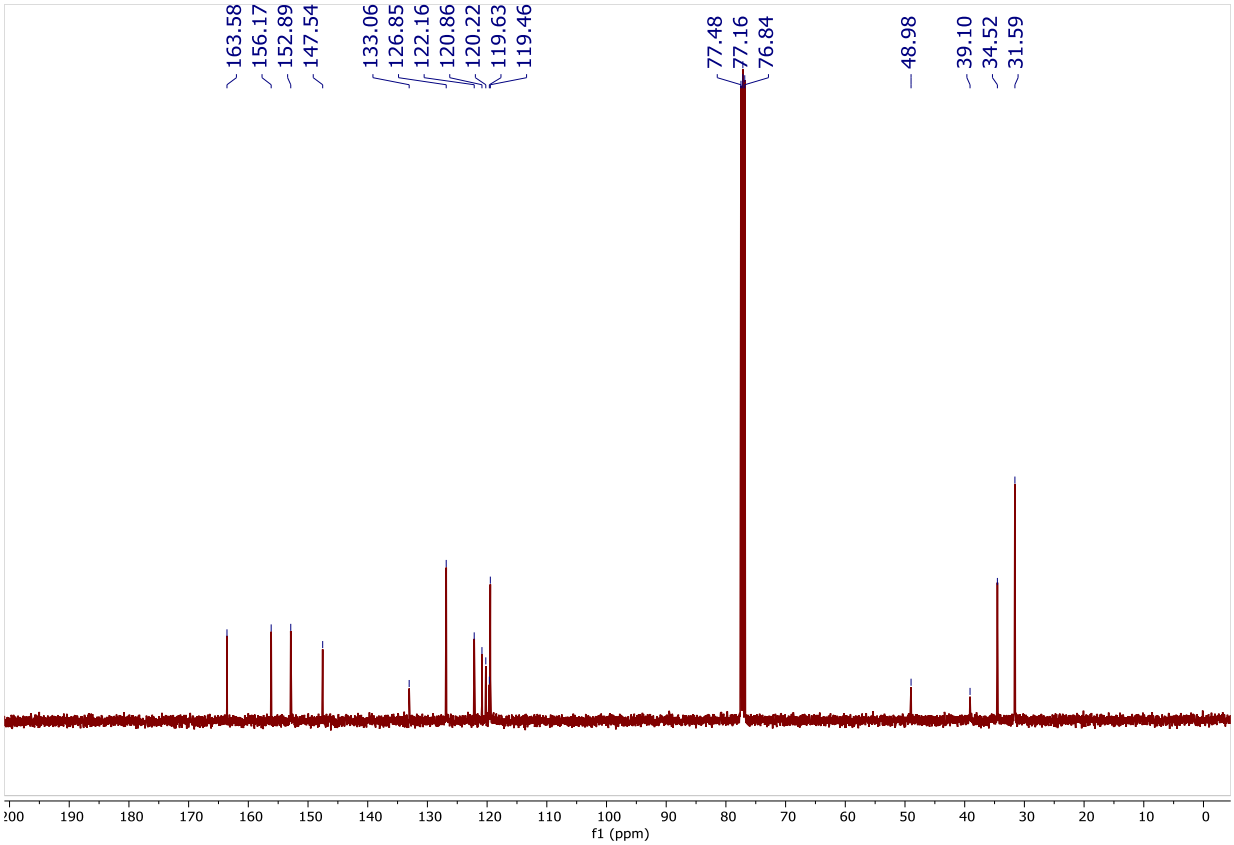

^{13}C NMR of compound **5** in $CDCl_3$.

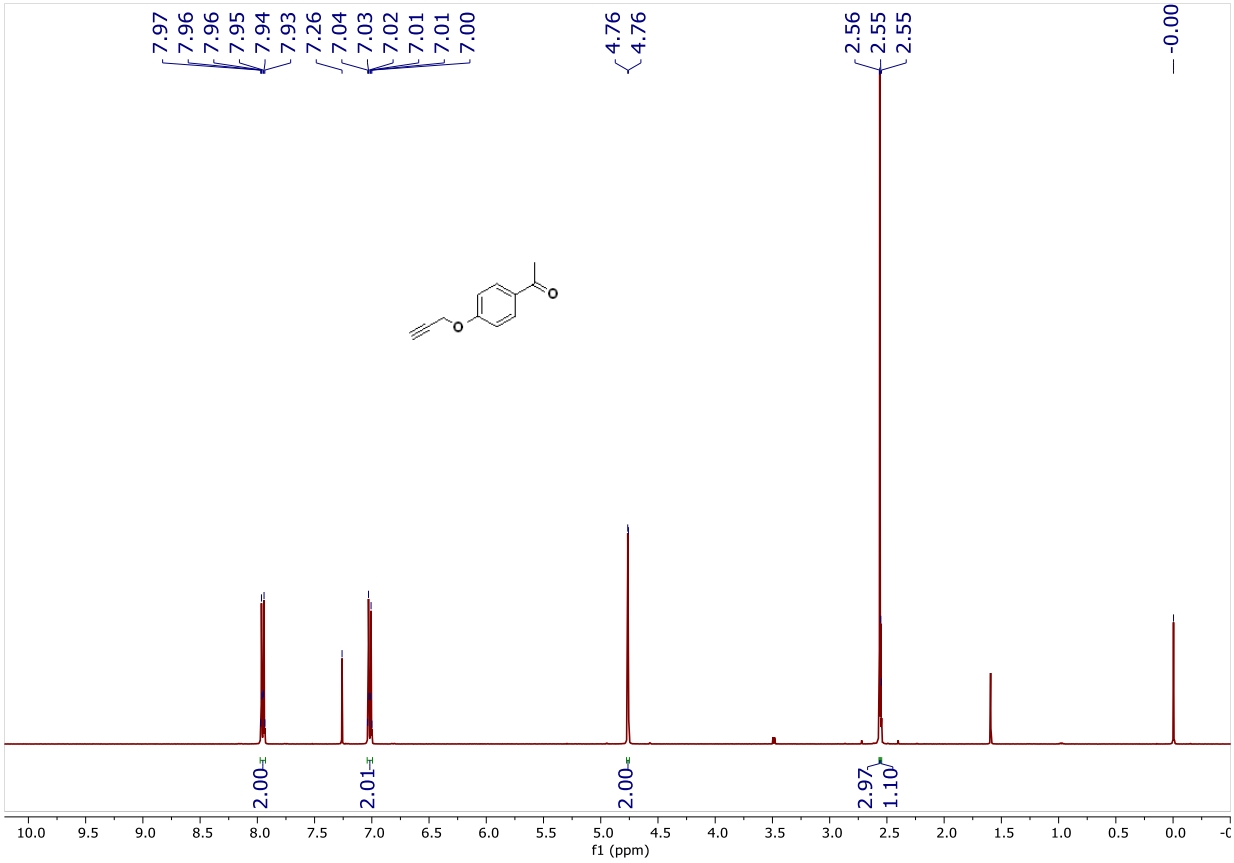

^{1}H NMR spectra of compound **6** in $CDCl_3$.

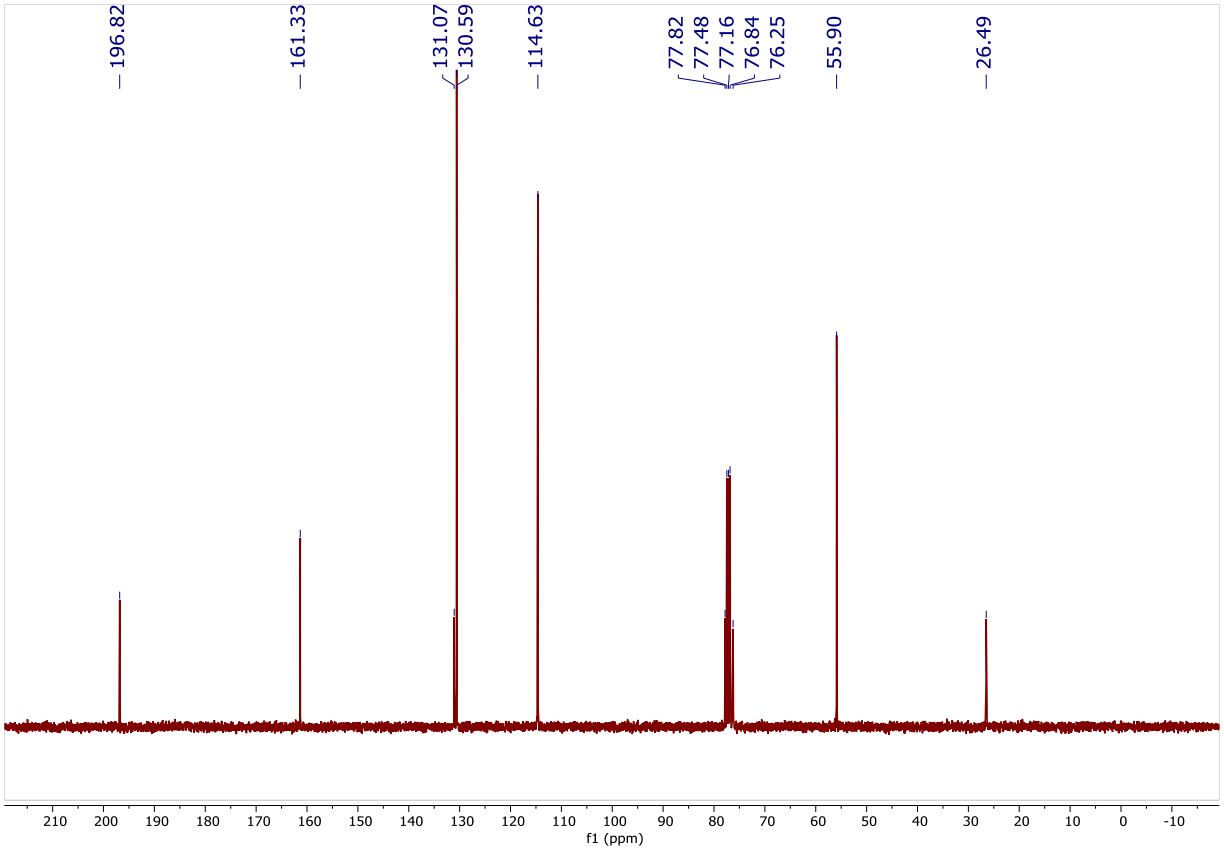

^{13}C NMR spectra of compound **6** in $CDCl_3$.

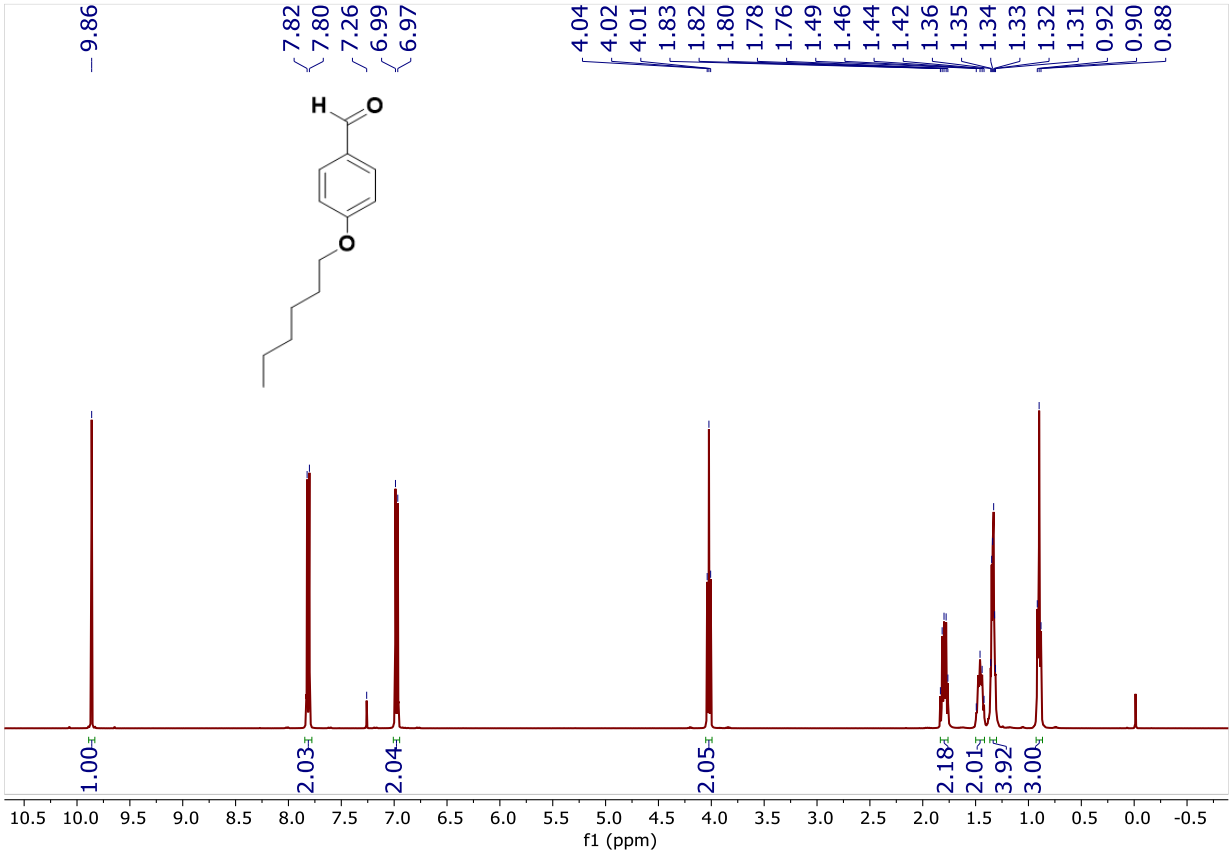

^{1}H NMR spectra of compound **7** in $CDCl_3$.

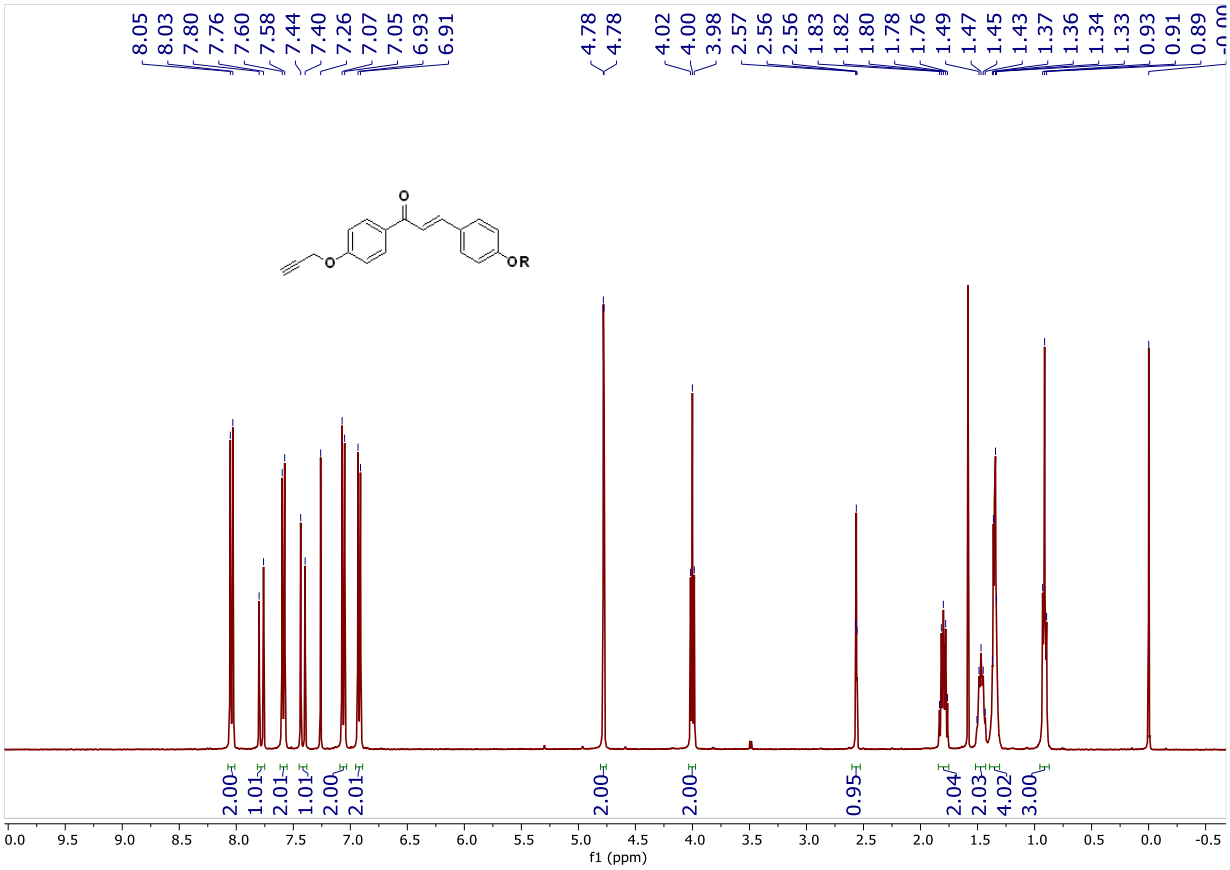

^{1}H NMR spectra of compound **8** in $CDCl_3$.

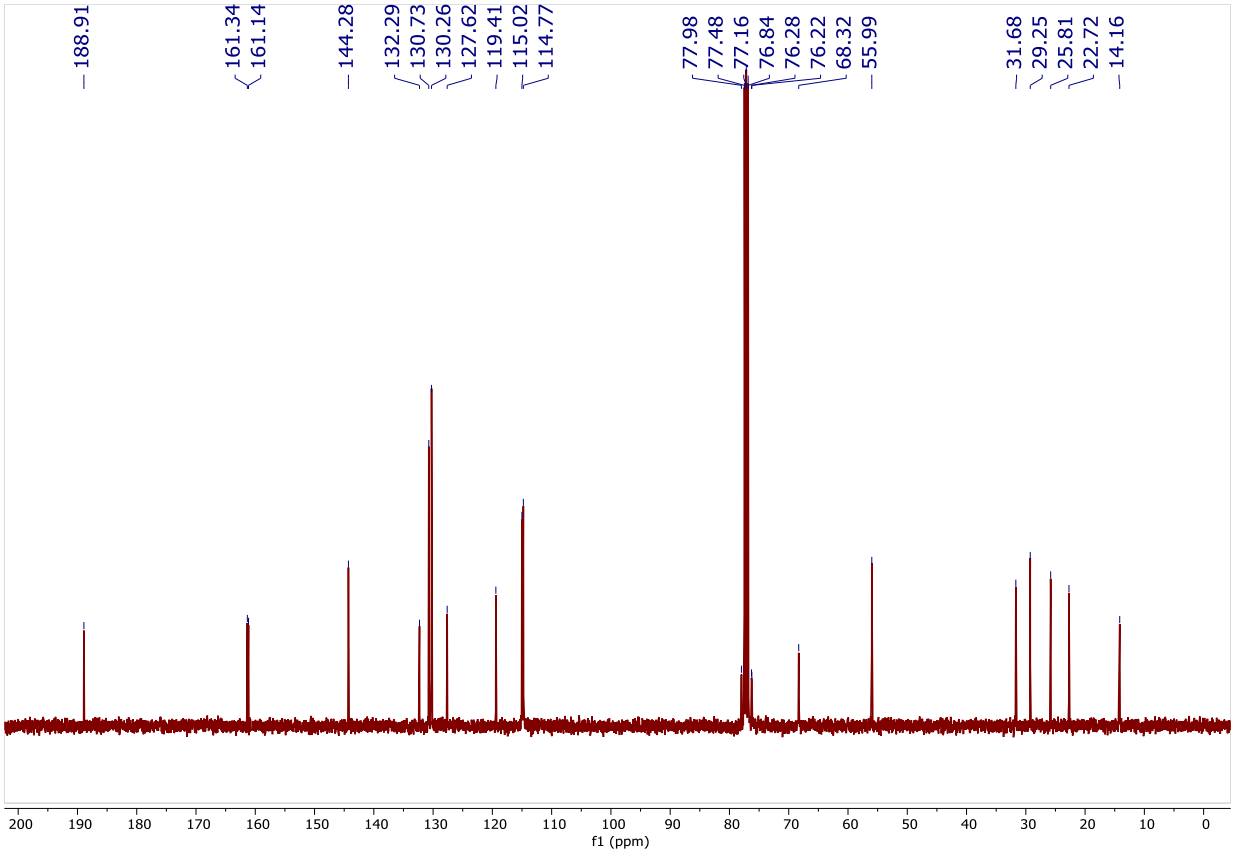

^{13}C NMR spectra of compound **8** in $CDCl_3$.

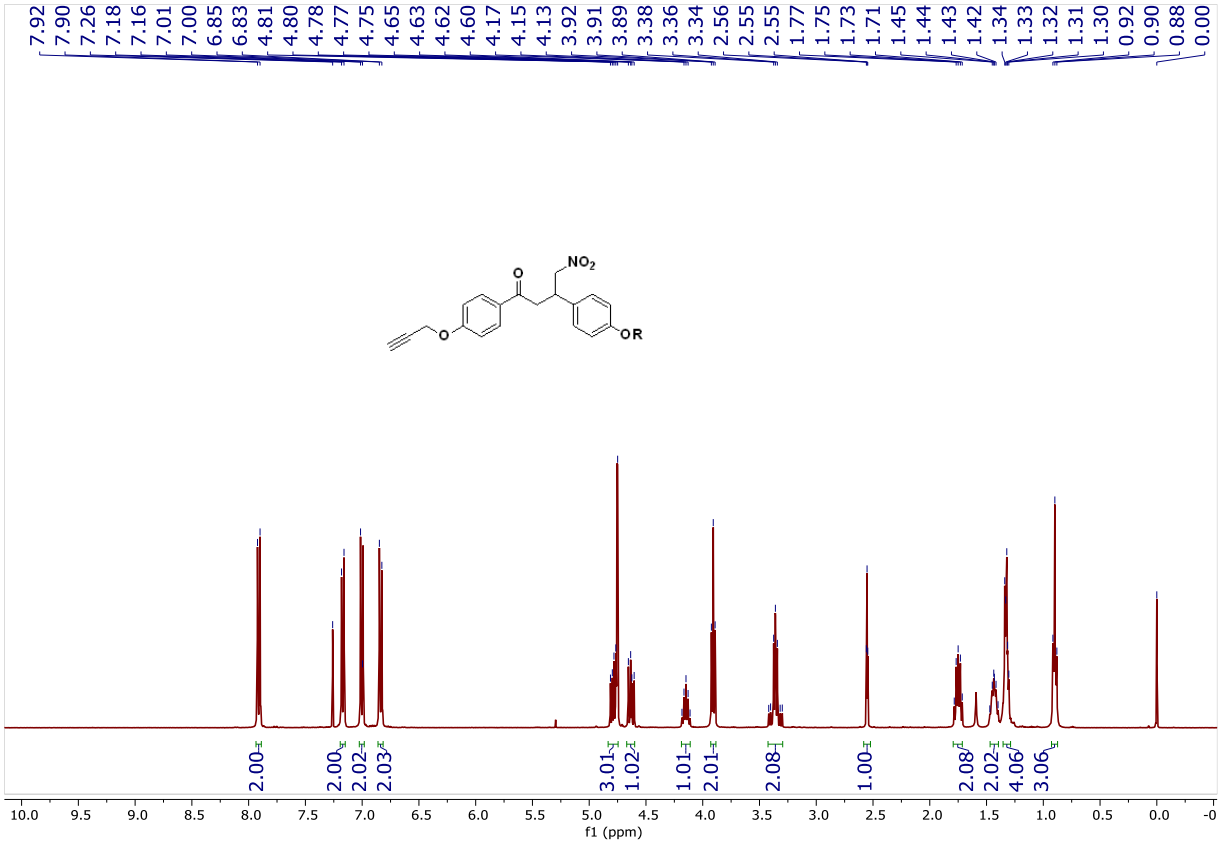

^{1}H NMR spectra of compound **9** in $CDCl_3$.

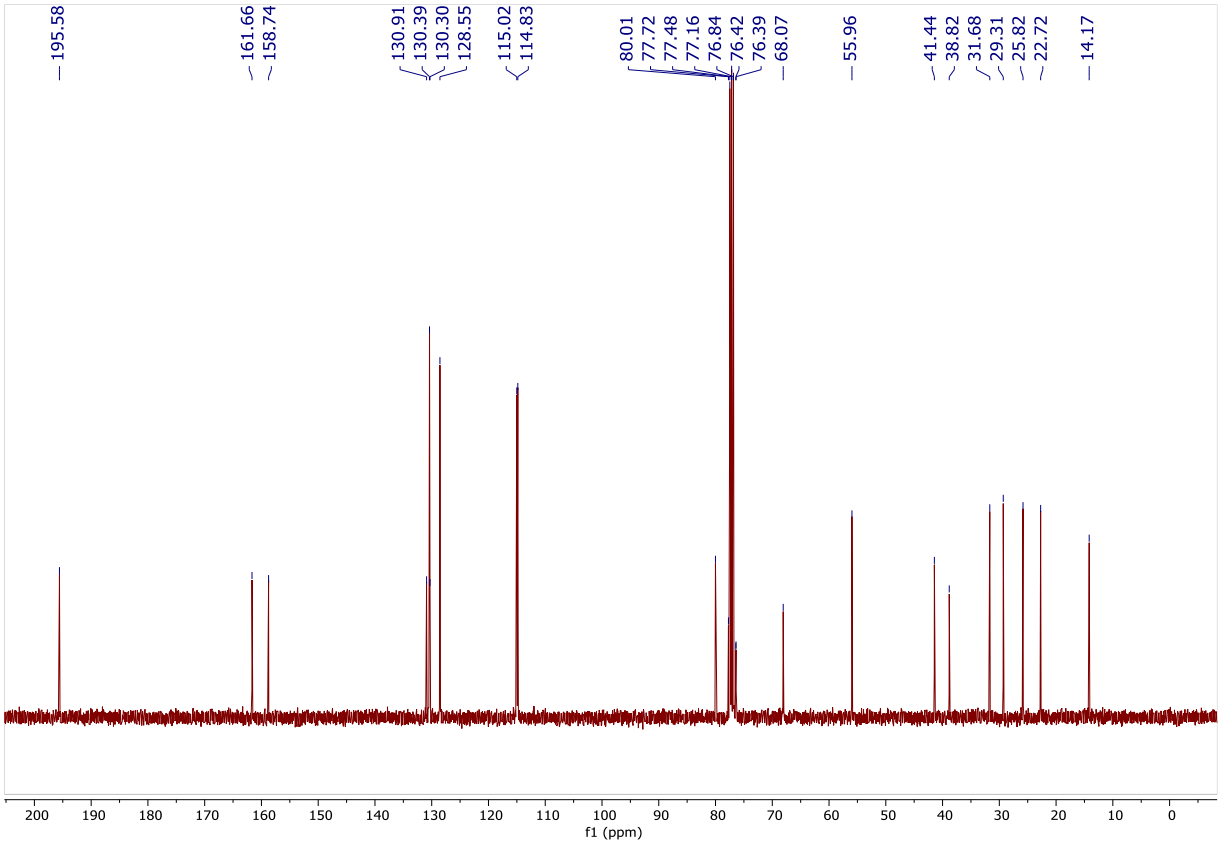

^{13}C NMR spectra of compound **9** in $CDCl_3$.

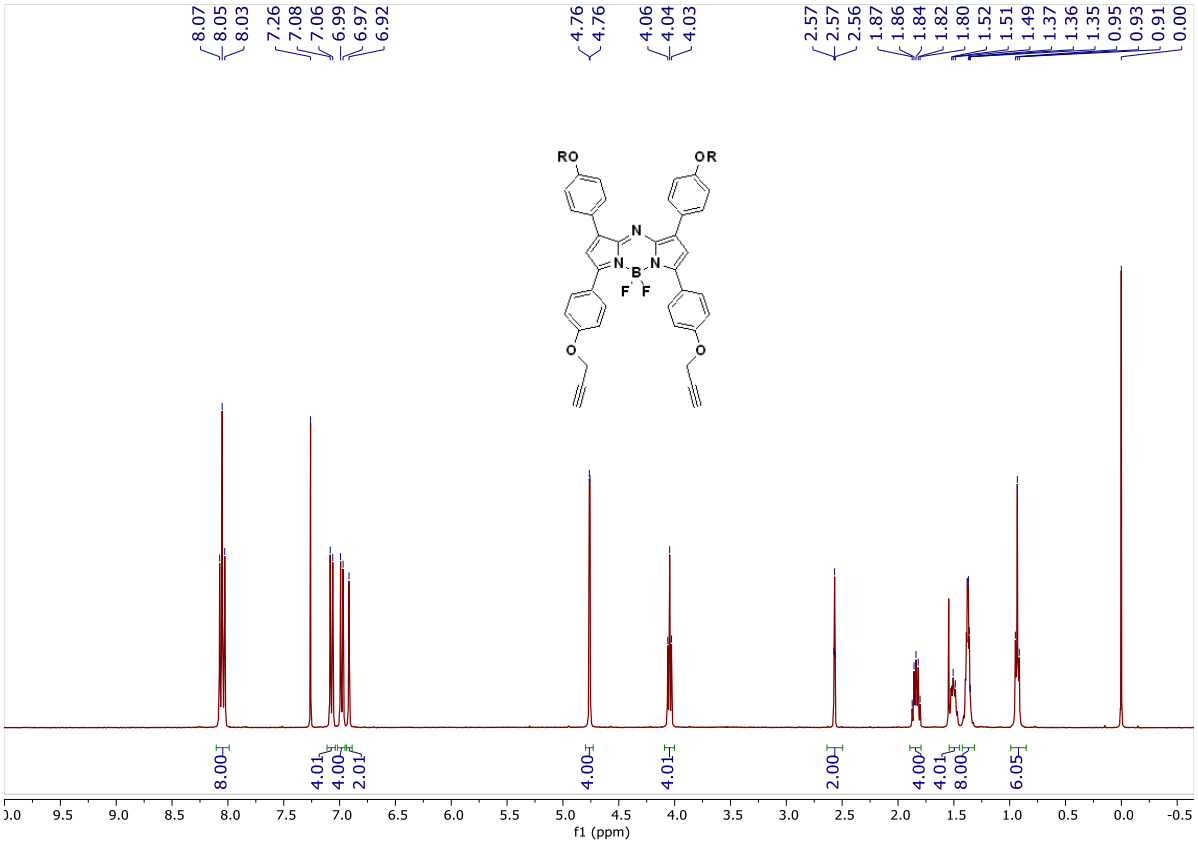

^{1}H NMR of compound **11** in $CDCl_3$.

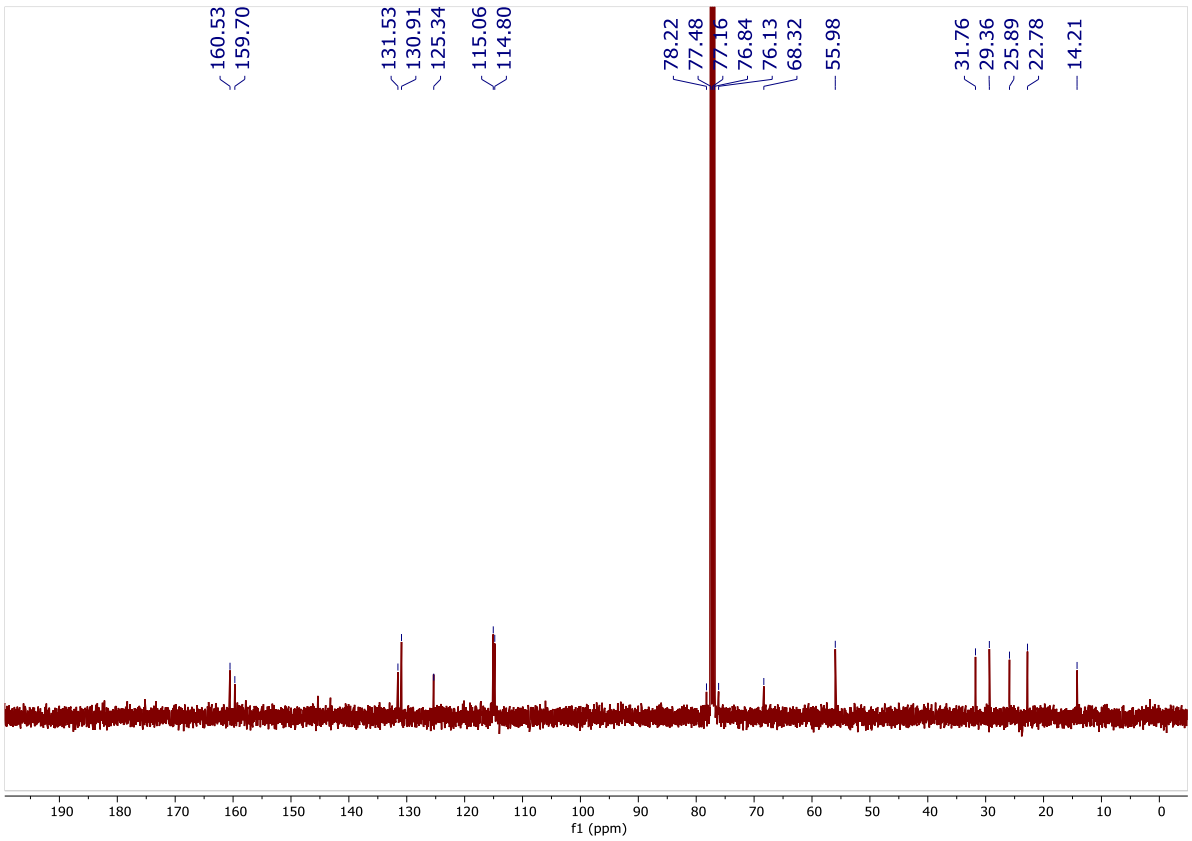

^{13}C NMR of compound **11** in $CDCl_3$.

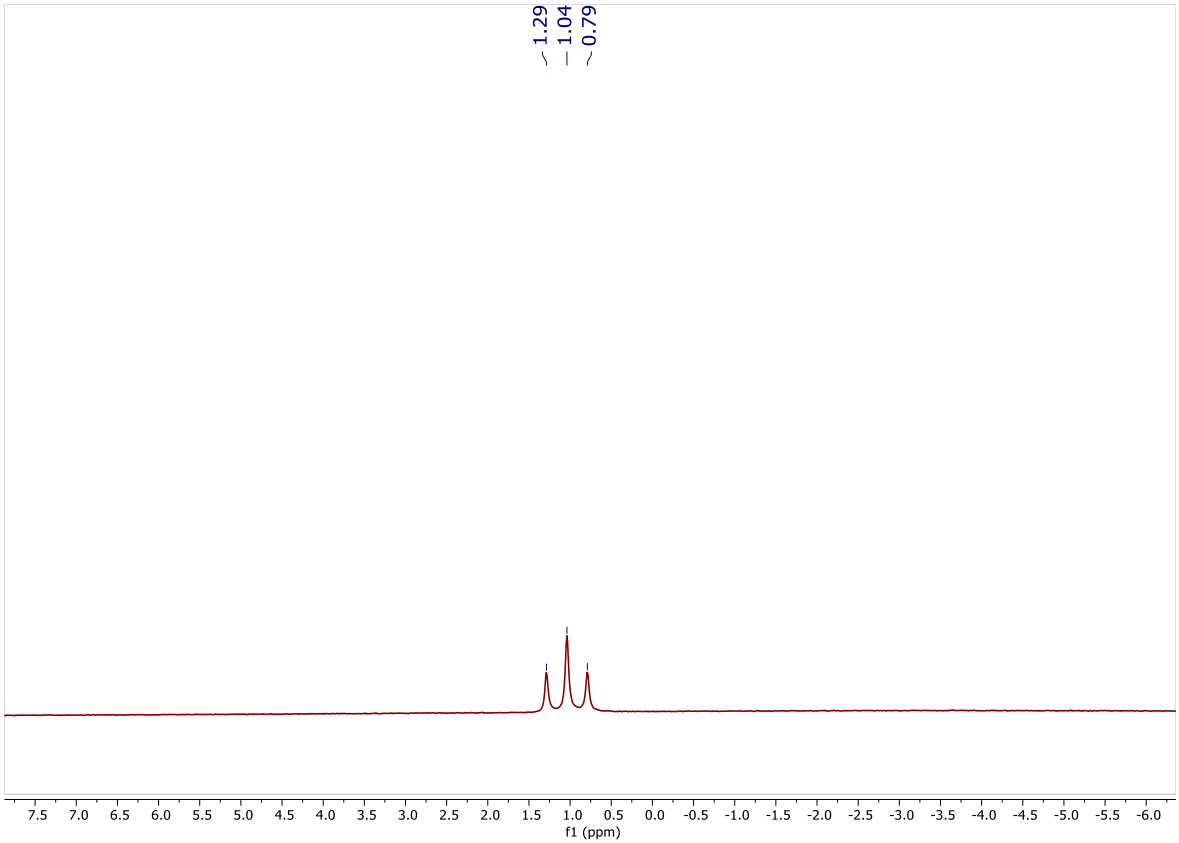

^{11}B NMR of compound **11** in $CDCl_3$.

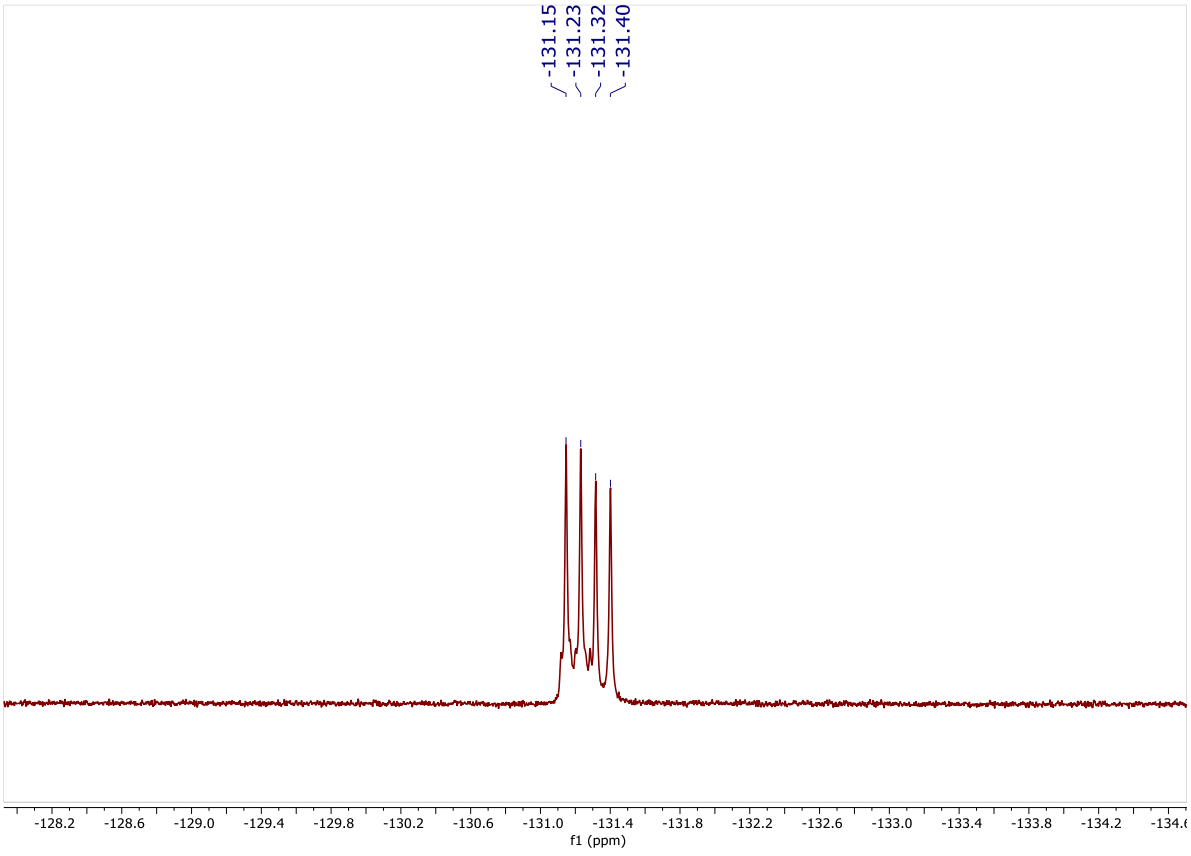

^{19}F NMR of compound **11** in $CDCl_3$.

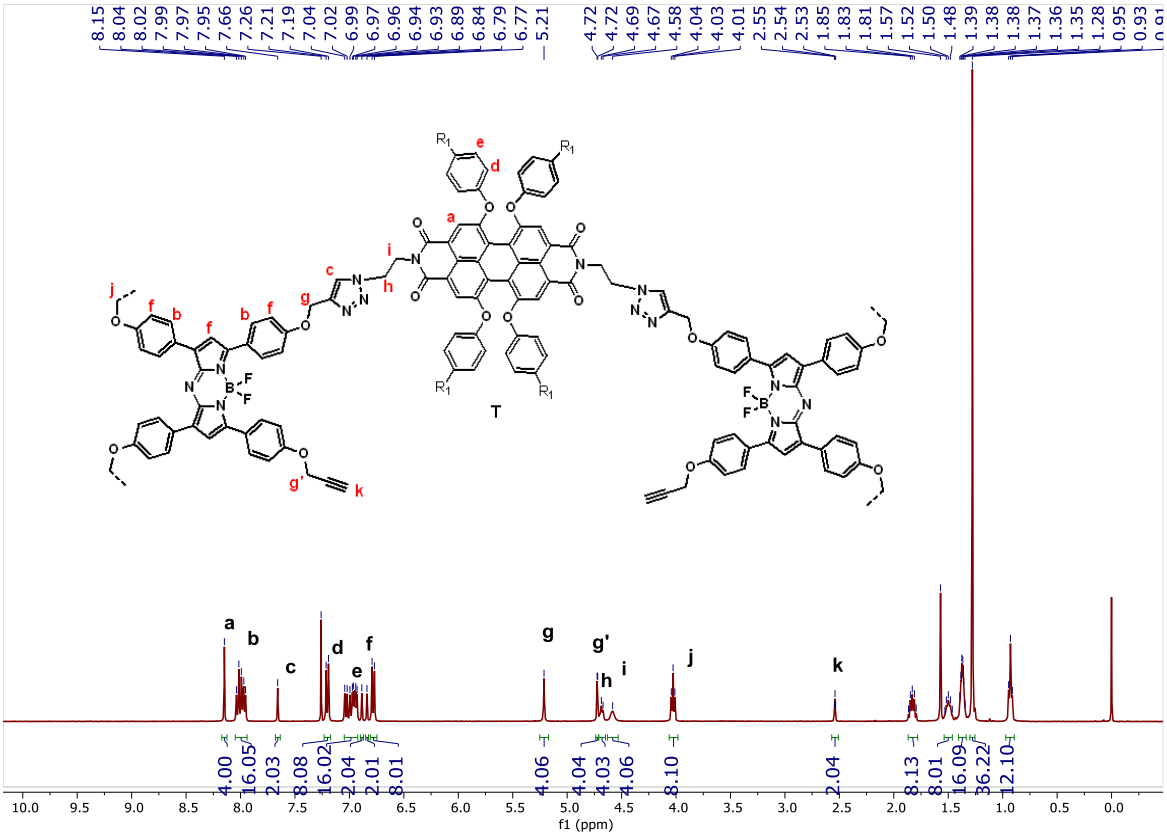

^{1}H NMR spectra of triad **T** in $CDCl_3$.

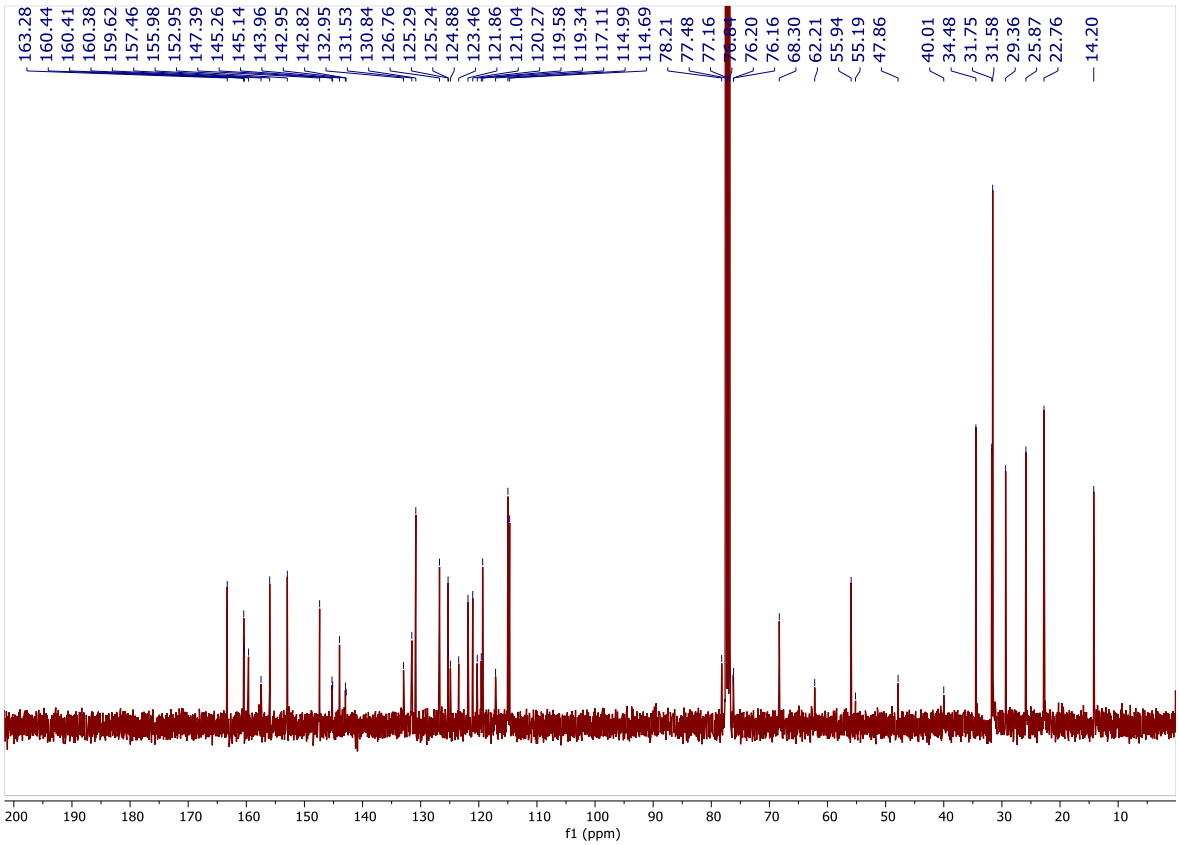

^{13}C NMR spectra of triad **T** in $CDCl_3$.

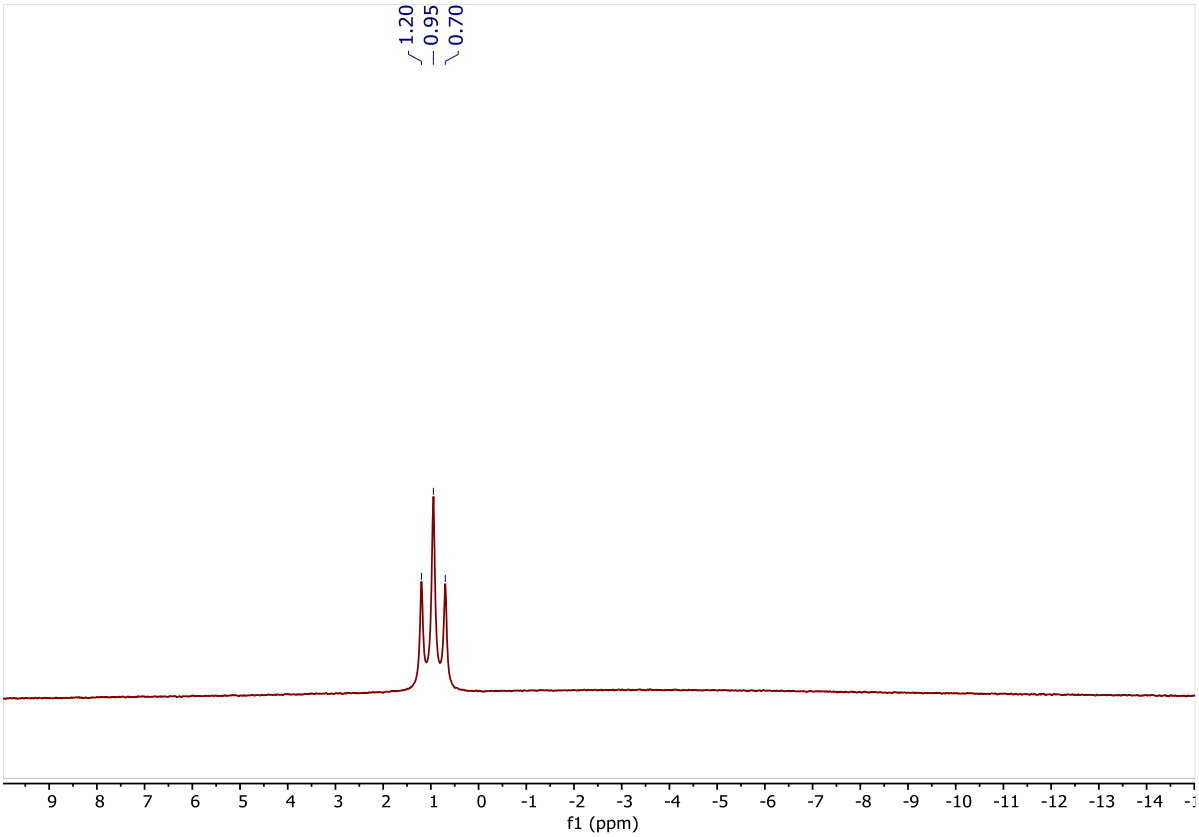

^{11}B NMR spectra of triad **T** in $CDCl_3$.

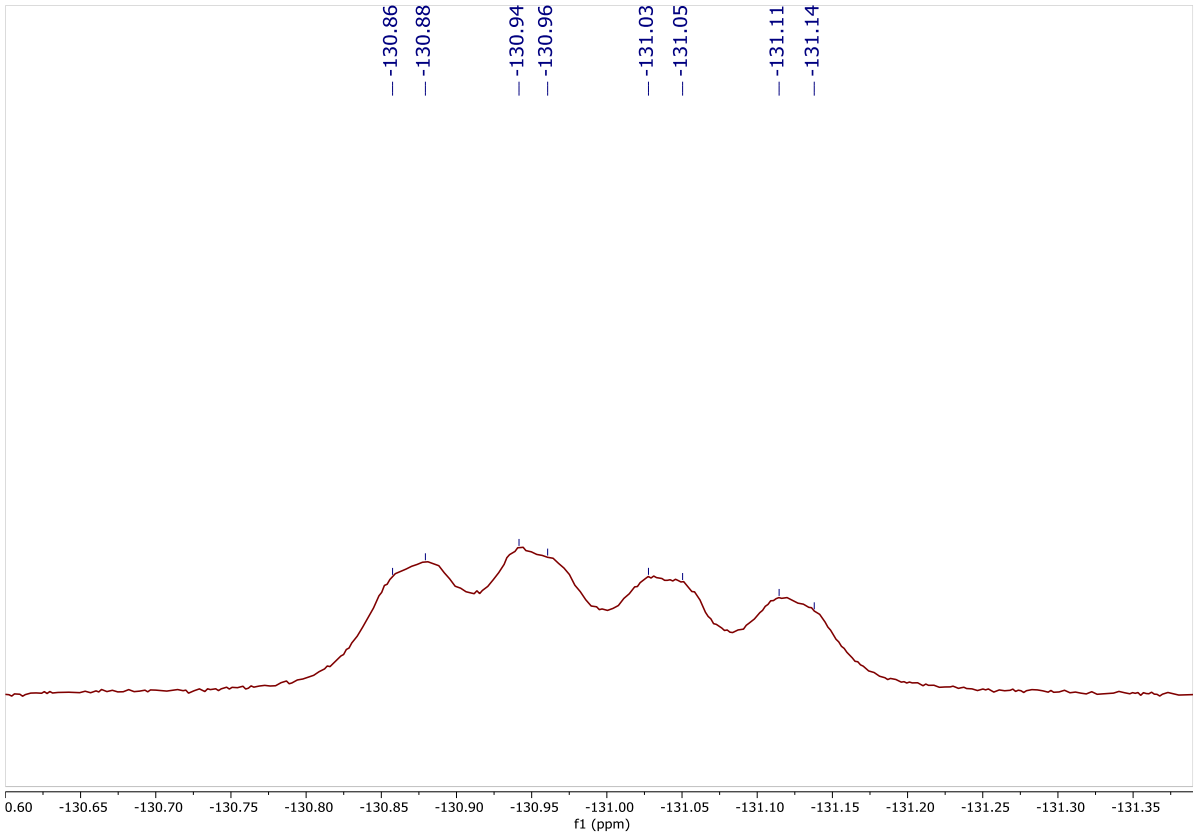

^{19}F NMR spectra of triad **T** in $CDCl_3$.

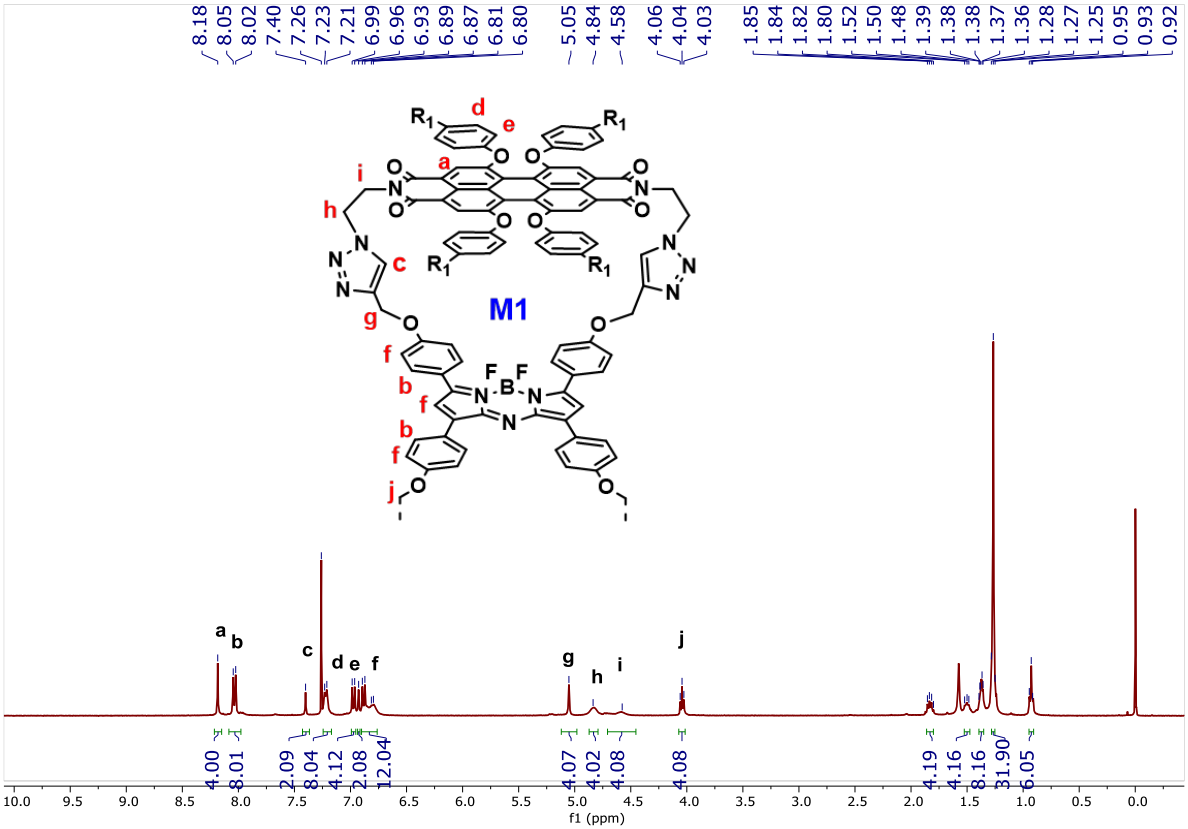

^{1}H NMR spectra of macrocycle **M1** in $CDCl_3$.

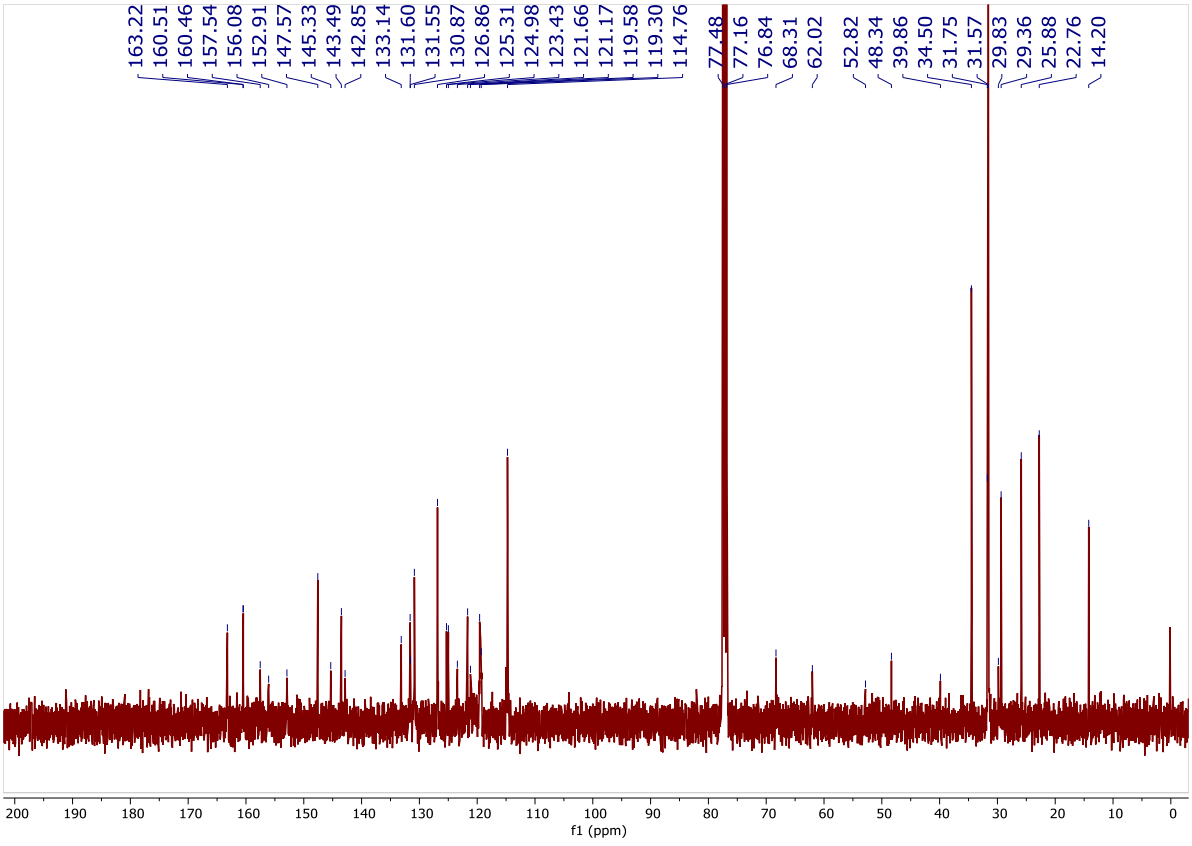

^{13}C NMR spectra of macrocycle **M1** in $CDCl_3$.

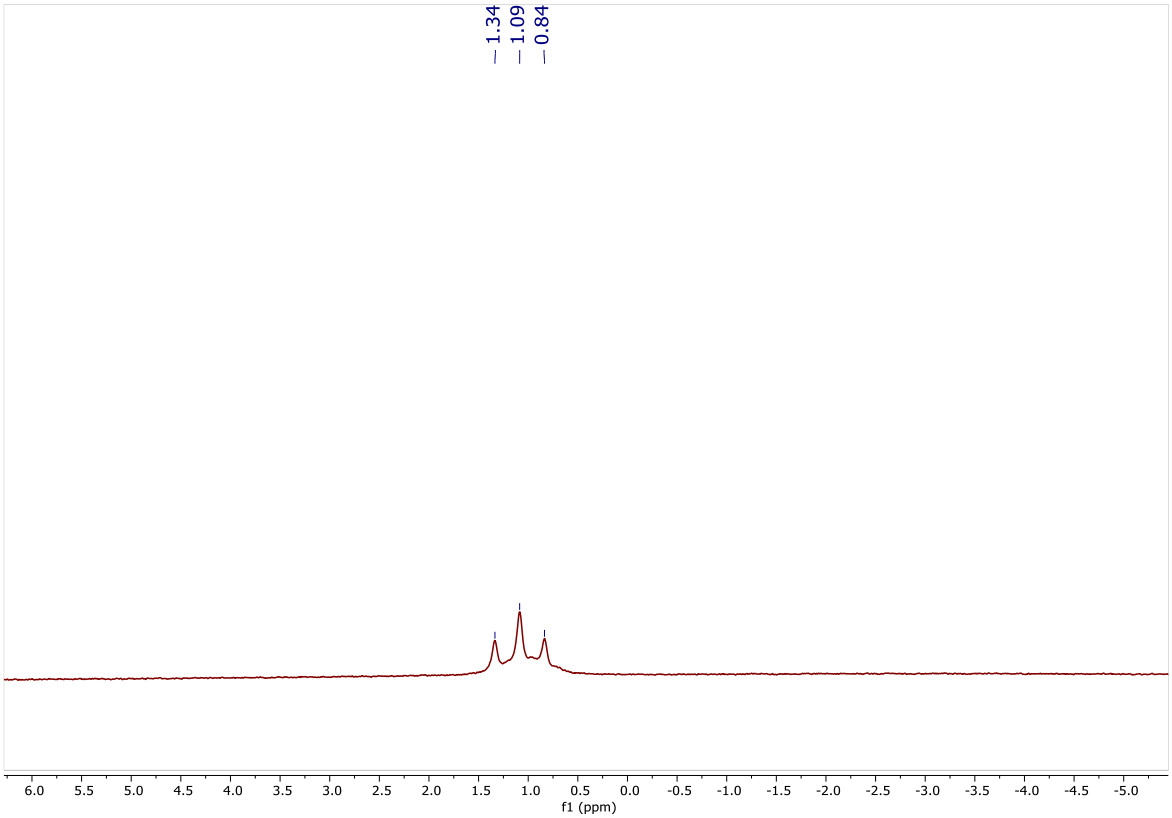

^{11}B NMR spectra of macrocycle **M1** in $CDCl_3$.

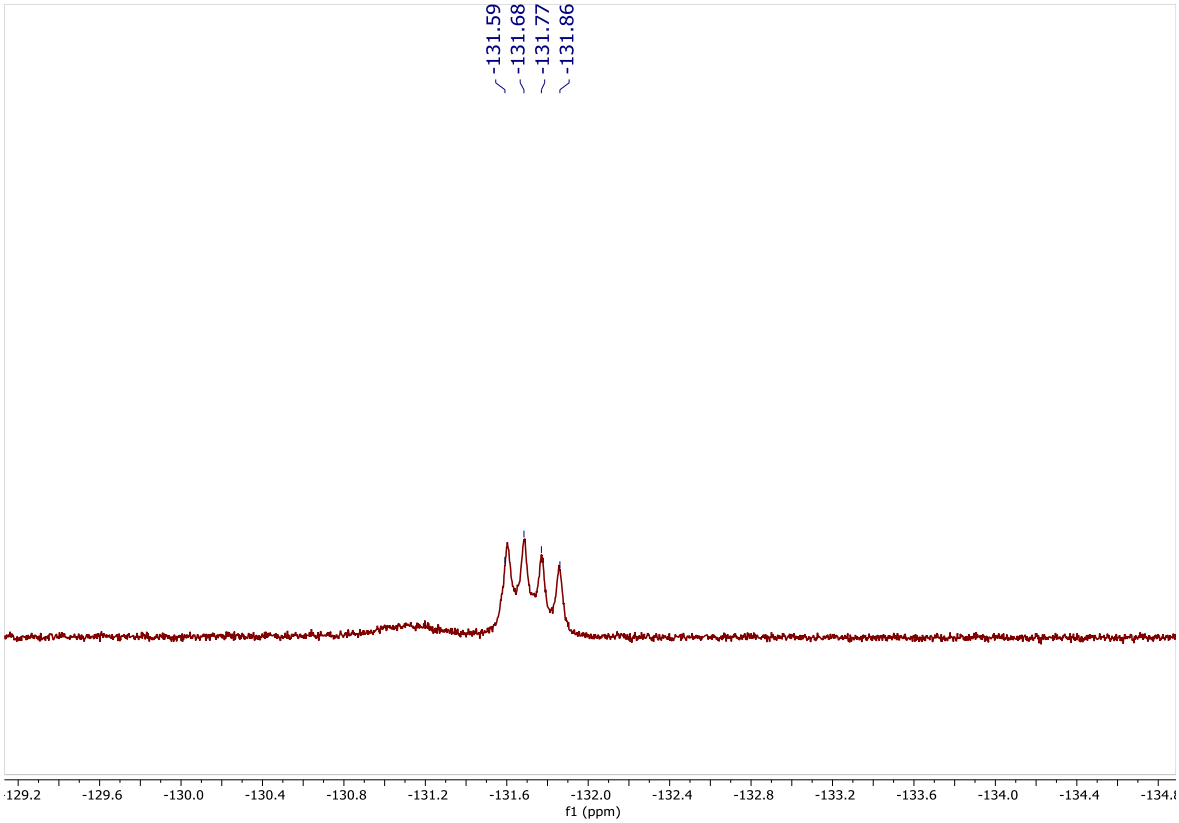

^{19}F NMR spectra of compound **M1** in $CDCl_3$.

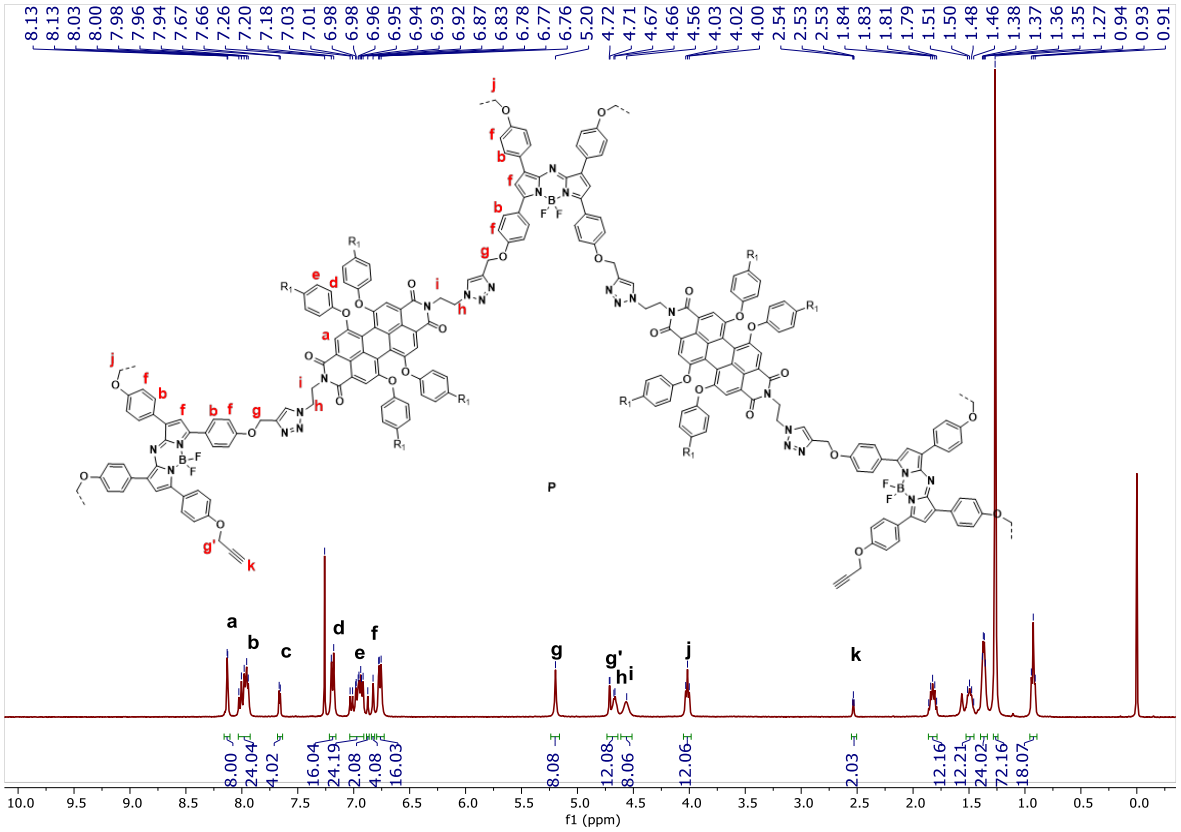

^{1}H NMR spectra of pentad **P** in $CDCl_3$.

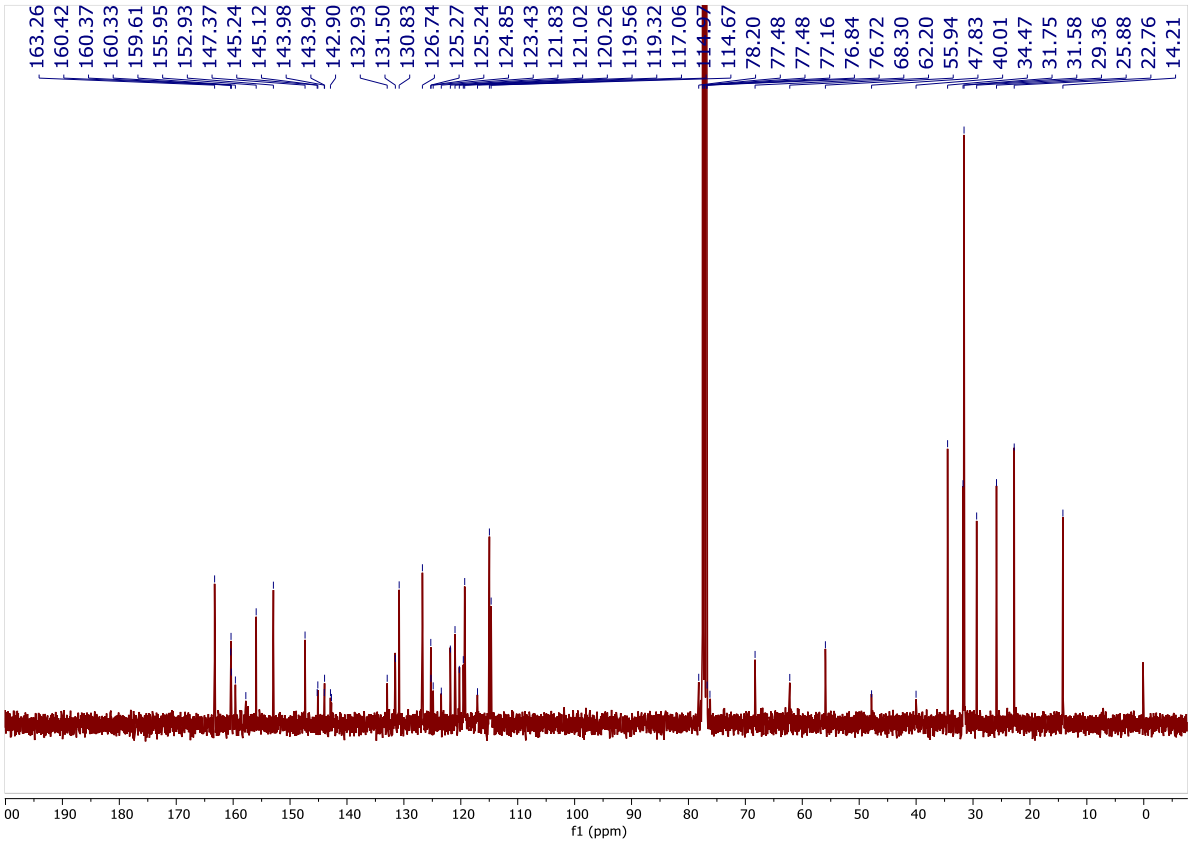

^{13}C NMR spectra of pentad **P** in $CDCl_3$.

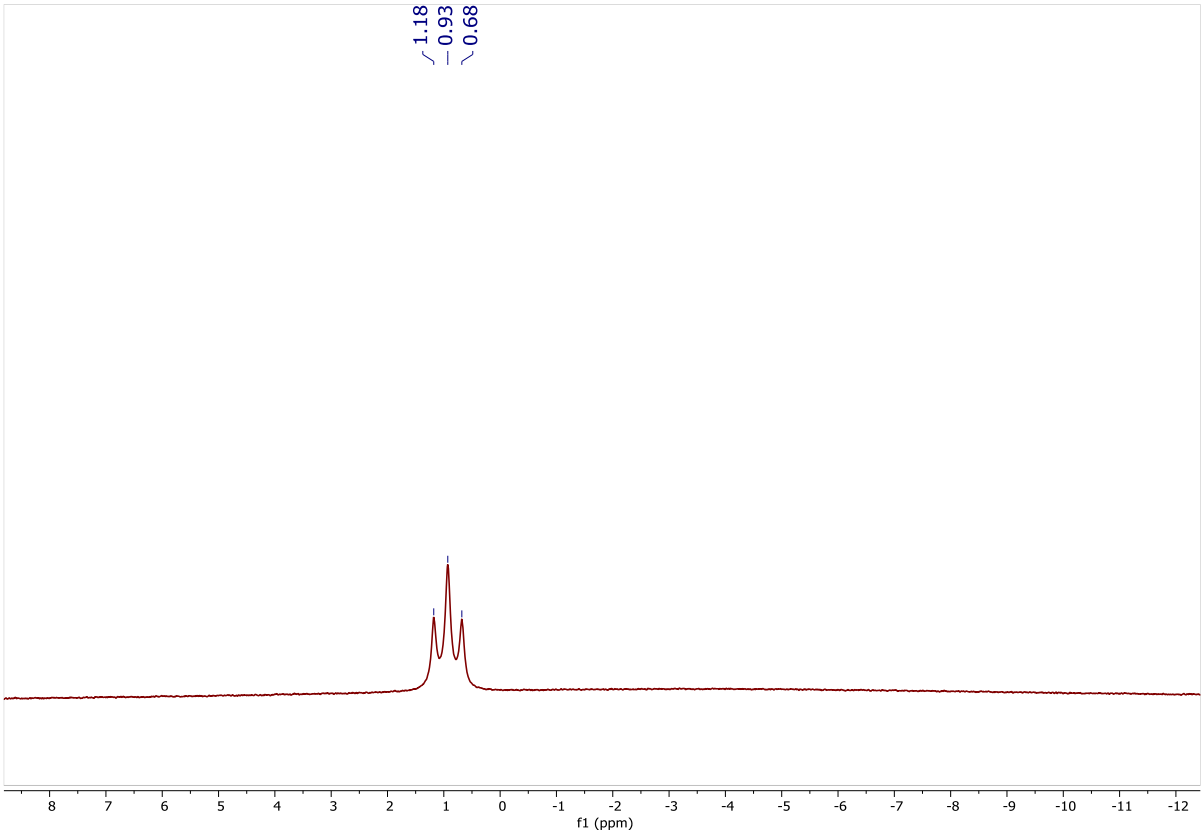

^{11}B NMR spectra of pentad **P** in $CDCl_3$.

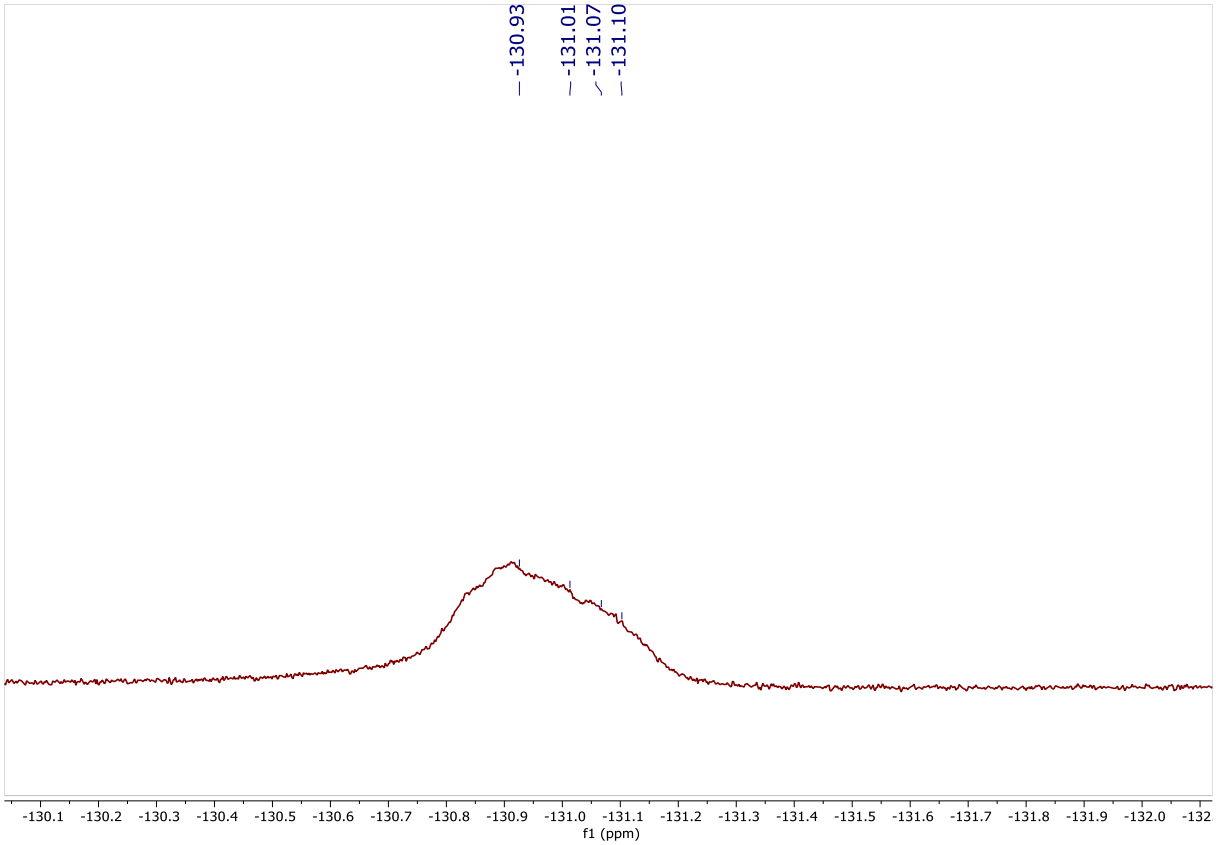

^{19}F NMR spectra of pentad **P** in $CDCl_3$.

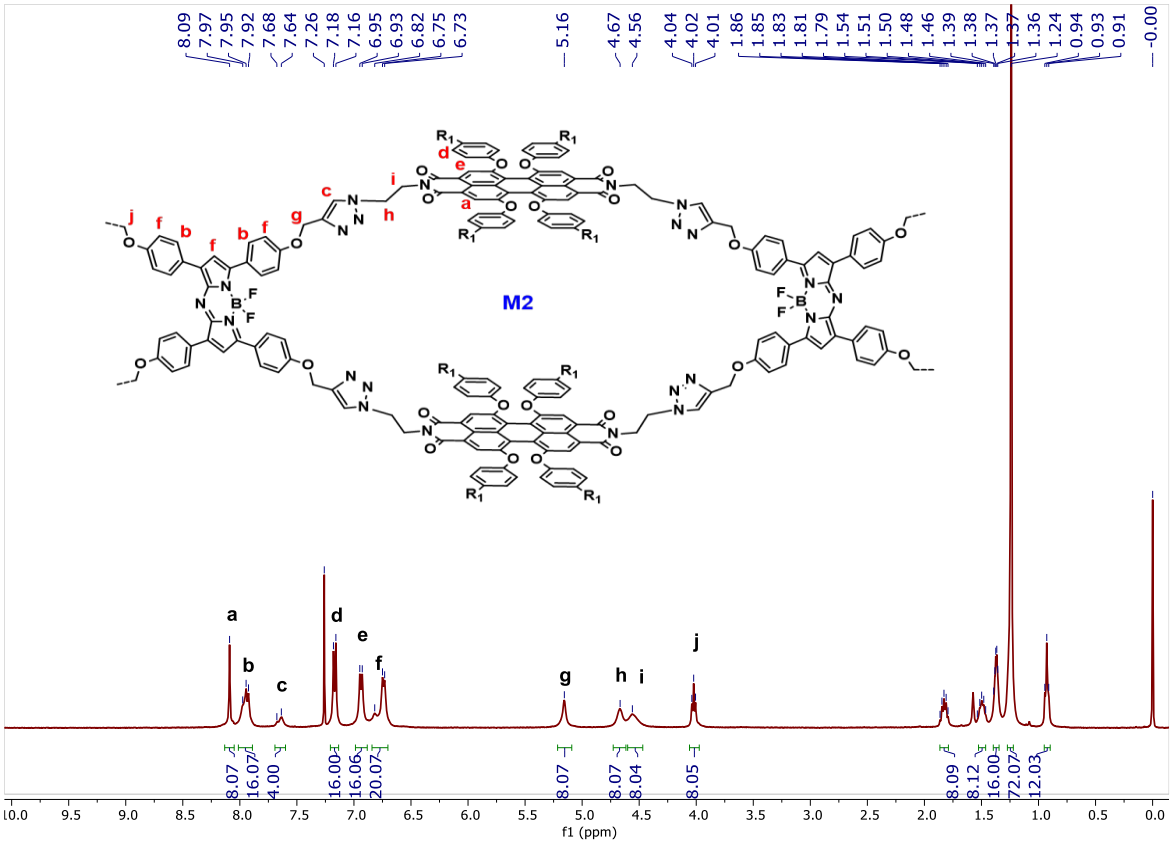

^{1}H NMR spectra of macrocycle **M2** in $CDCl_3$.

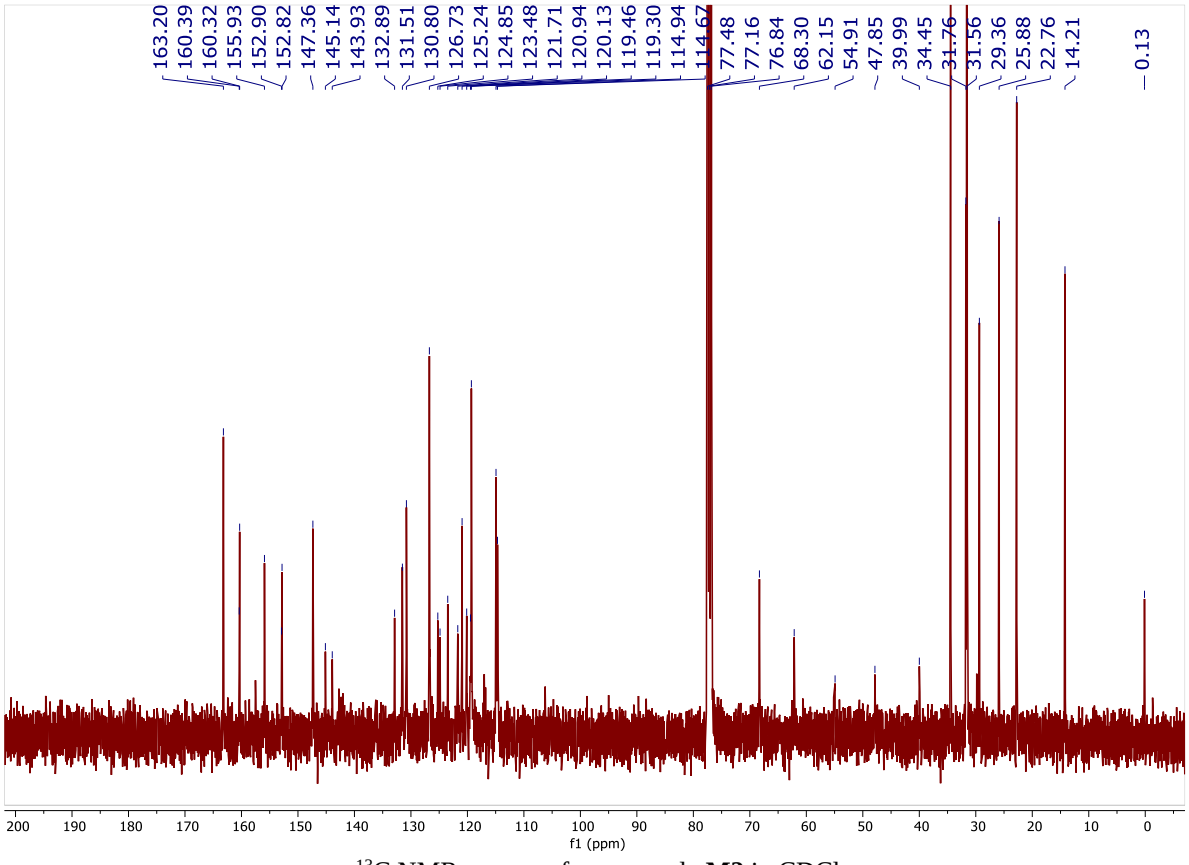

^{13}C NMR spectra of macrocycle **M2** in $CDCl_3$.

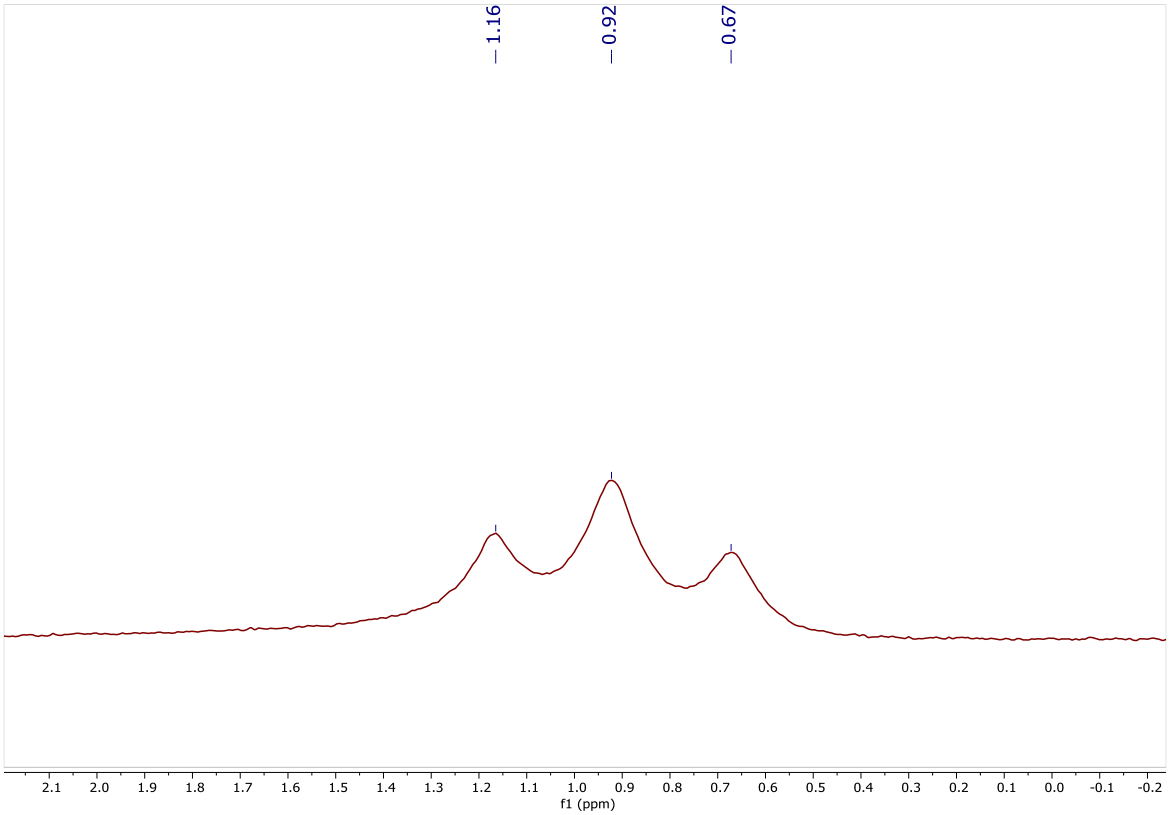

^{11}B NMR spectra of macrocycle **M2** in $CDCl_3$.

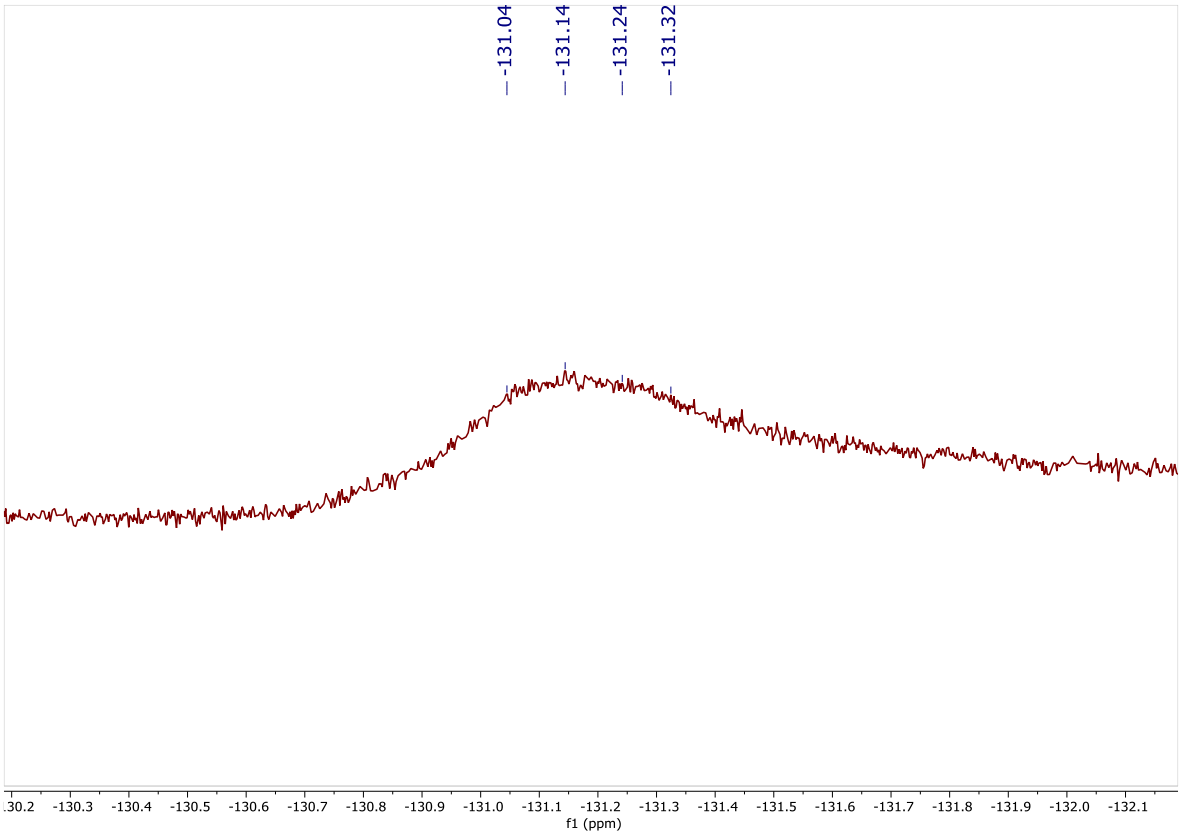

^{19}F NMR spectra of macrocycle **M2** in $CDCl_3$.

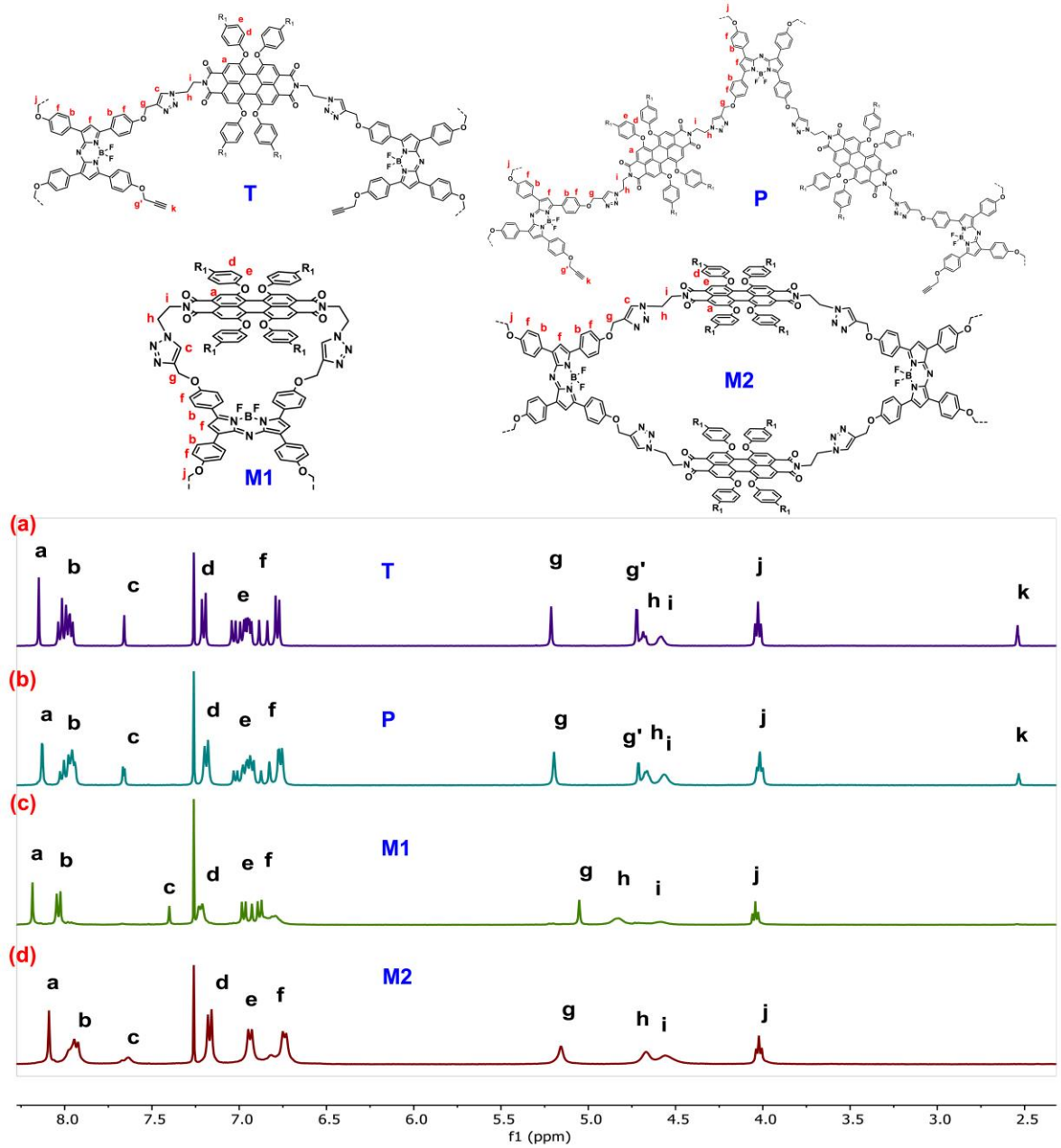

Figure S1. Comparison of ^{1}H NMR of (a) **T**, (b) **P**, (c) **M1**, and (d) **M2** in $CDCl_3$ (400 MHz).

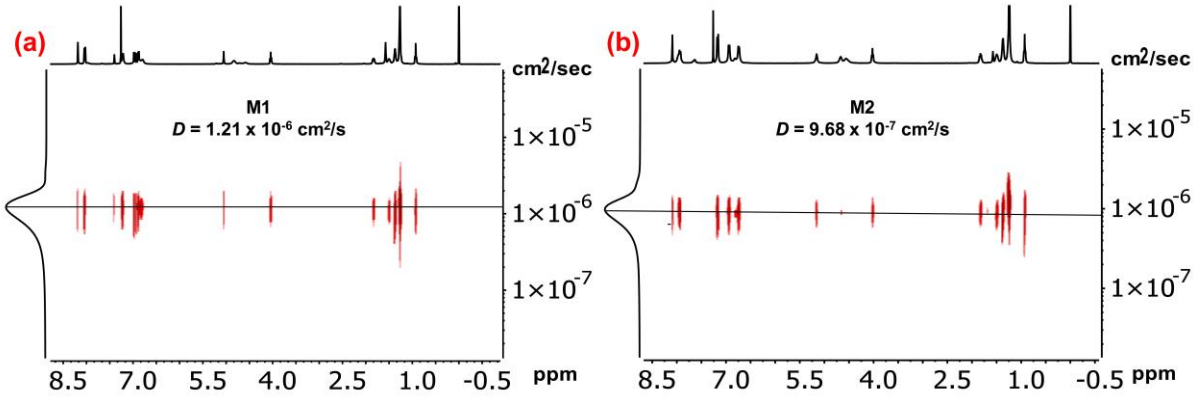

Figure S2. DOSY NMR spectra of (a) **M1** and (b) **M2** in $CDCl_3$ (400 MHz).

4. Mass spectra

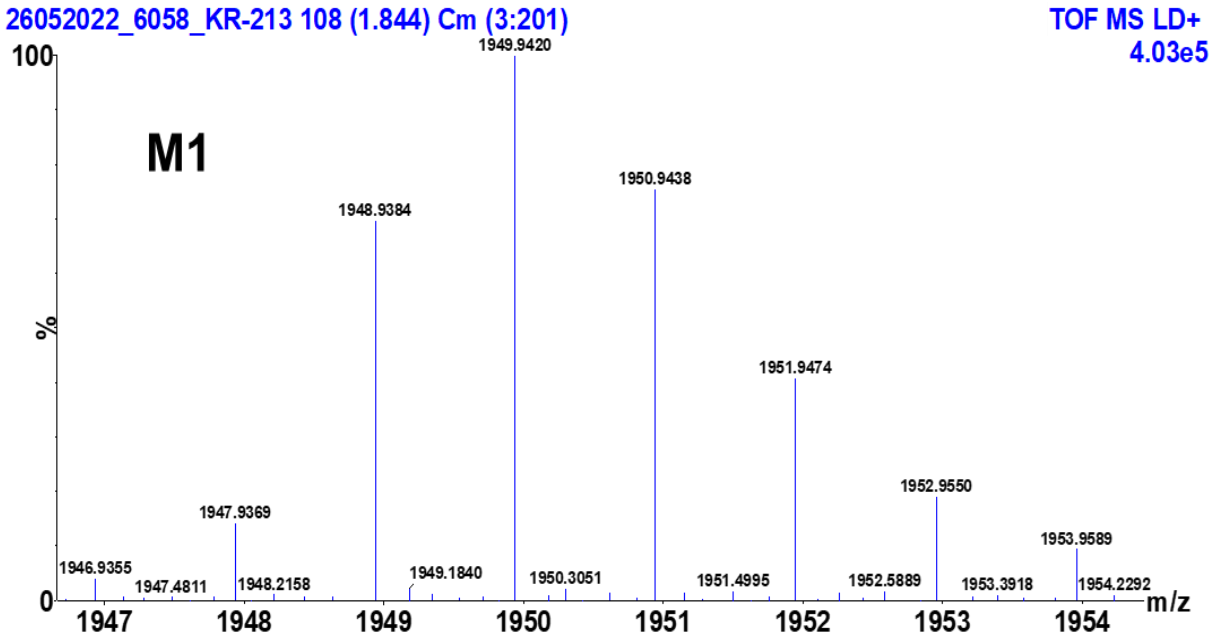

Figure S3. MALDI-TOF mass spectra of **M1**.

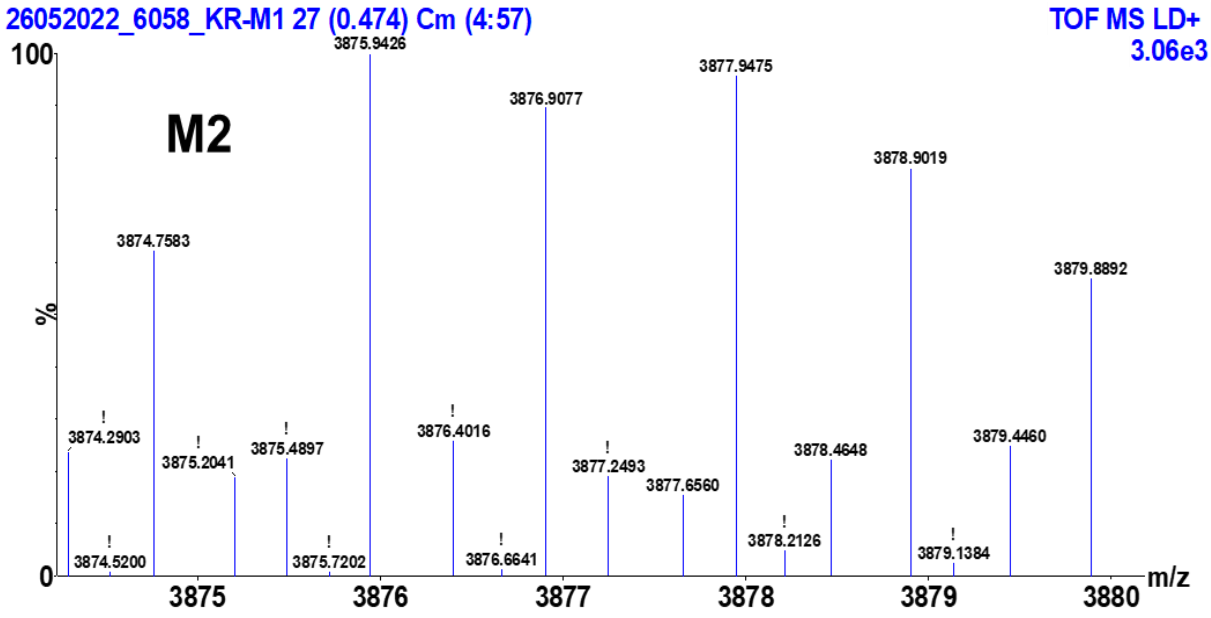

Figure S4. MALDI-TOF mass spectra of **M2**.

5. Photophysical studies

Steady-state emission

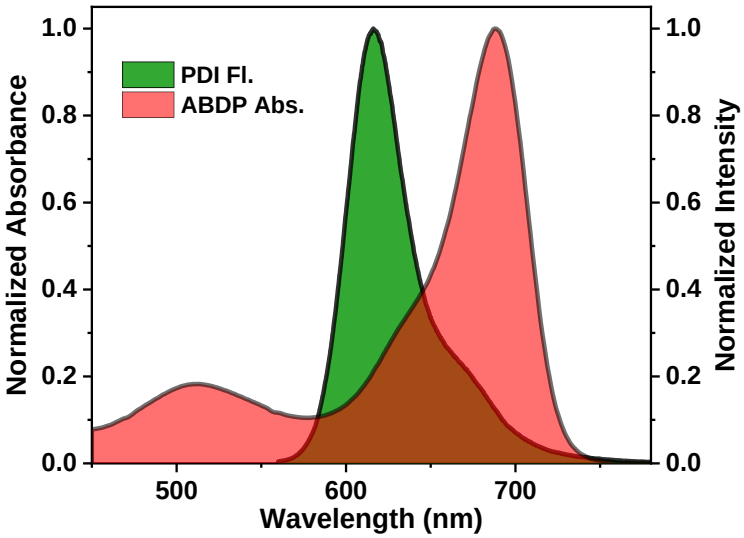

Figure S5. Spectral overlap of PDI emission and ABDP absorption spectra in chloroform ($c \sim 10^{-6}$ M).

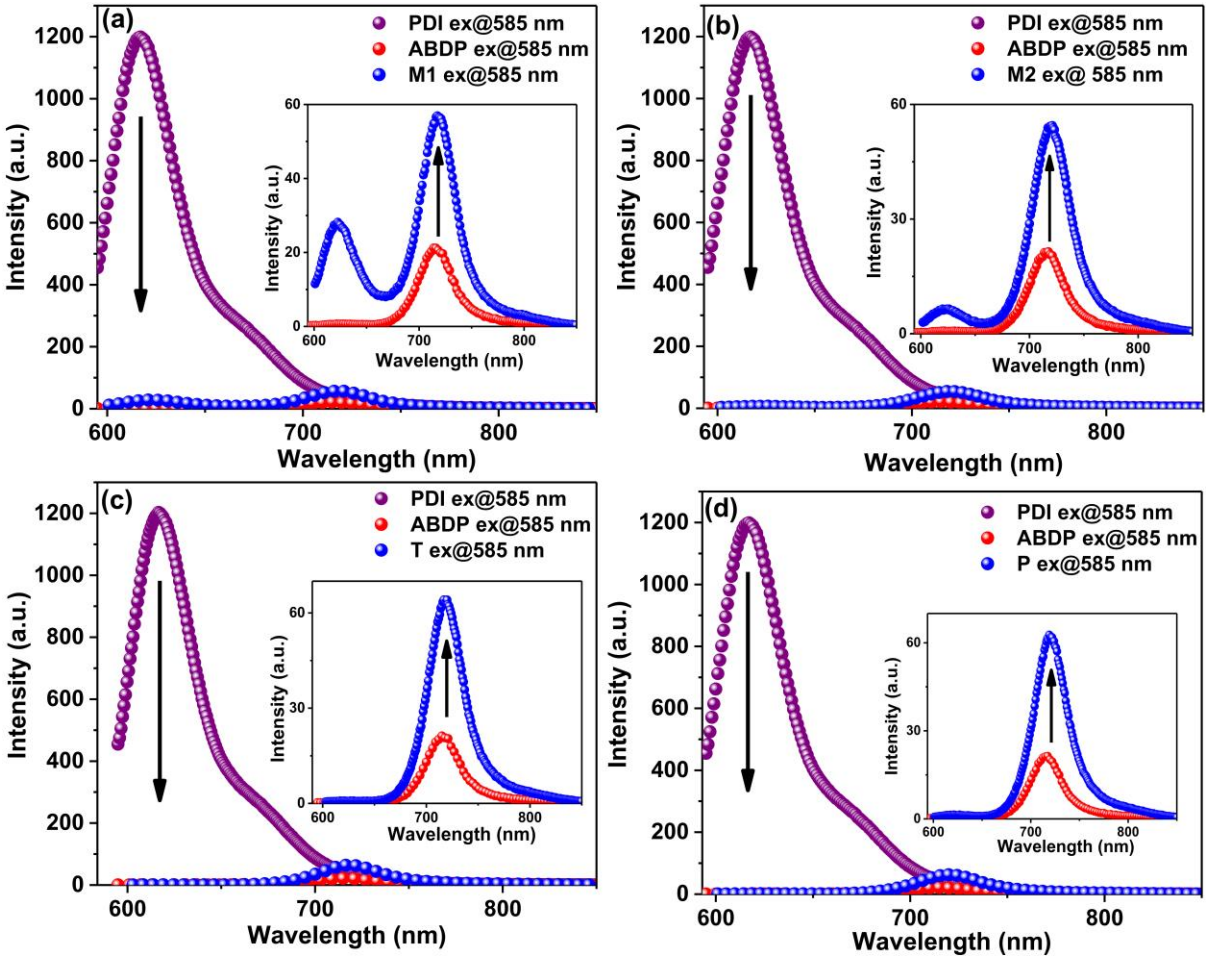

Figure S6. Steady-state emission spectra of (a) **M1**, (b) **M2**, (c) Triad **T**, and (d) Pentad **P** along with reference compound PDI and ABDP in chloroform ($c \sim 2 \times 10^{-6}$ M).

Table S1. Photophysical properties of reference as well as final compounds in $CHCl_3$.

Compound	λ_{abs}(nm)	ε (M^{-1} cm^{-1})	λ_{em} (nm)
PDI	585	50,791	617
ABDP	688	87,705	716
M1	591	58,072	623, 719 (λ_{ex} = 591 nm)
	694	80,366	
M2	592	1,04,410	621, 721 (λ_{ex} = 592 nm)
	694	1,51,260	
T	592	60,425	720 (λ_{ex} = 592 nm)
	691	1,63,220	
P	591	1,06,014	719 (λ_{ex} = 591 nm)
	692	2,29,570	

Fluorescence quantum yield

Table S2. The fluorescence quantum yields of PDI, Triad **T**, Pentad **P**, **M1** and **M2** by using relative method in $CHCl_3$.

Comp.	λ_{ex} (nm)	λ_{em} (nm)	Φ	ETE = 1- Φ_D/Φ_{DA}
PDI	585	616	~ 0.88	-
ABDP	688	716	~0.36	-
M1	591	623	~0.052	~ 94 %
	591	719	~0.22	-
	693	719	~0.23	-
M2	592	620	~0.009	~ 99 %
	592	721	~0.15	-
	694	721	~0.18	-
T	592	616	~ 0.005	~ 99 %
	592	720	~0.15	-
	691	720	~0.29	
P	591	616	~ 0.0034	~ 100 %
	591	720	~0.13	-
	692	720	~0.21	
[a]**Lumogen® F Red 305**	577	613	0.96 (reported in $CHCl_3$)[3]	-
[b]**ABDP Ref**	680	712	0.483 (reported in DCM)[2]	-

a. Reference dye for PDI part fluorescence quantum yield.[3]

b. Reference dye for aza-BODIPY part fluorescence quantum yield.[2]

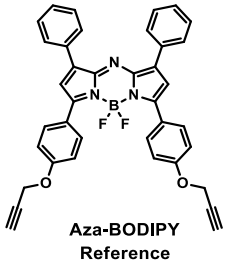

Aza-BODIPY Reference

Fluorescence excitation spectra

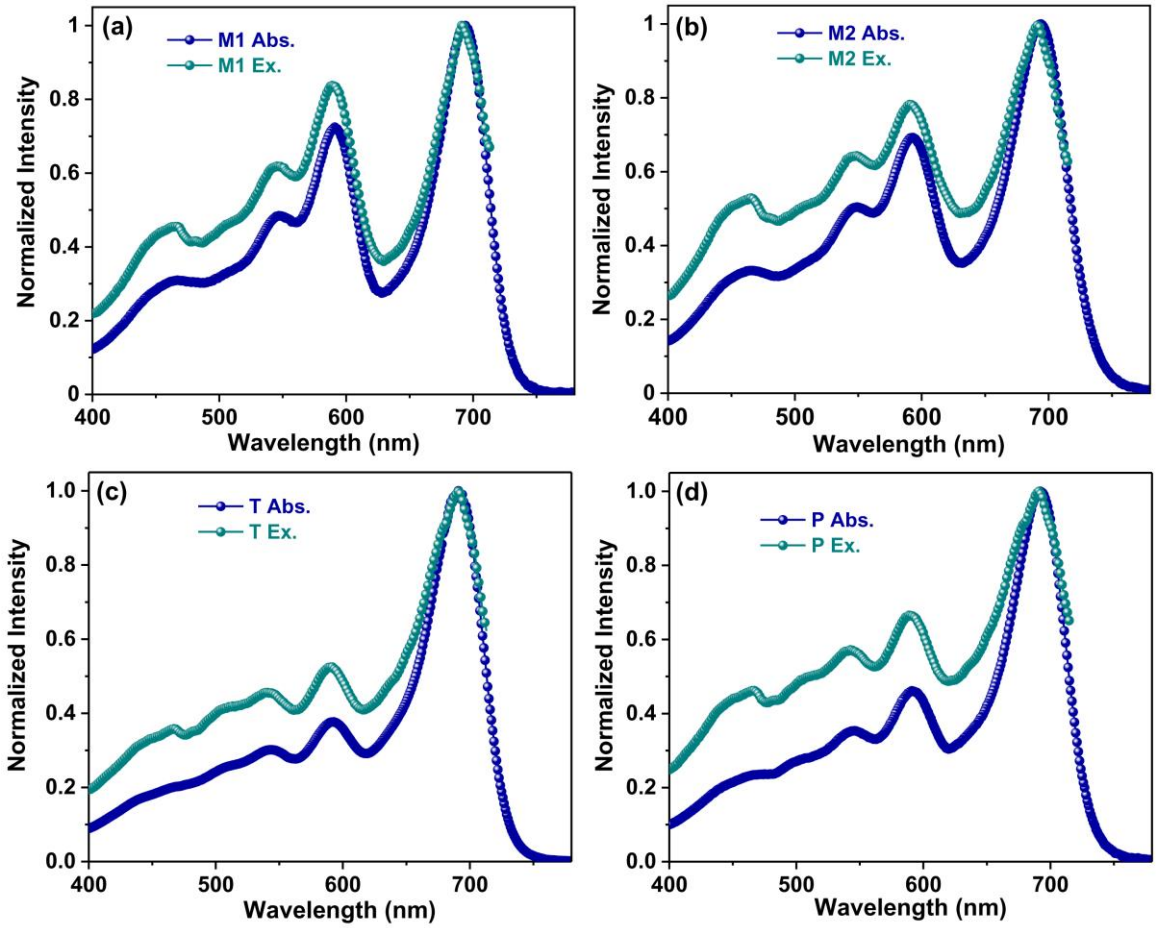

Figure S7. Comparison of absorption spectra with fluorescence excitation spectra of (a) **M1**, (b) **M2,** (c) **T** and (d) **P** in chloroform ($c \sim 2 \times 10^{-6}$ M).

Theoretical FRET Efficiency

FRET parameters such as spectral overlap integral, Förster radius, rate of FRET (k_{ET}) and energy transfer efficiency (ETE) were calculated according to the Förster theory.[1] The spectral overlap integral $J(\lambda)$ for the emission of the donor and absorption of the acceptor can be evaluated according to equation 1.

$$J(\lambda) = \int F_D(\lambda)\, \varepsilon_A(\lambda)\, \lambda^4\, d\lambda \qquad (1)$$

where, $F_D(\lambda)$ is the fluorescence intensity of the donor with total intensity normalized to unity. The $\varepsilon_A(\lambda)$ refers to the molar extinction coefficient of the acceptor expressed in units of $M^{-1}cm^{-1}$ and λ in nm. Accordingly, the $J(\lambda)$ values calculated using the a|e (Fluor Tools) software for **M1** was 5.28×10^{15} nm^4 M^{-1} cm^{-1}.

Subsequently, the Förster radii (R_0) for **M1** were calculated using equation 2 as follows:

$$R_0 = 0.211\, [(k^2 \Phi_D\, J(\lambda))/n^4]^{1/6} \qquad (2)$$

where, k^2 is the orientation factor and a value of $k^2 = 2/3$ was used considering randomly oriented transition dipoles, Φ_D was the donor only quantum yield and n was the refractive index of the solvent used (1.445 for $CHCl_3$). Accordingly, R_0 of 63.09 Å was obtained for M**1**.

Utilizing the calculated Förster radii as well as experimentally obtained fluorescence lifetimes (τ_D) of donor subchromophores PDI (6.49 ns) and centre-to-centre distances of 9.14 Å obtained from optimized geometry of **M1** (Figure S8), energy transfer rate (k_{ET}) were obtained according to the equation 3:

$$k_{ET} = 1/\tau_D\,[R_0/R]^6 \qquad (3)$$

and accordingly, k_{ET} of 1.80×10^{13} s^{-1} was obtained for **M1**.

Finally, the energy transfer efficiencies (ETE) were obtained for **M1** according to equation 4:

$$E = 1/[1+(R/R_0)^6] \qquad (4)$$

and ETE of ~ 99.9 % was obtained for **M1**.

This theoretically calculated ETE is in good agreement with ETE calculated from steady-state fluorescence quenching and fluorescence quantum yield measurements for **M1**.

The theoretically calculated FRET parameters have been presented in Table S3.

Table S3. Calculated FRET parameters for **M1** using theoretical and experimental results.

Comp.	$J(\lambda)$ (M^{-1} cm^{-1} nm^4)	R_0 (Å)	k_{ET}(s^{-1})	ETE (%)
M1	5.28×10^{15}	63.09	1.80×10^{13}	99.9

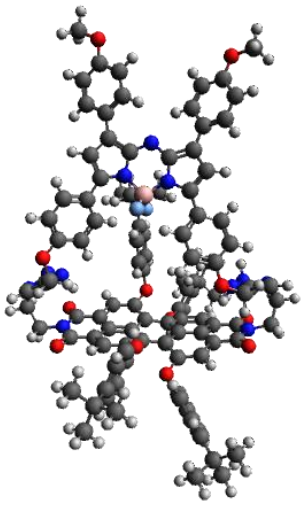

Figure S8. Optimized geometry of macrocycle **M1** by DFT method at B3LYP 6-31G (d,p) level.

Because of large structure of macrocycle **M2**, the geometric optimization by B3LYP/631G basis set was not possible.

Fluorescence lifetime

Table S4. Fluorescence lifetime analysis of **PDI**, Triad **T**, Pentad **P**, **M1** and **M2** at different excitation and emission wavelengths in toluene and $CHCl_3$.

Comp.	Solvent	λ_{ex} (nm)	λ_{em} (nm)	$\tau_1(\alpha_1)$ (ns)	$\tau_2(\alpha_2)$ (ns)	τ_{avg} (ns)	χ^2
PDI	Toluene	590	602	6.05 (1.00)	-	6.05	1.00
	$CHCl_3$	590	616	6.49 (1.00)	-	6.49	1.07
ABDP	Toluene	635	717	2.40 (1.00)	-	2.40	1.09
	$CHCl_3$	635	716	2.27 (1.00)	-	2.27	1.04
M1	Toluene	590	720	5.56 (0.12)	2.80 (0.88)	3.13	1.00
		635	720	2.24 (0.36)	3.02 (0.64)	2.74	1.04
	$CHCl_3$	590	719	6.37 (0.10)	1.59 (0.90)	2.05	1.06
		635	719	4.91 (0.06)	1.64 (0.94)	1.83	1.12
M2	Toluene	590	721	1.73 (0.28)	3.04 (0.72)	2.68	1.00
		635	721	1.40 (0.12)	2.75 (0.88)	2.59	1.08
	$CHCl_3$	590	721	1.46 (0.47)	2.69 (0.53)	2.11	1.03
		635	721	0.74 (0.27)	2.32 (0.73)	1.90	1.08
T	Toluene	590	721	4.07 (0.12)	2.27 (0.88)	2.48	1.11
		635	721	1.19 (0.07)	2.40 (0.93)	2.32	1.00
	$CHCl_3$	590	720	1.78 (0.29)	2.47 (0.71)	2.27	1.02
		635	720	0.06 (0.36)	2.07 (0.64)	1.35	1.06
P	Toluene	590	721	1.10 (0.32)	2.44 (0.68)	2.01	1.02
		635	721	0.69 (0.23)	2.29 (0.77)	1.93	1.10
	$CHCl_3$	590	721	0.58 (0.21)	2.12 (0.79)	1.79	1.01
		635	721	0.37 (0.22)	1.96 (0.78)	1.62	1.02

Solvatochromism

The absorption and emission spectra (Figure S9-S11, Table S5) of macrocycles and acyclic compounds were recorded in solvents of increasing polarity from toluene to benzonitrile. Solvent polarities did not show a significant impact on the absorption and emission maxima and spectral features, except in case of pentad **P**, where spectral broadening of PDI band was observed in toluene (Figure S11c) suggesting the aggregation of **P** in toluene.

With the increase in solvent polarity, triad **T** and macrocycle **M2** showed decrease in fluorescence intensity of aza-BODIPY from toluene to chloroform, THF and DCM, however, other compounds did not follow any trend.

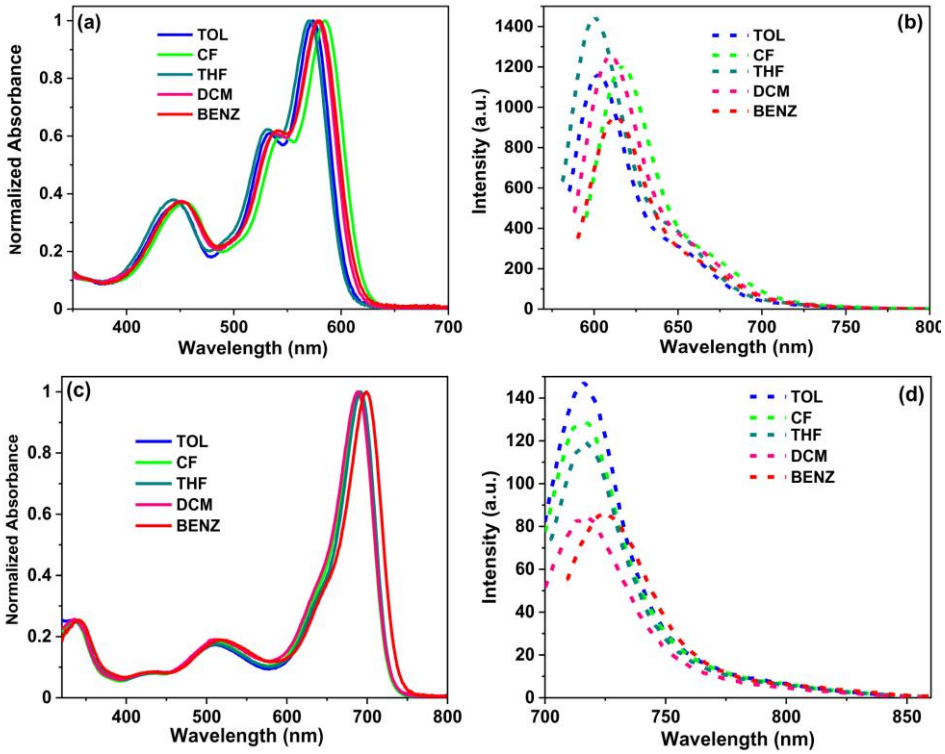

Figure S9. Absorption and emission spectra of (a), (b) **PDI** and (c), (d) **ABDP** ($c \sim 2 \times 10^{-6}$ M) in solvents with different polarity. TOL - Toluene, CF - Chloroform, THF - Tetrahydrofuran, DCM - Dichloromethane, BENZ – Benzonitrile.

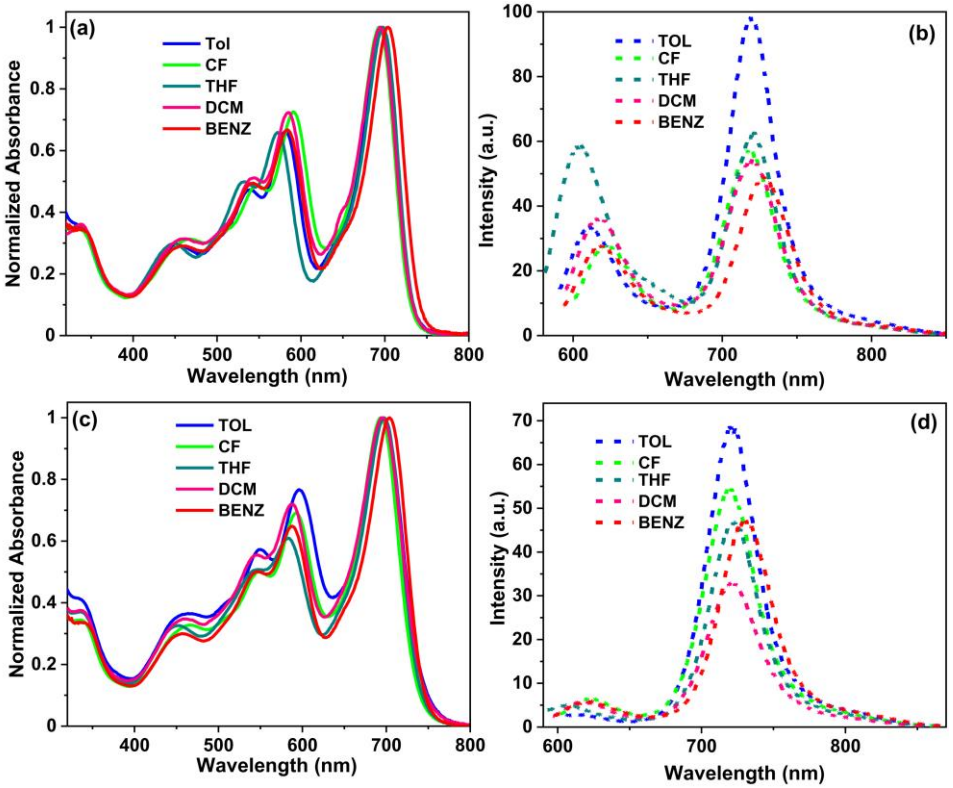

Figure S10. Absorption and emission spectra of (a, b) **M1** and (c, d) **M2** ($c \sim 2 \times 10^{-6}$ M) in solvents with different polarity.

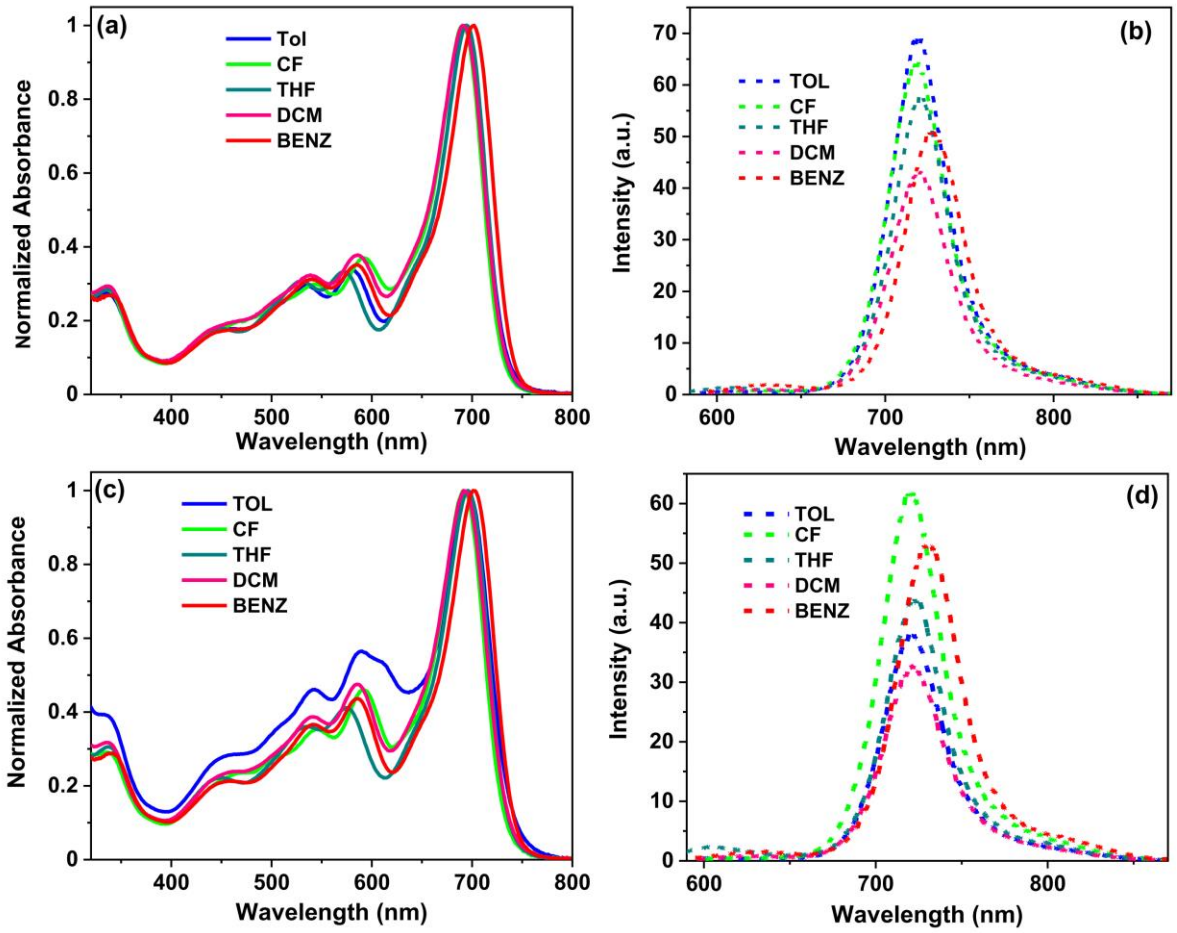

Figure S11. Absorption and emission spectra of (a, b) Triad **T** and (c, d) Pentad **P** ($c \sim 2 \times 10^{-6}$ M) in solvents with different polarity.

Table S5. Absorption and emission maxima of macrocycles **M1** and **M2**, acyclic triad **T** and pentad **P** and corresponding reference compounds in different solvents.

Comp.	Solvent	λ_{abs} (nm)	λ_{em} (nm)
PDI	Toluene	574	602
	$CHCl_3$	585	616
	THF	570	601
	DCM	578	611
	Benzonitrile	580	614
ABDP	Toluene	690	717
	$CHCl_3$	688	716
	THF	692	717
	DCM	689	717
	Benzonitrile	699	726
M1	Toluene	581, 696	611, 720 (λ_{ex} = 581 nm)
	$CHCl_3$	591, 693	623, 719 (λ_{ex} = 591 nm)
	THF	572, 697	605, 721 (λ_{ex} = 572 nm)
	DCM	585, 694	618, 721 (λ_{ex} = 585 nm)
	Benzonitrile	584, 703	621, 727 (λ_{ex} = 584 nm)
M2	Toluene	596, 696	619, 721 (λ_{ex} = 596 nm)
	$CHCl_3$	592, 694	620, 721 (λ_{ex} = 592 nm)
	THF	583, 697	605, 723 (λ_{ex} = 583 nm)
	DCM	588, 695	618, 721 (λ_{ex} = 588 nm)
	Benzonitrile	588, 704	622, 728 (λ_{ex} = 588 nm)
T	Toluene	581, 694	721 (λ_{ex} = 581 nm)
	$CHCl_3$	592, 691	720 (λ_{ex} = 592 nm)
	THF	572, 695	721 (λ_{ex} = 572 nm)
	DCM	586, 691	721 (λ_{ex} = 586 nm)
	Benzonitrile	585, 702	729 (λ_{ex} = 585 nm)
P	Toluene	589, 696	721 (λ_{ex} = 589 nm)
	$CHCl_3$	591, 692	720 (λ_{ex} = 591 nm)
	THF	575, 696	723 (λ_{ex} = 575 nm)
	DCM	586, 692	722 (λ_{ex} = 586 nm)
	Benzonitrile	585, 701	730 (λ_{ex} = 585 nm)

Absorption and emission spectra in THF/H_2O mixtures

To probe the aggregation induced emission (AIE) behaviour of **M1** and **M2** along with triad **T** and pentad **P** in semi-aqueous media, absorption/emission spectra (Figure S12-S13) were recorded in water/tetrahydrofuran (THF) mixtures. From the absorption spectra, broadening as well as a redshift of both the PDI (~ 10-30 nm) and ABDP (~ 12-41 nm) bands were observed with an increase in water fraction. However, the emission spectra showed aggregation caused quenching behaviour with the increase of water fraction (Figure S12-13). Dynamic light scattering (DLS) measurements (Figure S14) revealed that **M1** formed closely packed aggregates with an average hydrodynamic diameter of ~ 68 nm while **M2** due to its large size formed loosely bound aggregates with an average hydrodynamic diameter of ~ 295 nm.

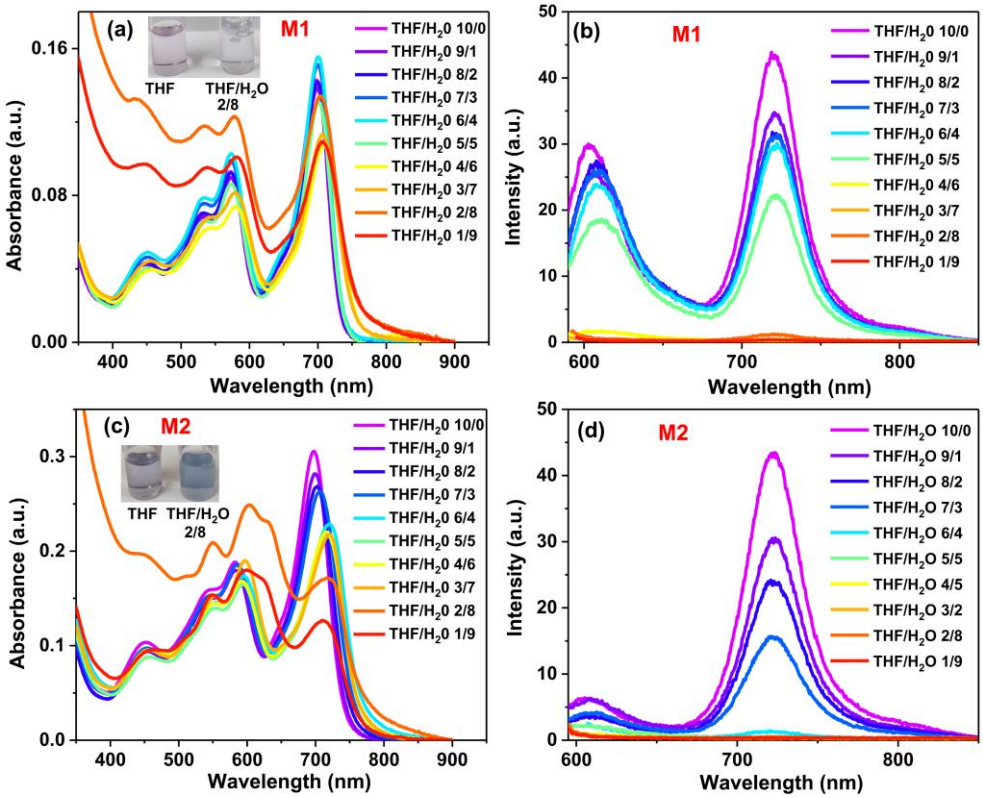

Figure S12. Changes in absorption and emission spectra of (a, b) **M1** and (c, d) **M2** in different THF/H_2O (v/v) mixtures (c ~ 2 ×10^{-6} M).

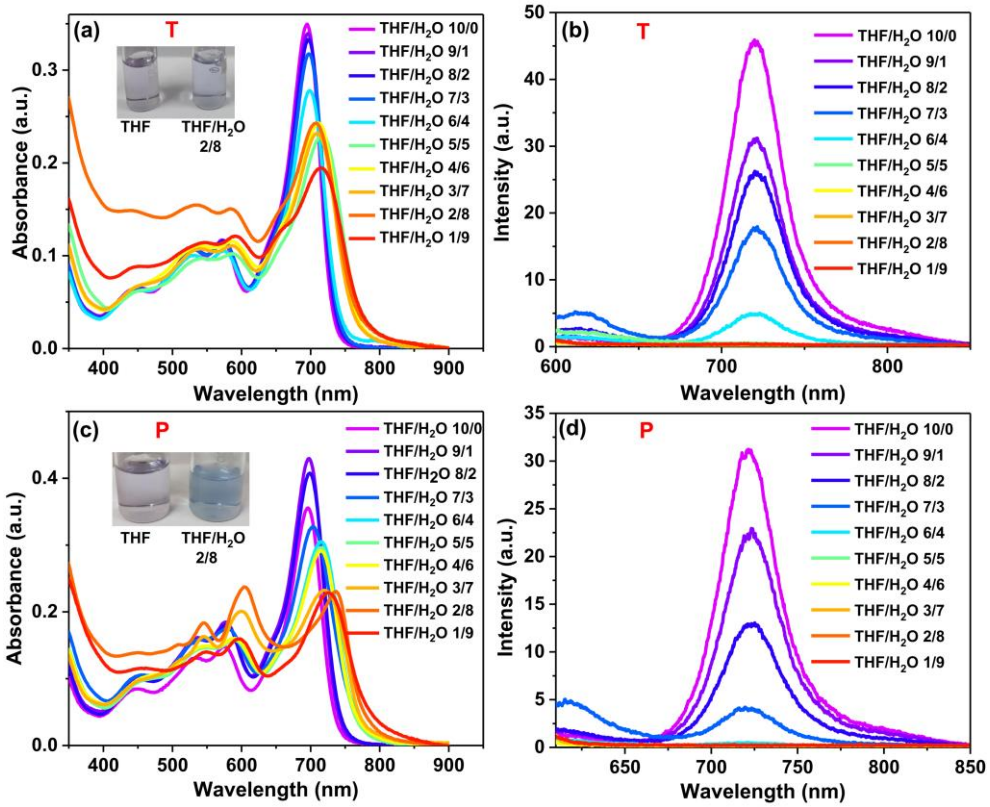

Figure S13. Changes in absorption and emission spectra of (a, b) Triad **T** and (c, d) Pentad **P** in different THF/H_2O (v/v) mixtures ($c \sim 2 \times 10^{-6}$ M).

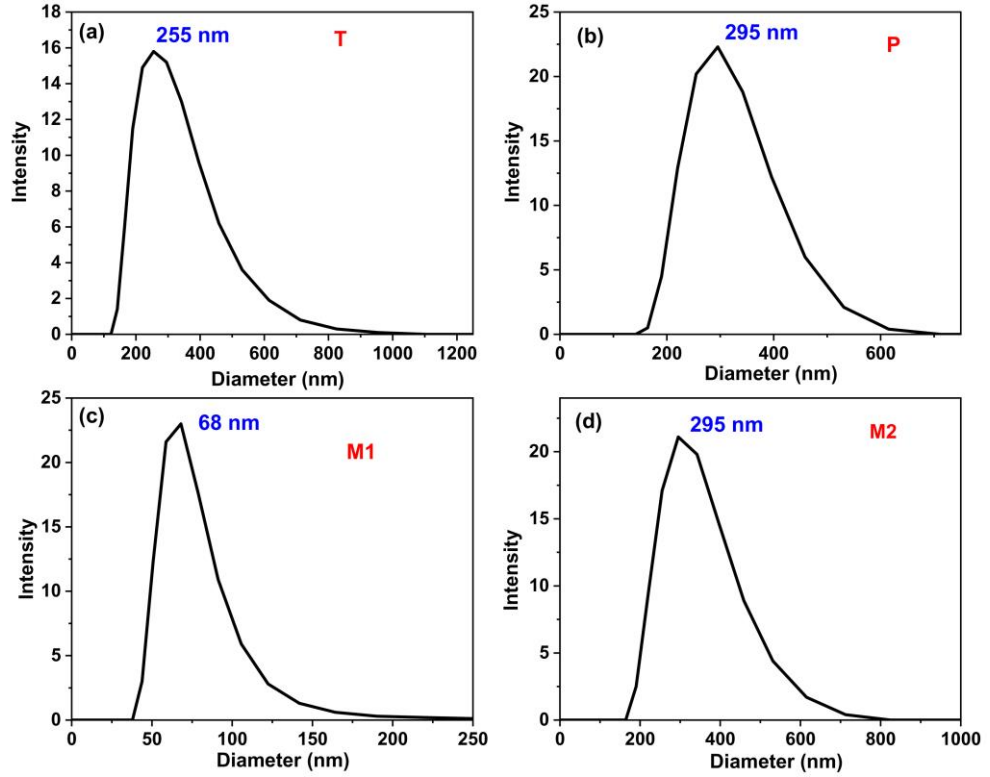

Figure S14. DLS profiles of (a) **T**, (b) **P**, (c) **M1** and (d) **M2** in water/THF (8:2; v/v) mixture ($c \sim 2 \times 10^{-6}$ M).

6. Temperature-dependent emission study

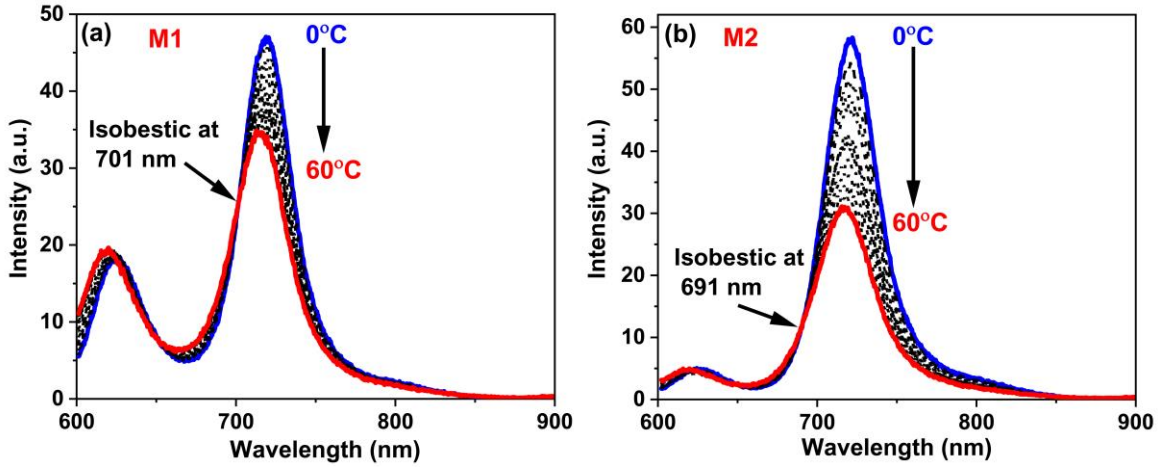

Figure S15. Temperature responsive emission spectra of (a) **M1** and (d) **M2** from 0 to 60 ˚C in chloroform (c ~ 2 $\times 10^{-6}$ M).

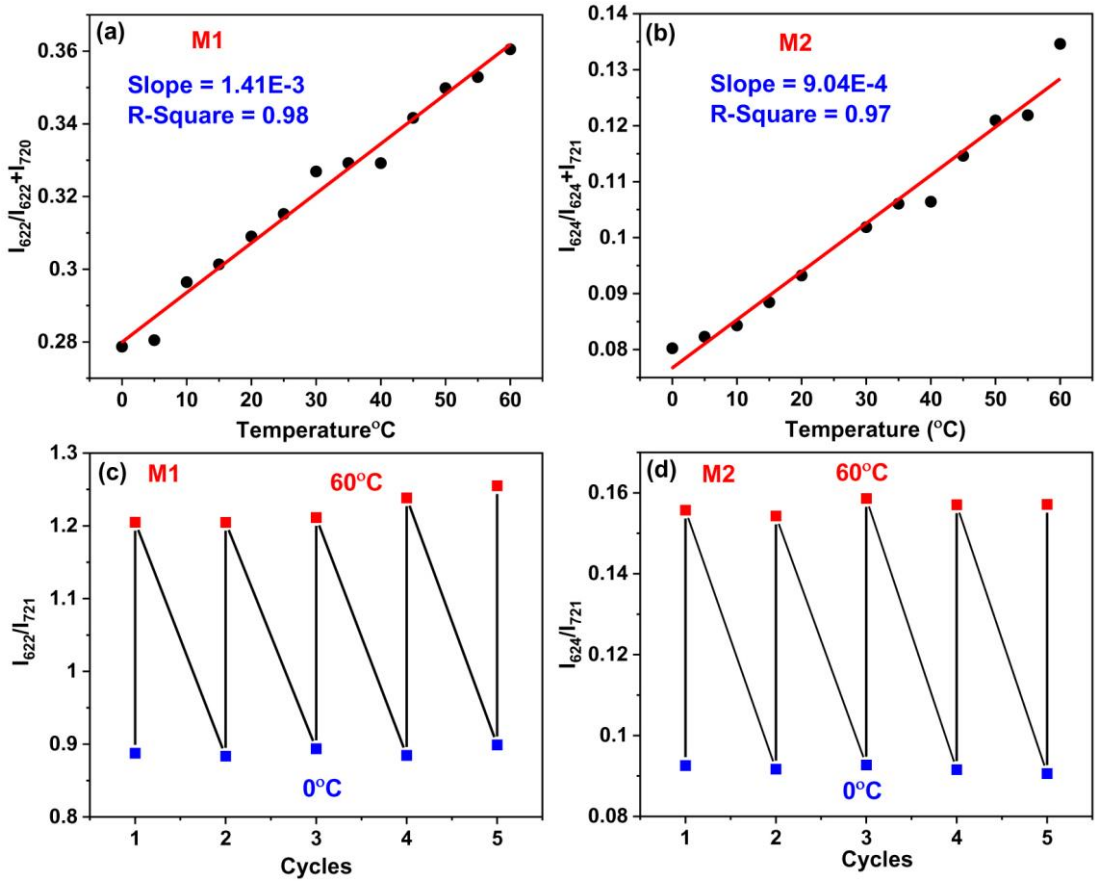

Figure S16. Plots of (a) $I_{614}/I_{614}+I_{721}$ for **M1** and (b) $I_{616}/I_{616}+I_{723}$ for **M2** *vs*. temperature; Cyclic switching of emission intensity ratio upon heating and cooling for (c) **M1** and (d) **M2** in chloroform (c ~ 2 $\times 10^{-6}$ M).

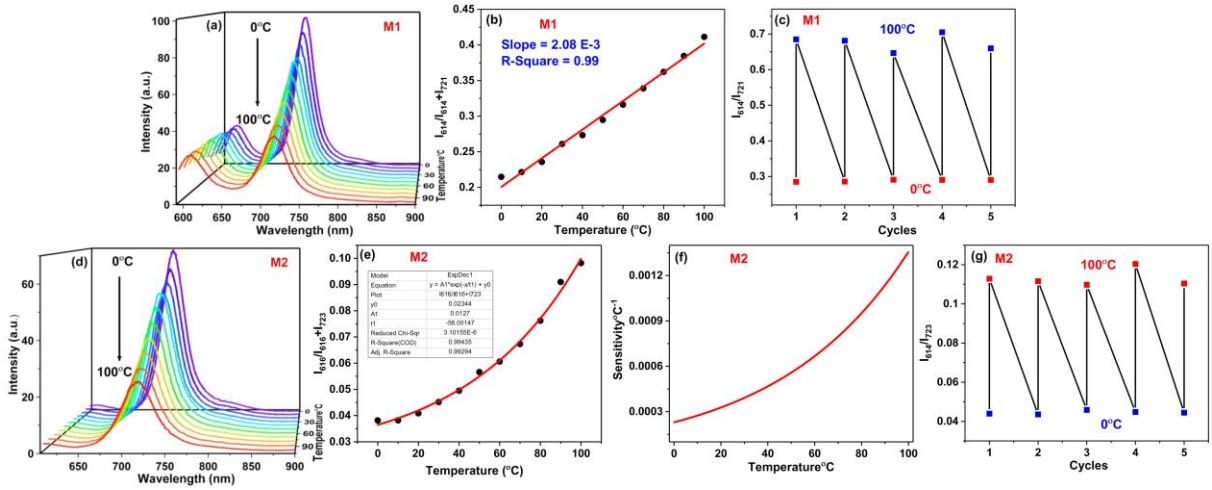

Figure S17. Temperature responsive emission spectra of (a) **M1** and (d) **M2** from 0 to 100 ˚C; Plots of (b) $I_{614}/I_{614}+I_{721}$ for **M1** and (e) $I_{616}/I_{616}+I_{723}$ for **M2** *vs*. temperature; (f) Sensitivity plot for **M2**; Cyclic switching of emission intensity ratio upon heating and cooling for (c) **M1** and (g) **M2** in toluene ($c \sim 2 \times 10^{-6}$ M).

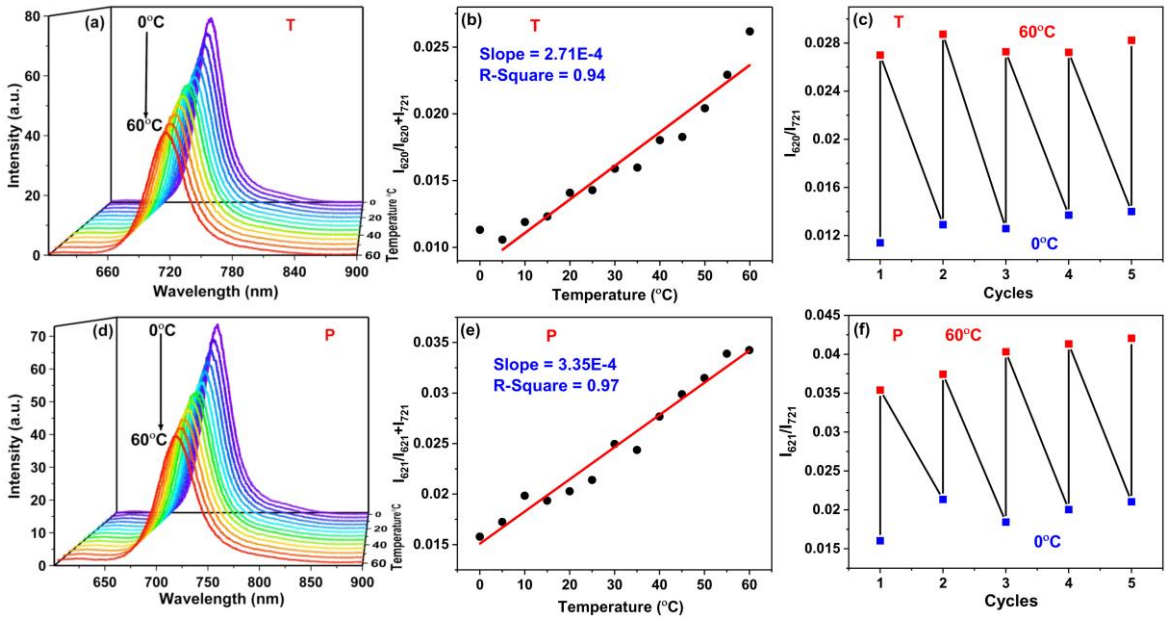

Figure S18. Temperature responsive emission spectra of (a) triad **T** and (d) pentad **P** from 0 to 60 ˚C; Plots of (b) $I_{620}/I_{620}+I_{721}$ for triad **T** and (e) $I_{621}/I_{621}+I_{721}$ for pentad **P** *vs*. temperature; Cyclic switching of emission intensity ratio upon heating and cooling for (c) triad **T** and (f) pentad **P** in chloroform ($c \sim 2 \times 10^{-6}$ M).

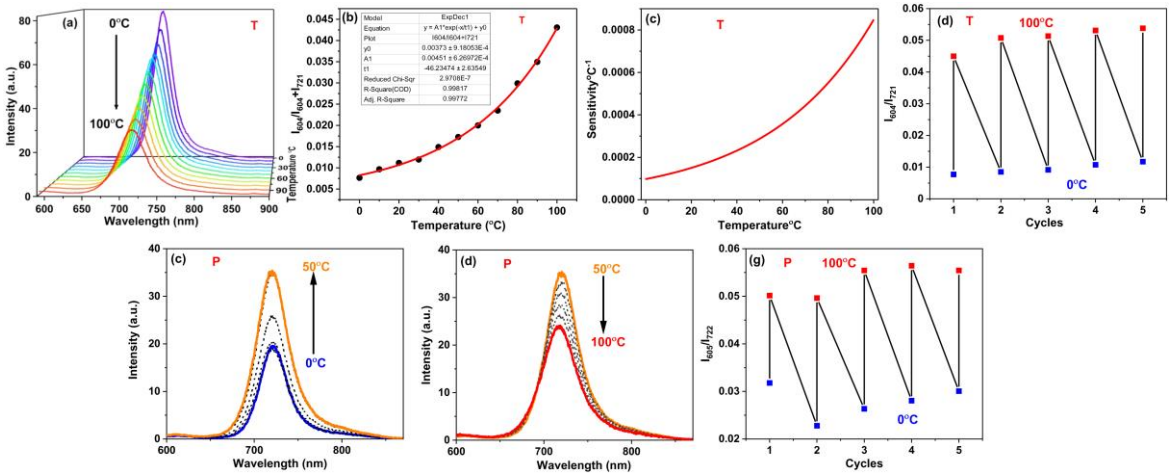

Figure S19. Temperature responsive emission spectra of (a) triad **T** and (e), (f) pentad **P** from 0 to 100 ˚C; (b) Plots of $I_{604}/I_{604}+I_{721}$ *vs*. temperature for triad **T**; (c) Sensitivity plot for triad **T**; Cyclic switching of emission intensity ratio upon heating and cooling for (d) triad **T** and (g) pentad **P** in toluene ($c \sim 2 \times 10^{-6}$ M).

Table S6. Fitted parameters for temperature-dependent fluorescence intensities and sensitivities for **T**, **P**, **M1** and **M2** in chloroform and toluene.

Comp.	Solvent	R^2	Equation	Sensitivity (°C^{-1})
M1	$CHCl_3$	0.98	y = 0.00143 x + 0.459	0.14 (0 to 60 °C)
	Toluene	0.99	y = 0.00208 x + 0.205	0.21 (0 to 100 °C)
M2	$CHCl_3$	0.97	y = 0.00090 x + 0.0783	0.09 (0 to 60 °C)
	Toluene	0.99	y = 0.0162 exp(x/49.67) + 0.0277	0.023 to 0.13 (0 to 100 °C)
T	$CHCl_3$	0.94	y = 0.00027 x + 0.0092	0.027 (0 to 60 °C)
	Toluene	0.998	y = 0.0051 exp(x/43.36) + 0.00465	0.0098 to 0.085 (0 to 100 °C)
P	$CHCl_3$	0.97	y = 0.000335 x + 0.0156	0.034 (0 to 60 °C)
	Toluene	-	-	-

7. Redox behavior and spectroelectrochemistry

The electrochemical behaviour of all the compounds were assessed by performing cyclic voltammetry and differential pulse voltammetry experiments in dry dichloromethane (DCM) using tetrabutylammonium hexafluorophosphate (TBAHFP) as supporting electrolyte (Figures S20-S22). The calculated HOMO, LUMO energy values are presented in Table S7, deep lying LUMO values indicated their electron deficient character and deep lying HOMO values indicated their ambient stability. The alignment of frontier molecular orbitals is presented in Figure S23 that shows the HOMO/LUMO energy levels of energy acceptor ABDP lie well within the HOMO/LUMO levels of donor PDI and such band alignments rule out the possibility of photoinduced electron transfer process between donor and acceptor components.

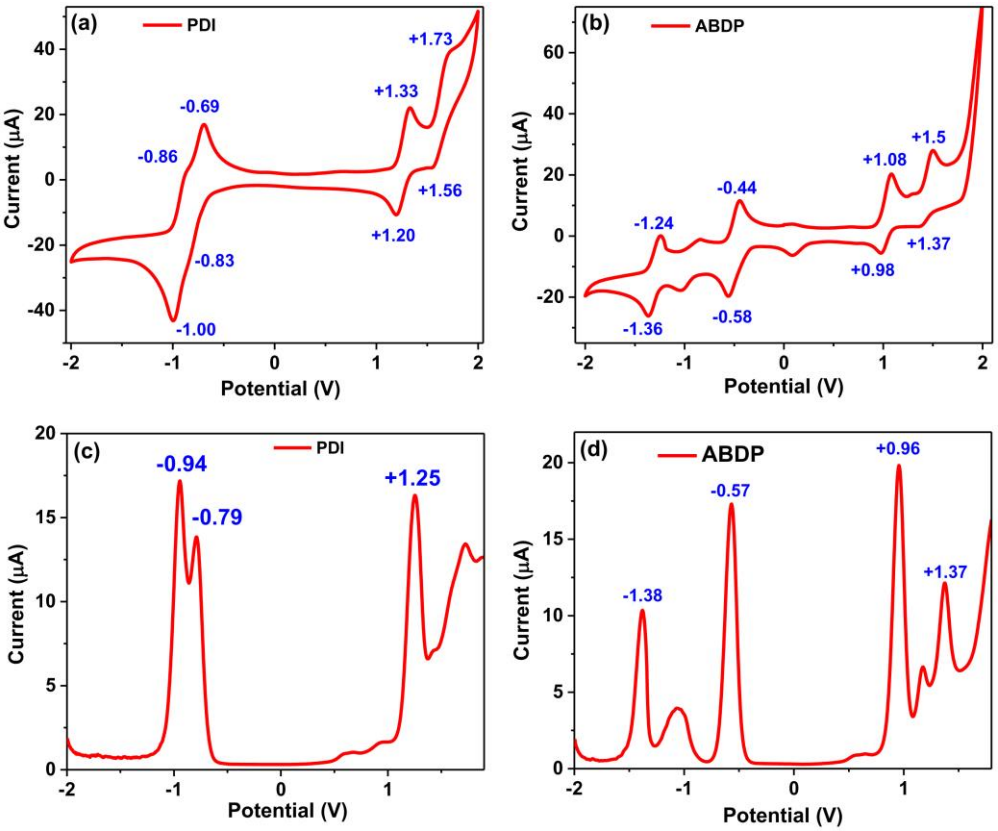

Figure S20. Cyclic voltammogram (a, b) and differential pulse voltammogram (c), (d) of **PDI** and **ABDP** respectively in dry DCM with 0.1 M TBAHFP at *c* ~ 0.5 mM vs. Ag/AgCl reference electrode at scan rate of 0.1 V s^{-1}.

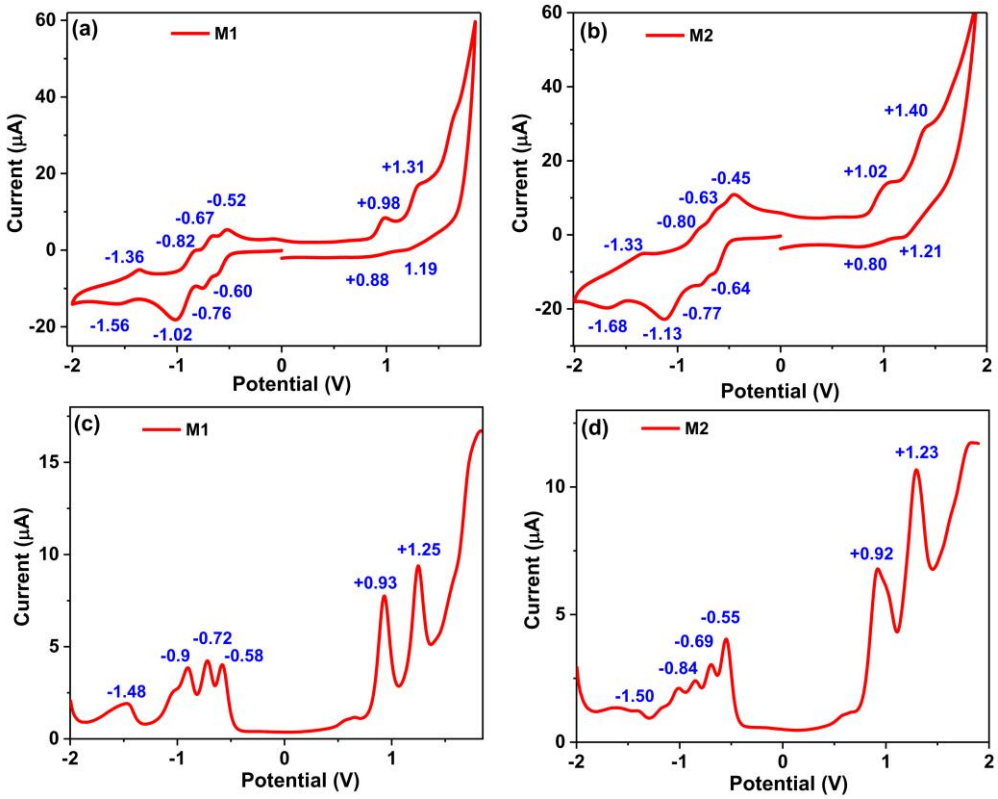

Figure S21. Cyclic voltammogram (a, b) and differential pulse voltammogram (c), (d) of **M1** and **M2** respectively in dry DCM with 0.1 M TBAHFP at *c* ~ 0.5 mM vs. Ag/AgCl reference electrode at scan rate of 0.1 V s^{-1}.

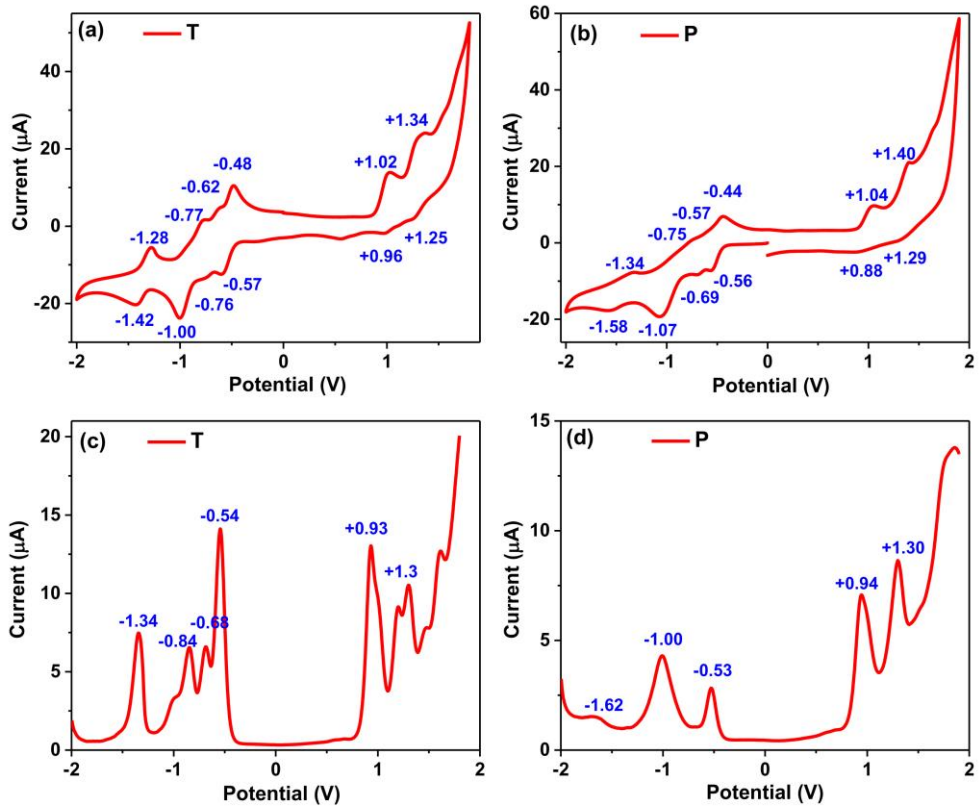

Figure S22. Cyclic voltammogram (a, b) and differential pulse voltammogram (c), (d) of **T** and **P** respectively in dry DCM with 0.1 M TBAHFP at *c* ~ 0.5 mM vs. Ag/AgCl reference electrode at scan rate of 0.1 V s^{-1}.

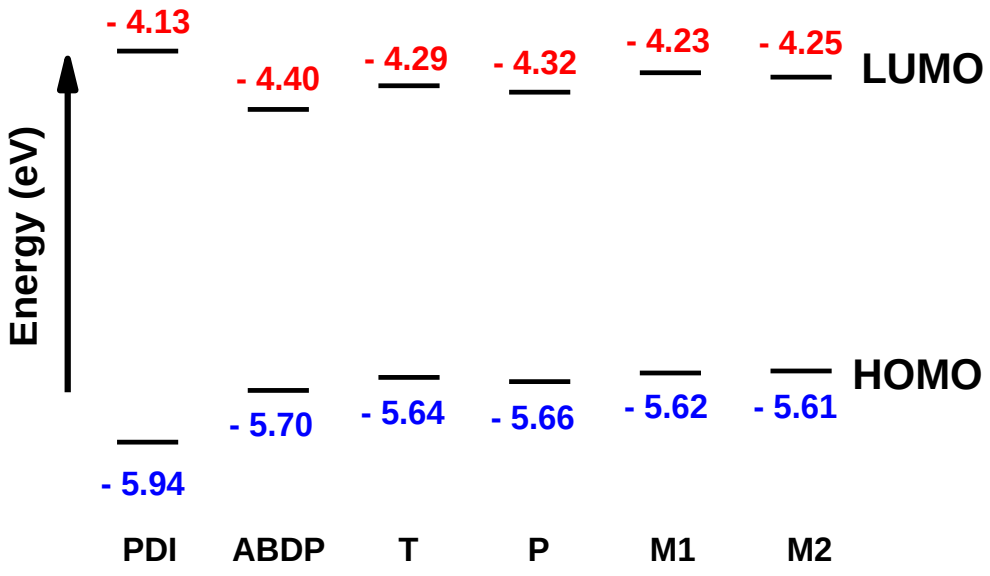

Figure S23. Alignment of frontier molecular orbital energy levels (in eV) obtained from cyclic voltammetry measurements for reference as well as for final compounds.

Table S7. Redox properties of all the compounds based on cyclic voltammetry.

Comp.	E_{Ox}^{onset} (V)	E_{red}^{onset} (V)	λ_{onset} (nm)	[a]HOMO (eV)	[b]LUMO (eV)	[c]E_g^{opt} (eV)	E_g^{cv} (eV)
PDI	1.18	-0.63	618	-5.94	-4.13	2.00	1.81
ABDP	0.94	-0.36	725	-5.70	-4.40	1.71	1.30
M1	0.86	-0.49	731	-5.62	-4.23	1.70	1.39
M2	0.85	-0.51	746	-5.61	-4.25	1.66	1.36
T	0.88	-0.47	736	-5.64	-4.29	1.69	1.35
P	0.90	-0.44	740	-5.66	-4.32	1.68	1.34

[a]HOMO = -(E_{Ox}^{onset} + 4.76) eV, [b]LUMO = -(E_{red}^{onset} + 4.76) eV and [c]E_g^{opt} = 1241/λ_{onset}.

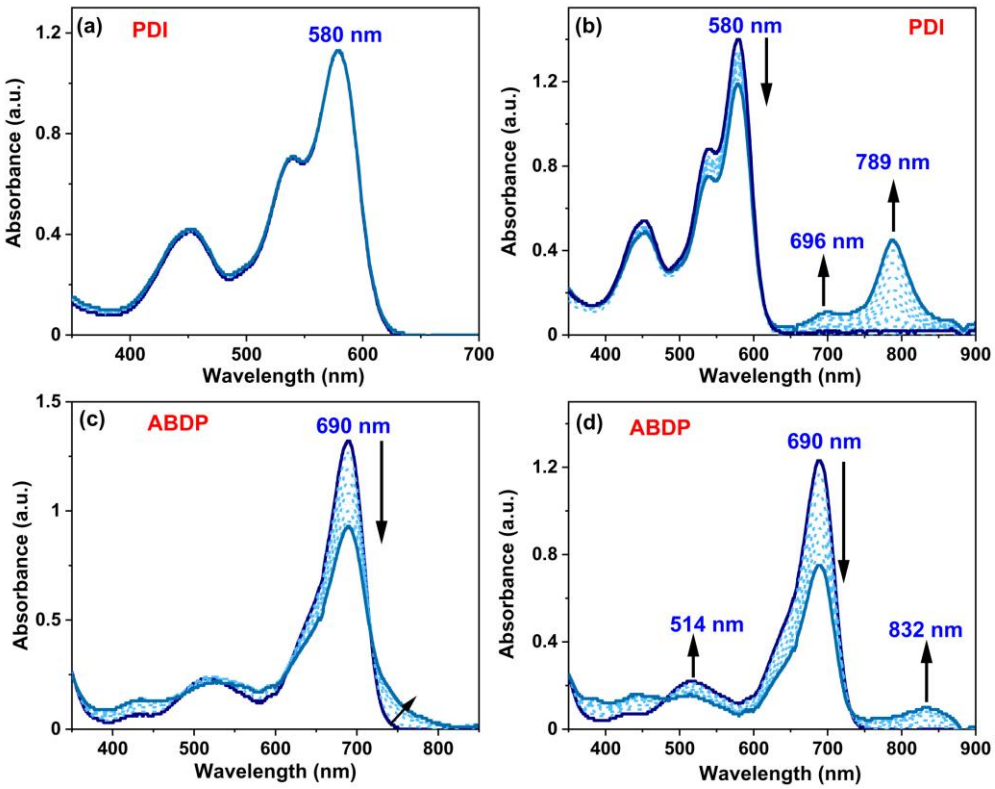

Figure S24. Spectroelectrochemical changes observed for (a), (b) **PDI** and (c), (d) **ABDP** during oxidation and reduction cycles.

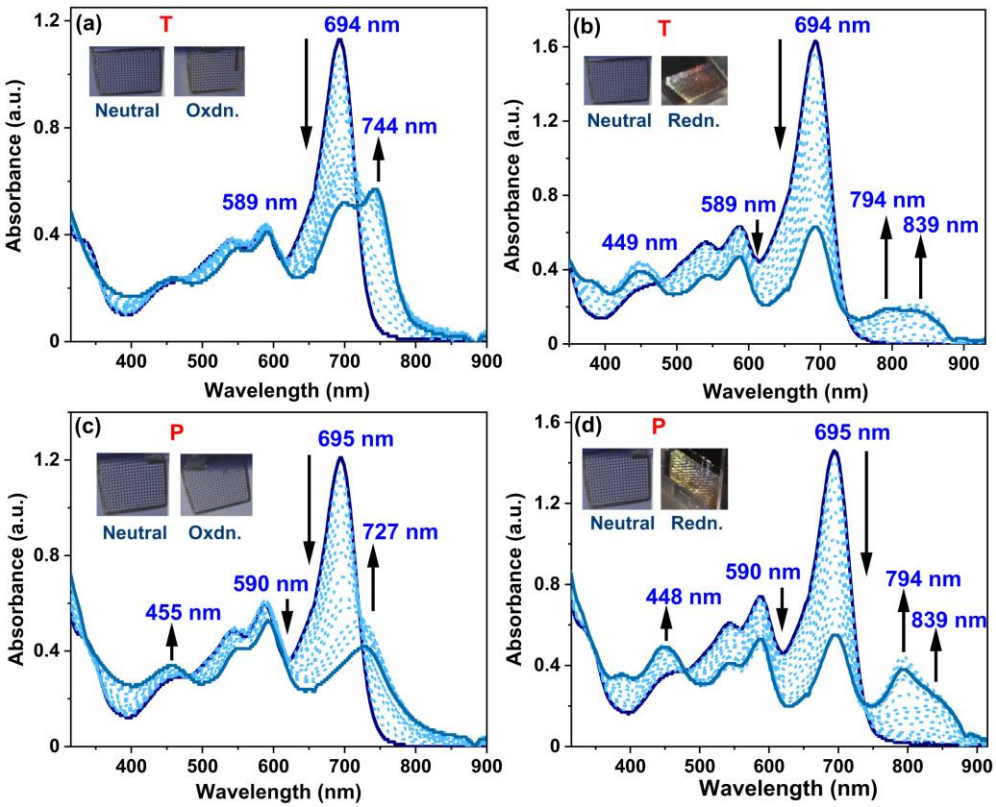

Figure S25. Spectroelectrochemical changes observed for (a), (b) Triad **T** and (c), (d) Pentad **P** during oxidation and reduction cycles (Inset figures represents the change in colour on oxidation and reduction stimuli).

8. Comparison of macrocycles and acyclic antenna

On comparison of macrocyclic systems **M1** and **M2** v*s* acyclic triad **T** and pentad **P**, the following observations were made:

(I) In macrocycles **M1** and **M2**, FRET efficiency was comparable to acyclic triad **T** and pentad **P**. (II) Pentad **P** showed exceptional behavior with the bidirectional response of emission intensity ratio towards temperature in toluene while others (**M1**, **M2**, and **T**) followed unidirectional response. In case of macrocycles, cyclic switchability of intensity ratio with temperature was more consistent as compared to open chain compounds due to conformational restrictions. (III) In the aggregation study of macrocyclic vs acyclic compounds, **M1** formed the most compact aggregate of average hydrodynamic diameter of ~ 68 nm compared to more loosely bound aggregates of **M2** (~295 nm), triad **T** (~255 nm), and pentad **P** (~295 nm).

9. References

1 K. Rani, U. K. Pandey and S. Sengupta, *J. Mater. Chem. C*, 2021, **9**, 4607–4618.
2 S. Guo, L. Ma, J. Zhao, B. Küçüköz, A. Karatay, M. Hayvali, H. G. Yaglioglu and A. Elmali, *Chem. Sci.*, 2014, **5**, 489–500.
3 G. Seybold and G. Wagenblast, *Dye. Pigment.*, 1989, **11**, 303–317.
4 K. Rani and S. Sengupta, *Chem. Sci.*, 2021, **12**, 15533–15542.